

AMERICAN UNIVERSITY OF BEIRUT

ANTI-TUMOR ACTIVITIES OF SALOGRAVIOLIDE A,
DERIVATIVES, AND NANOPARTICLE FORMULATIONS
IN BREAST AND COLORECTAL CANCER CELLS

by
ZAYNAB JABER

A thesis
submitted in partial fulfillment of the requirements
for the degree of Master of Science
to the Department of Biochemistry and Molecular Genetics
of the Faculty of Medicine
at the American University of Beirut

Beirut, Lebanon
June 2015

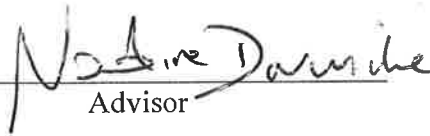
AMERICAN UNIVERSITY OF BEIRUT

ANTI-TUMOR ACTIVITIES OF SALOGRAVIOLIDE A,
DERIVATIVES, AND NANOPARTICLE FORMULATIONS IN
BREAST AND COLORECTAL CANCER CELLS

by
ZAYNAB JABER

Approved by:

Dr. Nadine Darwiche, Professor
Biochemistry and Molecular Genetics


Advisor

Dr. Walid Saad, Assistant Professor
Chemical Engineering Program


Co-Advisor

Dr. Najat A. Saliba, Professor
Chemistry


Member of Committee

Dr. Firas Kobeissy, Assistant Professor
Biochemistry and Molecular Genetics


Member of Committee

Date of thesis defense: June 10, 2015

AMERICAN UNIVERSITY OF BEIRUT

THESIS, DISSERTATION, PROJECT RELEASE FORM

Student Name: Jaber Zaynab
Last First Middle

Master's Thesis Master's Project Doctoral Dissertation

I authorize the American University of Beirut to: (a) reproduce hard or electronic copies of my thesis, dissertation, or project; (b) include such copies in the archives and digital repositories of the University; and (c) make freely available such copies to third parties for research or educational purposes.

I authorize the American University of Beirut, **three years after the date of submitting my thesis, dissertation, or project**, to: (a) reproduce hard or electronic copies of it; (b) include such copies in the archives and digital repositories of the University; and (c) make freely available such copies to third parties for research or educational purposes.

Signature

Date

This form is signed when submitting the thesis, dissertation, or project to the University Libraries

ACKNOWLEDGEMENTS

I would never have been able to finish my thesis without the guidance of my committee members, help from colleagues and friends, and support from my family. I would like to extend a sincere thanks to Hikma Pharmaceuticals, who took on the financial support of this project and made it all possible, and a special thanks to the board members of Hikma for their input and expertise on the path of translational research. I am also grateful to the staff of the AUB Nature Conservation Center.

To my advisor, Dr. Nadine Darwiche, I would like to express my deepest gratitude for her excellent guidance and providing me with an excellent atmosphere for doing research. Her believing in me as a researcher was sometimes all that kept me going. I would like to thank Dr. Walid Saad, my co-advisor, who introduced me to the interesting discipline of chemical engineering and nanotechnology. I would also like to thank Dr. Najat Saliba and Dr. Tarek Ghaddar, the co-investigators of this project whose chemistry expertise drove the project to success. I could not have asked for a better group of investigators on this enriching experience. Additionally, I would like to extend a sincere thank you to committee member, Dr. Firas Kobeissy, for his encouragement, insightful comments, and hard questions.

Many thanks to the engineers and staff of the Central Research Science Laboratory (CRSL) who trained me in the use of specialized analytical instruments that proved crucial to my research. Also thanks to chemical engineering lab staff Rita Khalil and Tala Bechara. I am also grateful to my colleagues and friends, Lamis Alaaraj and Melody Saikali, who were willing to help and give me their best suggestions. A special thanks goes to my colleagues of the Blue Lab past, present, and future: Rana Abdel-Samad, Patrick Aouad, Berthe Hayar, Raed Hmadi, Leeanna El-Houjeiri, Boutheina Ghandour, Melody Saikali, Houda Samman, Zeinab Sweidan, and Rita Tohme. I am thankful and indebted to them for sharing expertise and the sincere encouragement extended to me. Raed and Melody, who were more than colleagues, thanks for the memories.

I take this opportunity to express gratitude to my family and friends for the unceasing encouragement, support, and attention. I have been fortunate enough to meet and spend time with some great friends during my years here at AUB, and I would like to thank them for their support and friendship: Karine Baasiri, Minerva Faddoul, Rose Khouri, Mohammad Al Medawar, and Nour Salloum. Finally, I would like to thank my family for always believing in me and encouraging me to succeed in all of my endeavors: Mom, Dad, Hussein, Fatima, and Nora. In particular, my parents have been lifelong advocates of my education, and for this, I am extremely grateful.

I also place on record, my sense of gratitude to one and all, who directly or indirectly, have lent me their hands in this venture.

AN ABSTRACT OF THE THESIS OF

Zaynab Jaber for Master of Science
Major: Biochemistry and Molecular Genetics

Title: Anti-tumor Activities of Salograviolide A, Derivatives, and Nanoparticle Formulations in Breast and Colorectal Cancer Cells

We are currently witnessing a renewed interest in the use of natural compounds to treat cancer. Sesquiterpene lactones are plant secondary metabolites that possess a broad range of anti-tumor activities due to the reactivity of their alkylating centers, lipophilicity, and molecular geometry. We have isolated the sesquiterpene lactone, Salograviolide A (Sal A), from the indigenous Lebanese plant *Centaurea ainetensis*, and have previously shown that this compound exhibits promising anti-cancer properties in a variety of cancer cells, while sparing normal ones. Combining nanotechnology with medicine enables more efficient drug delivery; increasing stability, bioavailability, and reducing drug toxicity, which are common challenges in drug development. The general aim of this study is to develop more bioavailable and clinically desirable derivatives of Sal A. We aimed to formulate and characterize nanoparticles of Sal A and its derivatives and assess the anti-cancer effects in established *in vitro* models of colorectal and breast cancer.

We have successfully scaled up the extraction and purification of Sal A using preparative high performance liquid chromatography during which another compound with similar physicochemical properties eluted at a later time point which was identified as Salograviolide B (Sal B). Importantly, this will be the first report revealing the biological activities of this sesquiterpene lactone. Furthermore, we have successfully synthesized derivatives of Sal A and Sal B: Sal A-1, Sal A-2, and Sal B-1 and have assayed their cytotoxicity on normal cells. These five compounds exhibited anti-cancer activities in a variety of human cancer cell lines where the different derivatives have shown at least a two-fold increased potency relative to Sal A. This increased potency may be attributed to their increased hydrophobicity, as confirmed through solubility experiments. By determining the aqueous and organic solubility of the compounds, we were able to ascertain their suitability for producing nanoparticles *via* Flash NanoPrecipitation. This is a recently developed technique for the production of controlled size nanoparticles of drugs, providing high active loading efficiencies and drug loading contents.

Sal A, Sal B, and derivatives were attempted to be formulated into nanoparticles. However, only Sal B proved most successful as a nanoparticle formulation and became our lead drug based on anti-tumor assays in colorectal and breast cancer cells. Our results showed that native Sal B and its nanoparticle formulation had comparable anti-tumor activities in colorectal and breast cancer cells independently of *p53* status, and both induced accumulation of cells in the S phase of the cell cycle and apoptosis. These promising drugs will be evaluated further in tumor animal models with the ultimate aim of providing novel colorectal and breast cancer therapies.

CONTENTS

	Page
ACKNOWLEDGEMENTS	v
ABSTRACT.....	vi
LIST OF ILLUSTRATIONS	x
LIST OF TABLES	xiii
LIST OF ABBREVIATIONS.....	xiv
 Chapter	
I. INTRODUCTION	1
A. Medicinal Plants and Cancer	1
B. Plant Secondary Metabolites	3
1. Definition.....	4
2. Classification	5
3. Sesquiterpene Lactones.....	6
C. The Indigenous Lebanese Medicinal Plant <i>Centaurea ainetensis</i>	9
D. Anti-tumor Activities of Salograviolide A	10
E. Breast Cancer	12
F. Colorectal Cancer	12
G. <i>In Vitro</i> Model Systems for Assessing Anti-tumor Activity	13
1. Breast Cancer Cell Lines	13
2. Colorectal Cancer Cell Lines	14
H. Treatment of Breast and Colorectal Carcinogenesis by Botanical Agents: A Step Towards Clinical Drug Development.....	14
I. Rationale for Drug Derivatization	16

J. Enhancing Drug Delivery: Nanotechnology	18
1. Definition	18
2. Nanoparticle Advantages	19
3. Flash NanoPrecipitation.....	21
4. Nanomedicine and Sesquiterpene Lactones	22
K. Aim of Study.....	24
1. Drug Extraction and Characterization	25
2. Drug Nanoparticle Formulation, Optimization, and Characterization	25
3. Anti-cancer Activities of Drugs and Nanoparticle Formulations	25
II. MATERIALS AND METHODS	26
III. RESULTS	38
A. Drug Extraction and Characterization	38
1. Extraction optimization and purification of Sal A from <i>Centaurea ainetensis</i>	38
2. Spectroscopic measurements reveal the structures of Sal A and Sal B	40
3. Sal A and Sal B derivatives were successfully synthesized and structurally elucidated	42
4. Sal B and derivatives were found to be more hydrophobic than Sal A	45
B. Drug Nanoparticle Formulation, Optimization, and Characterization	48
1. Nanoparticles were successfully formulated on a hydrophobic drug, ST1926	48
2. Nanoparticle formulation challenges for Sal A, Sal A-1, and Sal A-2	49
3. Nanoparticles were successfully formulated and characterized for Sal B.....	50
C. Anti-cancer Activities of Drugs and Nanoparticle Formulations.....	53
1. Sal B and derivatives reveal increased potency in human colorectal and breast cancer cells with different p53 status compared to Sal A.....	53

2. Sal A and Sal B are relatively non-cytotoxic to normal <i>versus</i> tumor cells	59
3. Nanoparticles show a similar cytotoxicity profile as native drug	63
4. Screening Sal A, B, A-2 on prevalent solid and liquid tumor cells	65
5. ST1926 nanoparticles have comparable anti-tumor activities to native drug in <i>in vitro</i> human colorectal and cancer models	72
6. Sal B nanoparticles have comparable anti-cancer activities to native drug <i>in vitro</i>	74
7. Native Sal B and Sal B nanoparticles-treated cells accumulate in the S phase of the cell cycle	78
8. Native Sal B and Sal B nanoparticles-treated cells show differential regulation of <i>p53</i> and <i>p21</i> proteins	79
9. Native Sal B and Sal B nanoparticles induce apoptosis in treated tumor cells	80
 IV. DISCUSSION	 82
 REFERENCES	 90

ILLUSTRATIONS

Figure		Page
1.	(A) Chemical structure of four major subclasses of sesquiterpene lactones (B) Chemical structure of functional group: α -methylene- γ -lactone ring	7
2.	(A) Parthenolide chemical structure (B) Dimethylaminoparthenolide (DMAPT) chemical structure	8
3.	<i>Centaurea ainetensis</i> (photos courtesy of the AUB NCC)	10
4.	Chemical structure of the sesquiterpene lactone Salograviolide A	10
5.	Illustration of enhanced permeability and retention effect.....	20
6.	Flash NanoPrecipitation Process	21
7.	Acid-Base extraction procedure to fractionate the methanolic crude extract of the aerial parts of <i>Centaurea ainetensis</i>	27
8.	Preparative chromatogram of the <i>Centaurea ainetensis</i> extract for purification of Sal A and the new sesquiterpene lactone Sal B.....	39
9.	Structures of Sal A, Sal B, and their synthesized derivatives.....	44
10.	Calibration curve of Sal A obtained by HPLC.....	45
11.	Calibration curve of Sal B obtained by HPLC.....	46
12.	Sample chromatogram of Sal A obtained by HPLC.....	46
13.	Sample chromatogram of Sal B obtained by HPLC.....	46
14.	Comparisons of Sal A solubility measurements obtained in each trial for H ₂ O and 10% THF.....	47
15.	Number-based Particle Size Distribution as attained by Dynamic Light Scattering at time 0 and 24 h.....	49
16.	Number-based particle size distribution for Sal B-NP stabilized with PS1.5-PEO2.4 as determined by DLS.....	51
17.	SEM images taken of Sal B Nanoparticles.....	52
18.	The effect of Sal A on the growth of colorectal and breast cancer cells.....	54

19.	The effect of Sal B on the growth of colorectal and breast cancer cells.....	55
20.	The effect of Sal A-1 on the growth of colorectal and breast cancer cells.....	56
21.	The effect of Sal A-2 on the growth of colorectal and breast cancer cells.....	57
22.	The effect of Sal B-1 on the growth of colorectal and breast cancer cells.....	58
23.	The normal-like colorectal cell line NCM460 was treated with (A) Sal A and derivatives (B) Sal A-1 and (C) Sal A-2 for 6 hours and the cytotoxic activity was determined by the lactate dehydrogenase assay as described in Materials and Methods.....	60
24.	The normal-like colorectal cell line NCM460 was treated with A) Sal B and B) Sal B-1 for 6 hours and the cytotoxic activity was determined by the lactate dehydrogenase assay as described in Materials and Methods.....	61
25.	The normal-like breast cell line MCF10A was treated with (A) Sal A, (B) Sal B and (C) Sal A-2 for 6 hours and the cytotoxic activity was determined by the lactate dehydrogenase assay as described in Materials and Methods.....	62
26.	Sal B and Sal B nanoparticles are relatively non-cytotoxic to HCT-116 cells.....	63
27.	Sal B and Sal B nanoparticles are relatively non-cytotoxic to MCF-7 cells.....	64
28.	The effect of Sal A on the growth of A) lung A549, B) prostate DU-145, and C) prostate PC-3 cells.....	66
29.	The effect of Sal B on the growth of A) lung A549, B) prostate DU-145, and C) prostate PC-3 cells	67
30.	The effect of Sal A-2 on the growth of A) lung A549, B) prostate DU-145, and C) prostate PC-3 cells	68
31.	The effect of Sal A on the growth of human hematological tumor cell lines.....	69
32.	The effect of Sal B on the growth of human hematological tumor cell lines.....	70
33.	The effect of Sal A-2 on the growth of human hematological tumor cell lines.....	71

34.	ST1926 and its nanoparticle formulation inhibit colorectal cancer cell growth independently of <i>p53</i>	73
35.	Sal B and its nanoparticle formulation inhibit colorectal cancer cell line HCT-116 cell growth.....	74
36.	Sal B and its nanoparticle formulation inhibit breast cancer cell line MCF-7 cell growth.....	75
37.	Sal B and its nanoparticle formulation affect the confluency and morphology of treated HCT-116 cells.....	76”
38.	Sal B and its nanoparticle formulation affect the confluency and morphology of treated MCF-7 cells.....	77
39.	Sal B and its nanoparticle formulation treatment of HCT-116 cells induces S phase accumulation in the cell cycle.....	78
40.	Sal B and Sal B-NP treatment of HCT-116 cells leads to differential upregulation of <i>p53</i> and <i>p21</i> proteins.....	79
41.	Sal B and Sal B-NP treatment of HCT-116 cells induces apoptosis as shown by PARP cleavage.....	80
42.	Sal B and its nanoparticle formulation induce apoptosis in HCT-116 cells 24 hours post-treatment.....	80
43.	Sal B and its nanoparticle formulation induce apoptosis in HCT-116 cells 48 hours post-treatment.....	81

TABLES

Table	Page
1. Groups of plant secondary metabolites	5
2. Description of tested human cancer cell lines	33
3. ¹ H-NMR spectral data for Sal A and Sal B (300 MHz, CDCl ₃ , and J, in Hz)	41
4. ¹³ C-NMR spectral data for Sal A and Sal B (300 MHz, CDCl ₃)	42
5. Table shows experimentally determined Sal A and Sal B aqueous solubility and calculated Log P values for Sal A, Sal B, and corresponding derivatives.....	48
6. Trials for nanoparticle formulation of Sal B	50
7. IC ₅₀ values of Sal A, Sal B, and derivatives for inhibition of tumor cell growth at 24 hours post-treatment.....	59
8. IC ₅₀ values of Sal A, Sal B, and Sal A2 for inhibition of solid tumor cell growth at 24 hours post-treatment	72
9. IC ₅₀ values of Sal A, Sal B, and Sal A-2 for inhibition of hematological tumor cell growth at 24 hours post-treatment	72
10. Effect of Sal B and Sal B nanoparticle treatment at 5 µg/ml for 48 hours on the cell cycle distribution of colorectal cancer cells.....	79

ABBREVIATIONS

α	Alpha
β	Beta
κ	Kappa
%	Percent
/	Per
:	Ratio
\pm	Plus or minus
$^{\circ}\text{C}$	Degree Celsius
μg	Microgram
μM	Micromolar
μm	Micrometer
ACN	Acetonitrile
BD	Brownian dynamics
CH_2Cl_2	Dichloromethane
CHCl_3	Chloroform
CO_2	Carbon dioxide
CTF	Confined tangential flow
d	Sphere diameter
DLS	Dynamic light scattering
DMAPT	Dimethylaminoparthenolide
DMEM	Dulbecco's minimal essential medium
DMSO	Dimethyl sulfoxide

DNA	Deoxyribonucleic acid
dUTP	2'-Deoxyuridine 5'-Triphosphate
EDTA	Ethylenediaminetetraacetic acid
EGCG	(-)-epigallocatechin-3-O-gallate
EGF	Epidermal growth factor
ELISA	Enzyme linked immunosorbant assay
EPR	Enhanced permeability and retention
EtOAc	Ethyl Acetate
FBS	Fetal bovine serum
FDA	Food and Drug Administration
fGn	Carboxyl-functionalized nanographene
FNP	Flash NanoPrecipitation
g	Gram
GAPDH	Glyceraldehyde 3-phosphate dehydrogenase
GC	Gas Chromatography
GSH	Glutathione
HCl	Hydrogen chloride
H ₂ O	Water
h	Hours
HPLC	High performance liquid chromatography
I κ B	Inhibitor of NF- κ B
IKK	Inhibitor of NF- κ B kinase
kDa	Kilodalton
LDH	Lactate dehydrogenase

mAb	Monoclonal antibody
MeOH	Methanol
mg	Milligram
min	Minute
ml	Milliliter
mM	Millimolar
MS	Mass Spectrometer
NCC	Nature Conservation Center
NCI	National Cancer Institute
NF- κ B	Nuclear factor kappa B
nm	Nanometer
nM	Nanomolar
NP	Nanoparticles
NMR	Nuclear magnetic resonance
PARP	Poly (ADP-ribose) polymerase
PBS	Phosphate buffered saline
PDI	Polydispersity index
PEG	Polyethylene glycol
PEO	Polyethylene oxide
PI	Propidium iodide
Prep-HPLC	Preparative high performance liquid chromatography
PS	Polystyrene
PSM	Plant secondary metabolites
ROS	Reactive oxygen species

rpm	Rounds per minute
RPMI	Roswell Park Memorial Institute medium
Sal A	Salograviolide A
Sal B	Salograviolide B
SCC	Squamous cell carcinoma
SD	Standard deviation
SDS	Sodium dodecyl sulfate
SE	Standard error
SEM	Scanning electron microscopy
SL	Sesquiterpene lactone
SPE	Solid phase extraction
Smac	Second mitochondria activator of caspases
T	Temperature
t	Time
TDT	Terminal Deoxynucleotidyl Transferase
TEMED	N,N,N',N'-Tetramethylethylenediamine
TG	Thapsigargin
THF	Tetrahydrofuran
TNF	Tumor necrosis factor
TUNEL	TDT-Mediated dUTP Nick-End Labeling
UV	Ultraviolet
V	Volts
WHO	World Health Organization

CHAPTER I

INTRODUCTION

A. Medicinal Plants and Cancer

Throughout history, humans have used natural products derived from plants for healing and wellbeing. The modern use of botanical medicines has historical roots in ancient medicine [1]. Since the beginning of humankind, phytotherapy has been pervasive across cultures and civilizations, and even today more than three-quarters of the world's population rely upon medicinal plants for health care. In many developed countries, 70% to 80% of the population has used some form of alternative or complementary medicine, where herbal medicine is ranked as the most popular form of traditional medicine and the most lucrative in the international marketplace, according to the World Health Organization (WHO).

Medicinal herbs such as Ginkgo, St. John's Wort, and Saw palmetto are gaining popularity. St. John's Wort in particular is more commonly used than any chemical medicine to treat mild to moderate depression. Today the impact of journals publishing data on medicinal plants is increasing. Additionally, there is a rising trend to include phytotherapy in the curriculum of medical schools in North America and Europe. Even here at the American University of Beirut (AUB), a new Master's Degree program in Complementary and Alternative Medicine (CAM) and graduate programs in herbal medicine will be launched soon.

In addition to the use of plants in their crude form in medicine, they have been the main source of chemical drugs. The initial spark that started the use of plant products and traditional remedies in the pharmaceutical industry was in 1897, when

Friedrich Bayer and Co. introduced synthetic acetyl salicylic acid (aspirin) to the world. Aspirin is a safer synthetic analogue of salicylic acid, which is the active ingredient of willow bark used as a remedy for aches and fevers [2].

Today, the search for plants exhibiting anti-cancer properties in particular, has been witnessing renewed attention [3, 4]. With the increase in cancer incidence and cancer holding steadfast as one of the major causes of death worldwide, there has been an increased interest in screening for anti-tumor agents from diverse sources including plants. This initiative began with the National Cancer Institute's launch of a large scale screening of 35,000 sample plants in 1960, which led to the discovery of the best-selling anti-cancer drug today, Taxol[®] [5, 6]. This breakthrough has boosted cancer researchers all over the world and especially those in regions of high diversity to explore the indigenous plants' active ingredients efficacy against cancer. Lebanon, with its high floristic diversity, is a prime location for this research endeavor. In Lebanon, there are over 2,600 plant species identified [7], where more than a hundred are reported to have medicinal properties [8].

Plant-derived medicine shows great promise. Today at least 25% of pharmaceuticals are plant-derived, and at least 75% have some plant-derived active ingredients [9]. For the period of 1981-2006, it was estimated that 47% of the 81 anti-cancer agents approved for use in the USA are derived from natural products [10, 11]. In fact, phytochemicals can act at any of the stages of carcinogenesis, namely tumor initiation, promotion, and progression. Agents that prevent initiation include such cancer blocking agents as ellagic acid, indole-3-carbinol, sulphoraphane, and flavonoids [12]. On the other hand, cancer-suppressing agents block the promotion stage or the progression stage. These include β -carotene, curcumin, epigallocatechin gallate,

genistein, resveratrol, gingerol, and capsaicin [12]. Many of these cancer-suppressing phytochemicals elicit their effect by acting on abnormally activated or silenced signaling molecules responsible for the activation of genes that regulate cell growth, differentiation, and cell death.

There is no doubt that recent advances in cancer therapies have increased the average lifespan of the cancer patient. However, with the WHO estimating that by 2030, there will be over 26 million cancer cases annually (World Cancer Report 2008, WHO) the need for novel anti-cancer agents persists. In investigating the anti-cancer properties of indigenous medicinal plants, the ultimate goal would be to identify the bioactive molecules responsible for their effects. Additionally, in order to facilitate the cancer drug discovery and developments, we need to consider new strategies such as biotechnology approaches to aid in obtaining more effective or lead compounds from the natural sources [13].

B. Plant Secondary Metabolites

Two centuries of modern chemistry and biology have described the role of primary metabolites in fundamental life functions such as cell division and growth, respiration, storage, and reproduction. It was not until 1891 that the concept of secondary metabolites was first introduced. Kossel was said to be the first to distinguish these metabolites from the primary ones [14]. Thirty years later, Czapek describes “endprodukts” in his plant biochemistry studies, suggesting that these compounds could derive from nitrogen metabolism by what he called “secondary modifications” such as deamination [15].

Ever since, studies on plant secondary metabolites (PSMs) have been increasing. Recently, following the advances in analytical techniques such as chromatography in the mid-twentieth century, a large quantity of new chemical molecules has become available from plant tissues which led the establishment of the discipline of phytochemistry. While in 1950 there were some 5000 or so characterized secondary plant products, now this figure is well over 100,000 [16]. From these discoveries, it has been shown that medicinal plants offer a wide range of these phytochemicals that are beneficial to human health and have been attributed to PSMs.

1. Definition

Among the thousands of plant metabolites that exist, PSMs serve as the largest group, whereas only a few are classified as “primary” [17]. PSMs, commonly known as phytochemicals, are plant components that usually have no nutritional value [18]. Compared to plant primary metabolites, PSMs are defined by their low abundance, constituting 1-3% of the plants’ dry weight, and are initially synthesized in specialized cells and organs, such as the flowers, roots or stems, at specific developmental stages [19].

PSMs contribute largely to plant fitness by interacting with the ecosystems in order to help ensure the survival and successful reproduction of plants. Their primary role is supporting the plants’ defense mechanisms against environmental threats such as microbes, fungi, viruses, herbivores and competing plants, as well as functioning as signaling compounds in pollination and seed dispersal [20]. Additionally, they constitute important ultraviolet (UV) absorbing compounds, thus preventing serious leaf damage from the light [21]. These molecules, besides playing a major role in the

adaptation of plants to their environment, also represent an important and diverse source of active pharmaceuticals.

2. Classification

PSMs are even taxonomically distinct, unlike the primary metabolites, namely lipids, proteins, nucleic acids, carbohydrates, and chlorophyll, which exist in all plants because they are involved in key metabolic processes that provide the building blocks for biosynthesis [22]. Four large molecule families are generally considered: acetogenins, alkaloids, phenolics, and terpenoids (Table 1). A good example of a widespread metabolite family is given by phenolics as these molecules are involved in lignin synthesis, making them common to all higher plants. However, other compounds such as alkaloids are sparsely distributed in the plant kingdom and are much more specific to defined plant genus and species.

Table 1. Groups of plant secondary metabolites

PSM subgroup	Chemical Structure	Drug Examples	Reference
Acetogenins	Long-chain aliphatic compounds with over 35 carbon atoms, ending with a γ -lactone	Asimicin Bullatacine	[23]
Alkaloids	Cyclic, nitrogen-containing metabolites derived from amino-acids	Narcotic analgesic morphine, codeine for treating coughs and the anti-cancer mitotic inhibitor drugs vincristine, vinblastine and colchicine	[24]
Phenols	Aromatic organic compounds with the molecular formula C_6H_5OH	Resveratrol Curcumin Cyanidine-3-glucoside (-)-Epigallocatechin-3-O-gallate	[25] [26] [27] [28, 29]
Terpenoid	Polymers of 5-C units (isoprene)	Paclitaxel	[30]

Terpenoids constitute the largest group of PSMs. They are found in important oils (mono-and-sesquiterpenes), resins (diterpenes and triterpenes), carotenoids (tetraterpenes), polyterpenes, perfumes (aromatic terpenes), turpentine, and saponins. In fact, the most widely used anti-cancer drug today, Taxol (Paclitaxel) from the Pacific Yew tree is classified as a terpene. Terpenoids can be further classified into monoterpenes (C10), sesquiterpenes (C15), diterpenes (C20), triterpenes (C30), and carotenoids (C40). Since we are particularly interested in studying the anti-cancer effect of sesquiterpenes, this will be described further in the next section.

3. *Sesquiterpene Lactones*

Sesquiterpene lactones (SLs) are PSMs that belong almost exclusively to the *Compositae (Asteraceae)* family [31, 32], and SL-rich plants commonly used in folk medicine [33]. These metabolites are colorless and bitter and constitute a stable family of terpenoids. Sesquiterpene lactones can be divided into four main groups (Figure 1A): 1) germacranolides (with a 10-member ring), including some common SLs such as costunolide and parthenolide; 2) eudesmanolides (6/6-bicyclic compounds), including santamarine and α -santonine; 3) guaianolides, including 3- β -methoxy-iso-seco-tanapartholide and Salograviolide (Sal A), the latter on which we are focusing our anti-tumor studies in this project and 4) pseudoguaianolides (both 5/7-bicyclic compounds), including helenalin and parthenin [31]. The suffix “olide” indicates the presence of a lactone group, and the biological activity of SLs is believed to be attributed to the presence of the α -methylene- γ -lactone ring (Figure 1B) [23]. This is because such structural elements tend to react with nucleophiles, particularly cysteine sulfhydryl groups through the Michael-type reaction. Hence, it is accepted that thiol groups such

as cysteine residues found in proteins, in addition to any free intracellular glutathione (GSH), pose as major targets of SLs. Consequently, this leads to the disruption of the crucial redox reactions that take place in the cell [34-36].

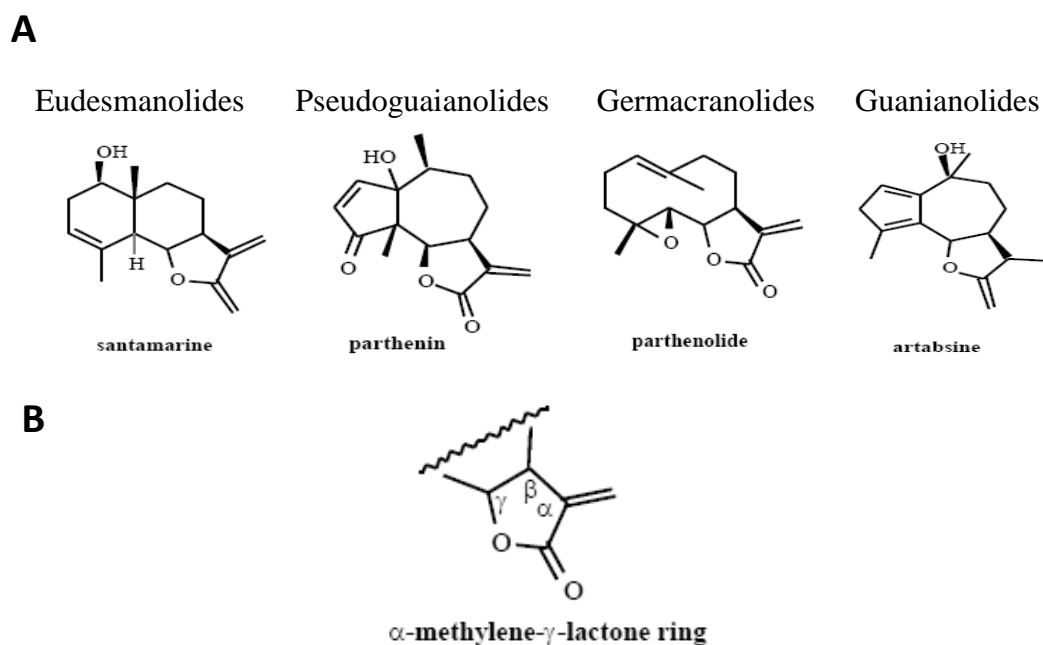


Figure 1. Chemical structure of four major subclasses of sesquiterpene lactones (1A). Chemical structure of functional group: α -methylene- γ -lactone ring (1B).

Source: Zhang, S *et al.* 2005. Anti-cancer Potential of Sesquiterpene Lactones: Bioactivity and Molecular Mechanisms. *Curr. Med. Chem. Anti-cancer Agents* 5: 239-249.

Plant extracts rich in SLs have gained considerable interest in treating human diseases such as cancer, inflammation, headaches, and infections [23, 31]. SLs possess a broad range of anti-tumor activities due to the reactivity of their alkylating centers, lipophilicity, and molecular geometry [37]. Moreover, several sesquiterpene lactones-derived drugs have been tested in cancer clinical trials as they are specific towards tumor and cancer stem cells, targeting specific signaling pathways. Such drugs include artemisinin, thapsigargin, and parthenolide [37].

Parthenolide (Figure 2A) is the major SL responsible for the bioactivity of feverfew (*Tanacetum parthenium*), a traditional herbal plant which has been used for the treatment of fever, migraine, and arthritis for centuries [38]. Parthenolide was shown to potently modulate proapoptotic activities in cancer cells and to inhibit NF- κ B-mediated antiapoptotic gene transcription and to stimulate the intrinsic apoptotic pathway [38]. It was determined through structure-activity studies that the α -methylene- γ -lactone moiety in parthenolide appears to be a critical functionality for its cytotoxic effect [39]. Parthenolide is a small molecule that has been reported to selectively target cancer stem cells (CSCs) while sparing normal counterparts; and was tested in clinical trials of several hematological cancers [37].

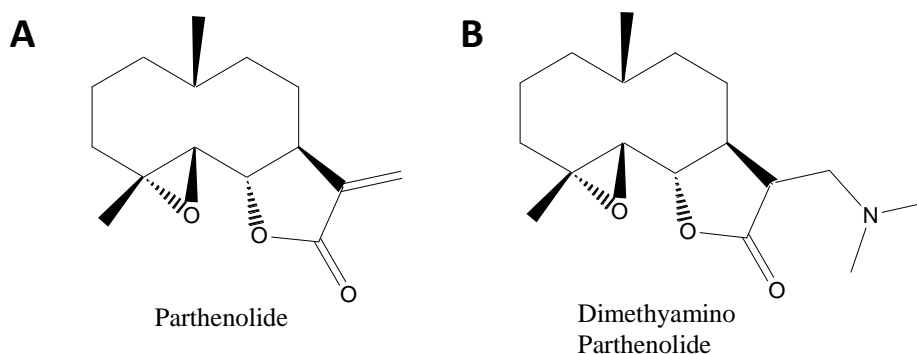


Figure 2. Parthenolide (A) and dimethylaminoparthenolide (DMAPT) (B) chemical structures

Despite the promising *in vitro* activities of parthenolide, this potent natural product exhibits poor water solubility *in vivo* [40]. Through functionalization of the exocyclic C-11 double bond of parthenolide, a diverse series of aminoparthenolide analogs have been derived from various arylalkyl, heteroarylalkyl, and alkyl amines [41]. The analogue Dimethylaminoparthenolide (DMAPT) (Figure 2B) was selected as a lead compound, based on favorable pharmacokinetic and pharmacodynamic

properties, and was tested in Phase I clinical trials against hematologic malignancies [41].

The potential of indigenous plants rich in SLs as “drug candidates”, in addition to the lack of information that exists about them in the region, highlights the importance of their identification, conservation, and sustainable use for drug discovery. Studies from the Nature Conservation Center (NCC) at AUB, identified and characterized a promising SL isolated from the Lebanese indigenous plant: Sal A from *Centaurea ainetensis* [42-46]. The promising anti-tumor properties of this SL are described in the Results chapter.

C. The Indigenous Lebanese Medicinal Plant *Centaurea ainetensis*

The genus *Centaurea* is one of the largest genera of the *Asteraceae* family, and consists of about five hundred species distributed in the Mediterranean and West Asia regions [47]. Interestingly the genus’ name is a dedication to the Greek mythological centaur Chiron, who is said to have used the flower to heal wounds, including his own, after battle. Indeed, the medicinal potential of these plants lives up to the name; plant extracts from this genus have shown to have antioxidant, antimicrobial, anti-tumor, and anti-inflammatory properties [33, 48, 49]. Furthermore, SLs isolated from the *Centaurea* genus have shown to possess growth inhibitory effects against lymphoma, breast, and lung cancer cells [50, 51].

The species *Centaurea ainetensis*, also known by its Arabic names Qanturyun Aynata or Shawk al-dardar, is indigenous to Lebanon [7] and is often used in folk medicine. Flowering from May to June, these plants have purplish tubes of anthers. Plants are grown in the Bekaa and mountainous regions of Lebanon, at high altitudes of

about 1600 m. They have been shown to exhibit anti-inflammatory [45, 46], as well as anti-cancer properties in colorectal and skin cancer cells [42, 44], in addition to reducing the number of adenomas in a mouse colorectal cancer model [42].



Figure 3. *Centaurea ainetensis* (photos courtesy of the AUB NCC)

D. Anti-tumor Activities of Salograviolide A

The purified bioactive SL, Sal A (Figure 4) from *Centaurea ainetensis* was isolated and reported to show potent anti-cancer activities in colorectal [42] and epidermal tumor cells [44], inducing apoptosis in both cell types, in addition to modulating NF- κ B signaling [44]. In this project, we have investigated the effect of Sal A against colorectal, breast, lung, prostate, and leukemic cell lines for the first time, as presented in the Results chapter.

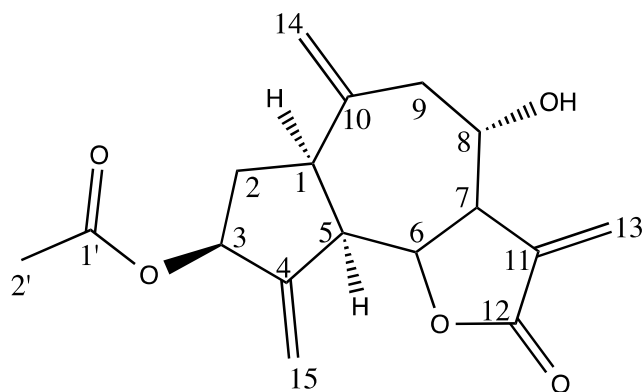


Figure 4. Chemical structure of the sesquiterpene lactone Salograviolide A
Source: Ghantous, A., Tayyoun, A., Abou Lteif, G., Saliba, N.A., Muhtasib, H.G, El-Sabban, M. and Darwiche, N.. 2008. Purified Salograviolide A isolated from *Centaurea ainetensis* causes growth inhibition and apoptosis in neoplastic epidermal cells. *International Journal of Oncology*. 32.841-849

The anti-tumor properties of Sal A have been further characterized using other human and murine *in vitro* models of cancers. In particular, Sal A increased pre-G₁ population and induced apoptosis in treated tumor cells [44]. Moreover, Sal A increased Bax/Bcl-2 ratio, p21 protein levels, and reduced cyclin D₁ protein expression. In colorectal and epidermal neoplastic cells, Sal A increased p16 protein levels and generated reactive oxygen species (ROS) [44]. It was demonstrated that ROS accumulation directly mediates Sal A-induced growth inhibition and cell death in colorectal and skin cancer cells suggesting that this molecule is a potent oxidant [42, 44]. Sal A, at concentrations not cytotoxic to normal keratinocytes, was shown to have promising chemopreventive activities, inhibiting anchorage-independent growth, thus cellular transformation in epidermal tumor cells [43]. These data support further investigation of Sal A and its derivatives, in the therapy of colorectal, skin, and other types of cancer.

E. Breast Cancer

Breast cancer is the most common cancer diagnosed among women in the United States, accounting for nearly 1 in 3 cancers, and it is also the second leading cause of cancer death among women after lung cancer [52]. It is not known when in the lifetime of a woman that initiation of breast cancer takes place, or whether a specific agent causes it. It is suggested that the period between menarche, or the first occurrence of menstruation, and first full-term pregnancy represents a window of high susceptibility for the initiation of breast cancer [53]. The public health problem of breast cancer necessitates the development of therapeutics against this neoplasm. We studied the anti-tumor properties of Sal A and its derivatives on representative early and late stage human breast cancer cell lines.

F. Colorectal Cancer

Colorectal cancer occurs in stages following a molecular evolution that manifests into histological changes. The *in situ* carcinoma starts as a polyp that enlarges and becomes more dysplastic, which is then followed by early invasive cancer, which precedes metastatic disease; a process that is estimated to take roughly five years. Colorectal cancer is one of the most common visceral malignancies, making it the third most common cause of cancer death in the United States [52]. In Lebanon, it is the second most frequently diagnosed cancer in women and the fourth most frequent cancer in men; with a yearly incidence of about 12 cases per 100,000 individuals [54]. Both genetic and environmental risk factors contribute to the risk of colorectal cancer. However, since the tumor tends to be diagnosed in its late stages and given the relatively low success of treatment strategies to reduce mortality, it is essential to adopt

an alternate approach to treat and/or reduce the risk of this deadly disease. There is compelling evidence from epidemiological and experimental studies that highlight the importance of compounds derived from plants to reduce the risk of colorectal cancer.

G. *In Vitro* Human Model Systems for Assessing Anti-tumor Activity

1. *Breast Cell Lines:*

- MCF-10A: MCF-10A is a spontaneously immortalized, but nontransformed human mammary epithelial cell line. It is derived from the breast tissue of a 36-year-old patient with fibrocystic changes. These cells exhibit the various features of normal breast epithelium, including the paucity of tumorigenicity in nude mice, lack of anchorage-independent growth, and dependence on growth factors and hormones for proliferation and survival [55]. Notably, MCF-10A cells express wild-type p53 [56, 57].
- MCF-7: MCF-7 is a breast adenocarcinoma cell line isolated in 1970 from a 69-year-old Caucasian woman. MCF-7 is the acronym of Michigan Cancer Foundation-7, which is the institute in Detroit where the cell line was established [58]. In fact, prior to MCF-7, it was not possible for cancer researchers to obtain a mammary cell line that was capable of living longer than a few months. MCF-7 cells have become the source of much of our current knowledge about breast cancer [58, 59].
- MDA-MB-231: Together with MCF-7 and T-47D (another breast cancer cell line), MDA-MB-231 account for more than two-thirds of all abstracts reporting studies on mentioned breast cancer cell lines, as concluded from a Medline-based survey [60]. MDA-MB-231 is a mammary gland epithelial cell line

derived from a metastatic site of an adenocarcinoma. It was taken from a 51-year-old female. This cell line is triple negative for estrogen receptor, progesterone receptor, and HER-2/Neu [61].

2. Colorectal Cell Lines:

- NCM460: Normal colorectal mucosa (NCM) is a nontransfected human colorectal epithelial cell line, originally derived from the normal colorectal mucosa of a 68-year-old Hispanic male, who underwent a partial gastrectomy. The margins of surgical resection extended into the transverse colorectal, which was designated as normal by the histopathologist and used as the tissue source for the NCM460 primary culture [62].
- HCT-116: HCT-116 is a colorectal carcinoma cell line taken from an adult male. In addition to HCT-116 (which is wild-type for p53), HCT-116 p53^{-/-} was also used. This cell line was originally created by homologous recombination by Bunz and colleagues [63].

Other types of cells of the most common types of cancer were also used to screen the drugs investigated (see Results).

H. Treatment of Colorectal and Breast Carcinogenesis by Botanical Agents: A Step Towards Clinical Drug Development

Plants have been a prime source of highly effective conventional drugs for the treatment of many forms of cancer. Though some actual compounds isolated from the plant frequently may not serve as drugs, they provide leads for the development of potential novel agents. In fact, more than 67% of the anti-cancer drugs today are natural

compounds or their derivatives, making the use of natural drugs or botanical agents in cancer therapy seem promising [64-66].

When it comes to cancer chemotherapy, natural products are often very potent but often have a setback: they have limited solubility in aqueous solvents and exhibit narrow therapeutic indices. This has led to the failure of a number of pure natural products, such as the plant-derived agent, maytansine [64]. Maytansine, isolated from the Ethiopian plant, *Maytenus serrata* in the early 1970s, exhibited extreme potency in testing against cancer models but the promising activity in preclinical testing did not translate into significant efficacy in clinical trials, and it was dropped from further study in the early 1980s. Recently, however, a derivative of maytansine, DM1, conjugated with a monoclonal antibody (mAb) targeting small cell lung cancer cells, was developed as huN901-DM1 for the treatment of small-cell lung cancer, and another conjugate of DM1 to J591, a mAb targeting the prostate specific membrane antigen (PSMA), is in clinical trials against prostate cancer. Other conjugates such as cantuzumab mertansine, produced by the coupling of DM1 to huC242, a mAb is directed against the muc1 epitope expressed in a range of cancers, including pancreatic, biliary, colorectal, and gastric cancers, is currently in Phase I clinical trials in the USA. The case of maytansine illustrates how the emergence of novel technologies can revive interest in these “old” agents. Notably, the development of effective drugs such as paclitaxel (Taxol[®]) and the camptothecin derivatives, topotecan and irinotecan required 20-30 years of dedicated research and patience, and considerable resources, to ultimately prove their efficacy as clinical agents [64].

Another interesting case is that of thapsigargin (TG), a compound isolated from the umbelliferous plant *Thapsia garganica*. TG has been shown to induce apoptosis in

quiescent and proliferating prostate cancer cells, but it does not show selectivity for prostate cancer cells. By conjugating TG to a small peptide carrier, a water-soluble prodrug has been produced that is able to target metastatic prostate cancer sites where prostate specific antigen (PSA) protease is overexpressed [64]. *In vivo* studies demonstrated complete tumor growth inhibition without significant toxicity, showing promise as a treatment for human prostate cancer. Therefore, by attaching agents to carrier molecules that are tumor-specific, effectively targeting highly cytotoxic natural products to the tumors while preventing cytotoxic side effects becomes possible.

Thus, molecularly targeted therapies represent the promise of a new paradigm in oncology [67, 68]. Since cancer is a heterogenous disease that is characterized by multiple genetic and epigenetic defects leading to dysregulation of processes controlling cell growth and survival, this disease certainly has a plethora of viable targets. With the strategy of developing agents that potently target only one or a few endogenous biomolecules, toxicity can be reduced [69]. Successful strategies can lead to positive implications in drug development and clinical application, allowing for a well resolved gap between efficacy and toxicity that is often problematic in research and development.

I. The Rationale for Drug Derivatization

As we have shown, Sal A has promising anti-cancer and anti-inflammatory properties. Today, there is an increased interest in synthesizing drugs with enhanced specificity and bioavailability without compromising the desirable inhibitory activities of the natural compound, and without depleting its natural resources. While Sal A is a SL with one active site, the α -methylene- γ -lactone moiety, it has been shown that SLs

with more than one active site show higher bioactivity and increased cytotoxicity *in vitro* [37]. Therefore, it was of interest to derivatize Sal A in a way to increase the number of active sites in this compound using routine organic chemistry synthesis protocols.

The α -methylene- γ -lactone moiety is a characteristic component of a large number of natural products that possess a wide range of biological activities, including anti-cancer. The structural requirement of the α -methylene- γ -lactone for achieving its cytotoxic and anti-inflammatory effects has been proposed to be the conjugated $O=C-C=CH_2$. In reference to the guaianolide Sal A, whose biological activities are summarized in earlier sections, its cytotoxicity can be attributed to the α -methylene- γ -lactone moiety. Considering the fact that: i) Sal A does not show cytotoxicity to normal cells relative to tumor cells at low concentrations, ii) possesses biological activities as was presented above, and iii) possesses a rigid molecular geometry that may show selectivity to specific proteins, through derivatization we are able to further investigate types of derivatives that maintain the unsaturated γ -lactone and those that do not keep this functional group.

In the case of SL parthenolide, for example, Kwok and colleagues showed that *in vitro* and *in vivo* anti-inflammatory activities of the compound were mediated through the α -methylene- γ lactone moiety [70]. Parthenolide binds inhibitor of nuclear factor kappa-B kinase subunit beta (IKK β), forming the IKK β :parthenolide protein adduct. Subsequently, parthenolide inhibits both TNF α -induced NF- κ B DNA binding activity and NF κ B-mediated transcription in HeLa cells. However, its reduced counterpart fails to show any of the prior activities [70].

Another goal of derivatization is to synthesize derivatives to enhance the drug's solubility and pharmacokinetic profile. Some synthesized derivatives have successfully reached clinical trials after overcoming solubility limitations [71, 72]. With its hydrophobic nature and low polarity, Sal A necessitates novel formulation of the bioactive molecule in order to improve its solubility and pharmacokinetic profile. To our knowledge, the derivatization of Sal A, solubility, and supersaturation levels are reported for the first time and will lead to a good knowledge of the most potent derivative bioavailability.

J. Enhancing Drug Delivery: Nanotechnology

1. Definition of Nanotechnology

“Nanotechnology” is the manipulation and control of nanoscale objects (one billionth of a meter). There are great benefits to being able to engineer at the scale of individual macromolecules, as discussed in the next section, and this holds true especially in medicine [73]. By building tiny molecular-scale devices capable of delivering drugs targeted to areas of disease has numerous benefits [74, 75]. Allowing for specific targeting, nanoparticles have emerged as great tools for efficient drug delivery because they are designed to target treatment selectively and specifically. Not only does this increase drug efficacy and bioavailability, but it can also reduce side effects [75]. Because of this, these tiny constructs have been extensively studied over the last decade. When designing nanoparticles as carriers of drugs, multifunctionality is easily manipulated and taken advantage of in order to engineer the drug to target a specific pharmacological site under particular physiological conditions. This has helped

with creating many cancer drugs currently in the market, with many other drugs targeted towards other diseases currently under research and development [74].

Key parameters of polymeric nanoparticle design need to be considered in order to make a successful formulation [76]. These factors include the size of the particle, polydispersity, surface properties, and shape. The chemical functionalities of the polymer affect essentially all aspects of nanoparticle performance, including the efficiency of drug encapsulation, the rate of polymer degradation and drug release, and toxicity at the injection site.

2. Advantages to Using Nanotechnology

Nanoparticle-based formulations of drugs offer several advantages, including improved bioavailability and drug targeting. In parenteral applications, nanoparticles can be used to modify the drug surface in order to optimize its residence time *in vivo* following injection. In cancer applications, where tumor vasculature is considered leaky, nanoparticles can be used to target tumor tissues *in vivo*, and concentrate the drug within the target site, thereby enhancing efficacy and reducing toxicity [77]. This enhanced accumulation at the tumor site is an effect known as the Enhanced permeability and retention (EPR) effect (Figure 12) and is a form of passive targeting (*versus* active targeting in which attachment of biochemical moieties facilitate delivery to unique tissues expressing specific biomarkers distinguishing it from surrounding healthy tissue) [78, 79]. Thus, poorly aligned endothelial cells in the fast growing tumor vasculature with fenestrations larger than 100 nm in size, and reduced lymphatic drainage in tumor tissue result in preferred accumulation of nanocarriers in these tissues over healthy tissue. The combination of reduced toxicity and enhanced efficacy greatly

improves the therapeutic window of the drug and is a main driver for the development of nanomedicines [80, 81].

In fact, the well-known anti-cancer therapeutic, paclitaxel, has been formulated as nanoparticles with enhanced cytotoxicity *in vitro* and enhanced therapeutic efficacy *in vivo* [82]. Interestingly, this nanoparticle formulation of paclitaxel is albumin bound, using the nanotech platform of albumin as an alternative to Cremophor, a toxic solvent in which water-insoluble paclitaxel was dissolved, thus enhancing the vehicle of administration. Marketed as Abraxane, it is approved to be used in the clinic against metastatic breast cancer [83].

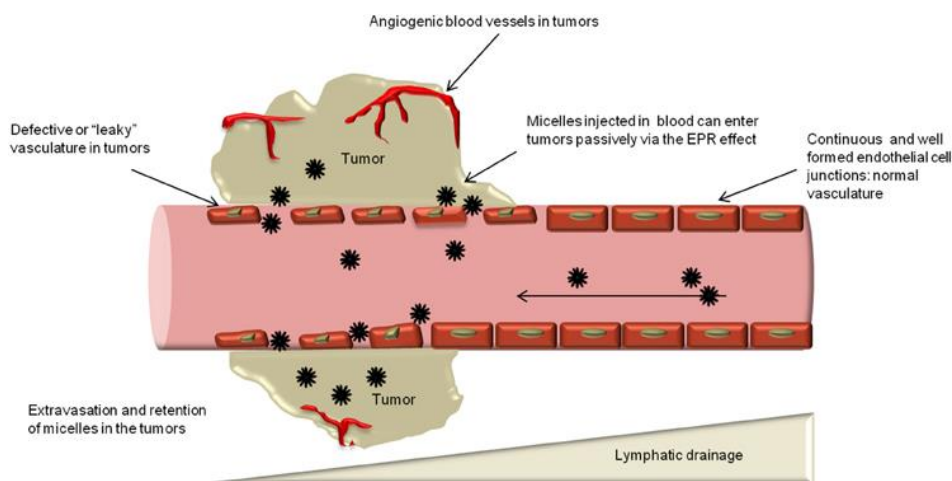


Figure 5. Illustration of enhanced permeability and retention effect. Nanoscale particles may penetrate leaky tumor vasculature and accumulate in diseased tissue. If the nanoparticle is a drug carrier for a chemotherapeutic, that chemotherapeutic may be more efficacious than in its free form due to the high concentrations of the carrier-bound particles which build up in the tumor.

Source: Jhaveri, A.M. and V.P. Torchilin, *Multifunctional polymeric micelles for delivery of drugs and siRNA*. *Frontiers in Pharmacology*, 2014. 5.

Another advantage of nanoparticle-based formulations of hydrophobic drugs is enhanced solubility. A large proportion of pharmaceuticals currently under development are based on drugs that suffer from low solubility and poor bioavailability [84]. It is estimated that 40% of new chemical entities in drug development are water

insoluble [85]. Thus an approach to overcome these limitations is the use of nanoparticle-based formulations where the hydrophobic drug is formulated as a suspension of controlled-size particles. Nanoparticles consisting of a hydrophobic core and a hydrophilic shell can solubilize hydrophobic agents in their core. Nanoparticles can enhance the dissolution rates in oral drug delivery applications by virtue of increasing the drug's surface area through particle size reduction. Hydrophobic drugs formulated as nanoparticles of ten to a few hundred nanometers and stabilized with polymeric or other surfactants at the surface (also termed nanosuspensions) become suitable for oral and parenteral administration [86].

3. Flash NanoPrecipitation

Flash NanoPrecipitation (FNP) is a newly developed experimental technique for producing polymer-protected nanoparticles with narrow size distributions through self-assembly. It provides high active loading efficiencies and drug loading contents [87]. Experimentalists have successfully used this process to produce different types of nanoparticles in the laboratory, such as nanoparticle formulations of the cancer drug paclitaxel resulting in improved *in vivo* efficacy compared with conventional formulations of the same drug [88]. In order to produce drug-loaded nanoparticles using FNP, the hydrophobic drug and stabilizing polymer are dissolved in a water-miscible organic solvent. The obtained solution is mixed through a confined tangential flow (CTF) mixer with a stream of water, at a high Reynolds number (>1600), causing precipitation of the drug, and simultaneous particle surface stabilization by the polymer due to the supersaturation condition produced in the CTF mixing cell. An illustration of the process is shown in Figure 6.

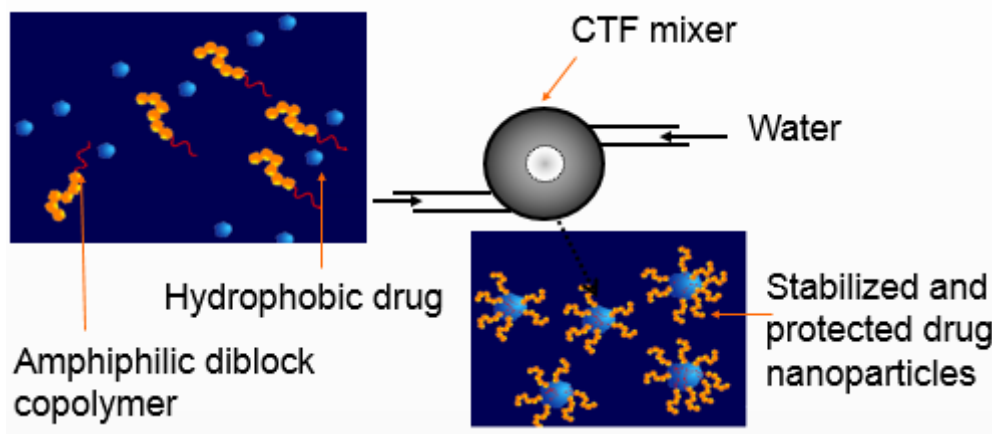


Figure 6. Flash NanoPrecipitation Process

In order to achieve surface stabilization in FNP, the polymers used are amphiphilic diblock copolymers, with one hydrophilic block and one hydrophobic block. Under conditions of supersaturation, these polymers form micelles and in the presence of a hydrophobic solute, the hydrophobic block adsorbs on the surface of the solute particles through hydrophobic interactions, while the hydrophilic block provides steric stabilization, resulting in stable nanoparticles. The hydrophilic block used is polyethylene glycol (PEG) of various molecular weights ranging from 2,000 to 10,000 g/mole. PEG has been shown to prolong the nanoparticles circulation time *in vivo*, which is crucial for the cancer application considered here. The hydrophobic blocks used include poly(ϵ -caprolactone), poly(lactide), and other biocompatible polymers. The hydrophobic block will be selected based on optimal nanoparticle formulation stability and will depend on the interaction of the Sal A derivative with the polymer, as well as the stability of the polymer following nanoparticle formation. The molecular weights of the hydrophobic block range typically from around 2,000 to 10,000 g/mole. The block molecular weight as well as the ratio of hydrophobic to hydrophilic blocks will dictate the surface coverage density of the particle, and will affect the nanoparticle

formulation stability. Therefore, the effect of polymer block molecular weight and ratio on the stability and the *in vitro* potency are explored for each Sal A derivative formulation.

4. *Nanomedicine and Sesquiterpene Lactones*

Nanomedicine, i.e. the application of nanotechnology in therapy is one of the fastest growing areas of nanotechnology [89, 90], and holds great promise for many therapeutics being developed today, especially in cancer therapies. In fact, the majority of preclinical research with nanoparticulate pharmaceutical drug delivery systems relates to cancer [91]. Encapsulating anti-cancer drugs into nanocarriers serves two purposes: 1) the body is protected against off-site toxicities, and 2) the drug is protected against the body's defense system.

Nanoparticles can play a role in the production of a smart herbal drug by addressing the problems that herbal drugs possess such as poor aqueous solubility, physical instability, low absorption, lower bioavailability and slow pharmacological actions [92]. To overcome these disadvantages, drug delivery system that contain nanocarriers have been developed [76]. In preclinical drug development, sesquiterpene lactone nanoparticle formulations are being pursued such as with parthenolide. In one recent study, carboxyl-functionalized nanographene (fGn) delivery of parthenolide was used to overcome the drug's extreme hydrophobicity [93]. Delivery by fGn was found to increase the anti-cancer/apoptotic effects of parthenolide when delivered to the human pancreatic cancer cell line, Panc-1.

Given that Sal A has potent anti-cancer effects in various solid and liquid tumors, makes it a very promising candidate for nanomedicine. By formulating

nanoparticles of Sal A, and its potentially more potent natural and synthetic derivatives, we would be able to enhance the drug's stability, bioavailability and accumulation at tumor sites *via* the EPR effect, in addition to protecting the native drug from exposure to catabolic enzymes.

K. Aim of Study

The general purpose of this project is to enhance the therapeutic properties of the SL Sal A, by synthesizing and optimizing potential derivatives with increased selectivity, specificity, bioavailability, and potency against cancer cells. Given the potential of nanotechnology in cancer therapeutics, we also aimed to establish parameters and techniques for optimal drug delivery using nanoparticle-based strategies to address any solubility limitations associated with Sal A and its derivatives, and to optimize drug bioavailability and drug efficacy in order to achieve a more clinically desirable product. The drugs were chemically characterized and the biological properties were tested for anti-tumor properties using well established biological assays on human *in vitro* tumor models. We therefore aimed to optimize these drugs for *in vivo* preclinical testing and eventually to clinical development. We undertook this study with the following specific aims.

1. Drug Extraction and Characterization

- a) Scale up the extraction and purification of Sal A from *Centaurea ainetensis* using a newly acquired preparative high performance liquid chromatography (prep-HPLC)
- b) Based on feedback from biological assays, determine the solubility and optimize the synthesis of the most potent derived structure (s)

2. Drug Nanoparticle Formulation, Optimization, and Characterization

- a) Formulate Sal A and its derivatives into nanoparticles using FNP
- b) Characterize the produced formulations: nanoparticle size, stability, and drug loading content
- c) Optimize the nanoparticle formulation efficacy through particle surface and particle size modification based on the biological assays results

3. Anti-cancer Activities of Drugs and Nanoparticle Formulations

- a) Assess the cytotoxicity effects of Sal A, derivatives, and corresponding nanoparticle formulations in *in vitro* human tumor models
- b) Characterize the anti-tumor activities of Sal A, derivatives, and corresponding nanoparticle formulations on cell growth and cell death

CHAPTER II

MATERIALS AND METHODS

A. Extraction, Purification, and Identification of Sal A from *Centaurea ainetensis*

1. Plant Material

The plant material of *Centaurea ainetensis* was collected from the Bcharre Cedars area in Lebanon at an altitude of 1330 m during the flowering stage in June 2012 and June 2013 by Mr. Khaled Sleem, AUB NCC. Voucher specimens were deposited in the herbarium of the Faculty of Agriculture and Food Sciences at the American University of Beirut (Beirut, Lebanon). The aerial parts were dried by leaving the plant sample in the shade for two weeks before grinding it into around 10 mm pieces using a blender.

2. Extraction and Purification

Extraction, purification and identification of the SLs were performed in the laboratory of Dr. Najat Saliba (Chemistry Department, American University of Beirut) as described in Figure 7. The aerial parts of *Centaurea ainetensis* (300 g) were soaked, separately, in 3 L methanol (MeOH) for 16 hours at room temperature. The crude methanolic extracts "I" were concentrated to 1/10 of their volumes and acidified to pH=2 with a sulfuric acid solution. This was followed by liquid-liquid extraction using a mixture of chloroform (CHCl₃): water (2:1 v/v) and the organic layer was collected and labeled as "I.2". The aqueous layer was then basified to pH 10 by adding concentrated ammonium hydroxide (NaOH) solution drop-wise and then suspended in CHCl₃: MeOH

mixture (3:1 v/v). It was later separated into organic and aqueous layers labeled “I.3” and “I.4”, respectively.

Only fraction I.2 which exhibited antiproliferative activity was further fractionated by column chromatography. Five grams of fraction I.2 was applied to a chromatographic column consisting of 400 g of silica gel (0.035-0.07 mm and 6 nm pore diameter). A gradient elution was performed to separate the molecules found in *Centaurea ainetensis*: Petroleum ether: CHCl₃: EtOAc (2:1:2), followed by petroleum ether: CHCl₃: EtOAc (2:2:1), CHCl₃: EtOAc: MeOH (3:3:1), CHCl₃: MeOH (3:2) and MeOH successively.

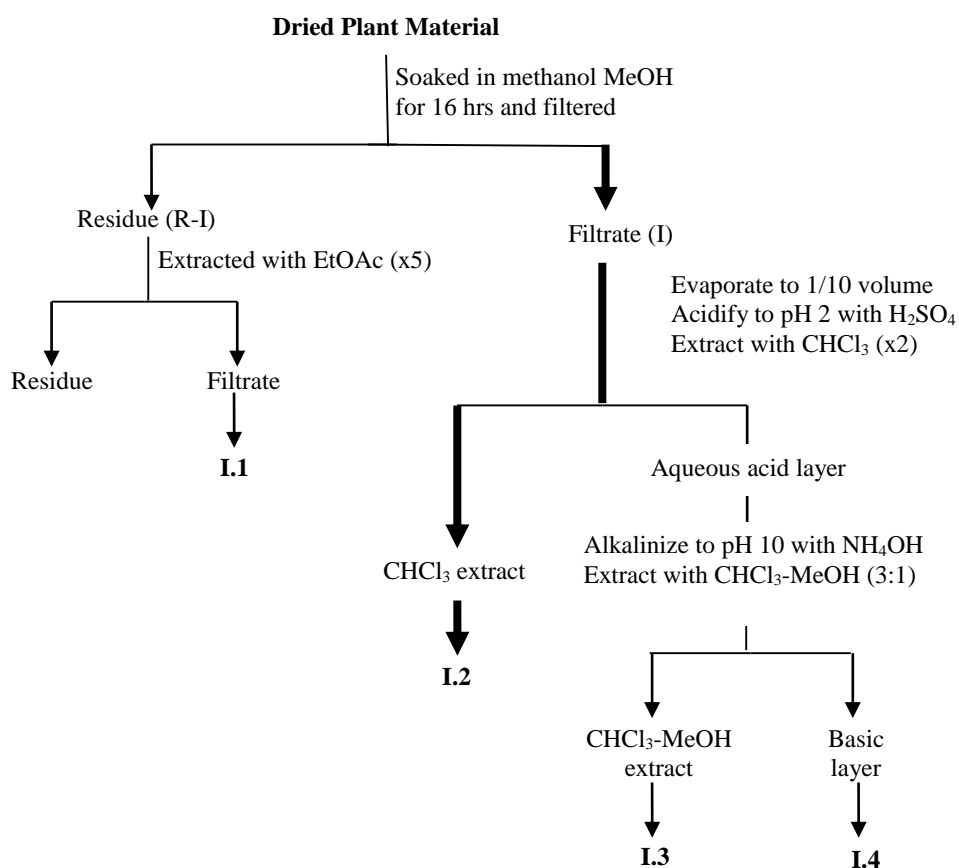


Figure 7. Acid-Base extraction procedure to fractionate the methanolic crude extract of the aerial parts of *Centaurea ainetensis*.

Source: Harborne, B. 1998. *Phytochemical Methods. A guide to modern techniques of plant analysis.* Third edition: Chapman and Hall.

3. Structure Elucidation

Structural elucidation of the bioactive components was performed using several spectroscopic techniques. A Nicolet AVATAR 360 FTIR spectrometer equipped with a KBr pellet cell holder. Spectrum was collected by averaging 128 scans at wave numbers ranging from 750 to 4000 cm^{-1} at a resolution of 1 cm^{-1} . NMR data were obtained using a Bruker 300 MHz spectrometer where TMS is used as an internal standard and deuterated chloroform (CDCl_3) as a solvent. Gas Chromatography- Mass Spectrometry (GC-MS) analysis was performed using a TraceTM gas chromatograph equipped with HP-5 capillary column (30 m long, 250 μm i.d, and 0.25 μm film thickness) and Helium as a carrier at a flow rate of 1ml/min. The maximum temperature was 350 °C. The column was heated from 35 °C to 290 °C. The injector temperature was set at 300 °C in a splitless mode. Results were recorded as percent of total peak areas. The mass spectrometer employed in the GC-MS analysis was a Polarization Q series mass selective detector in the electron impact (EI) ionization mode (70 eV).

B. Solubility Experiments

In order to quantify the supersaturation levels under the process conditions, determination of the solubility in water and in water: tetrahydrofuran (THF) (9:1 vol/vol) was pursued by adding an excess amount of Sal A or its derivatives to each solution which were subject to vortexing, sonication and shaking for at least 24 hours. The solutions were then centrifuged and the supernatants were filtered and analyzed by reverse-phase HPLC. The concentrations of the solutes were calculated against a prepared calibration curve based on known concentrations of solute.

C. High Performance Liquid Chromatography

The solute content of the nanoparticle formulations were quantified using analytical High Performance Liquid Chromatography (HPLC). HPLC is a chromatographic technique based on the partitioning of analytes between two phases, stationary phase and mobile phase. While the stationary phase remains immobilized in the column, the mobile phase flows through the column. When a mixture containing many components is introduced to this system, each analyte behaves in a characteristic way depending on its affinity for each phase. The analyte's affinity for either mobile or stationary phase will influence its retention time in the column. The goal, usually achieved during method development, is to find the optimum conditions such that analytes go through the column at speeds that allow for separation.

An isocratic elution was used with a C18 reverse phase column (250 x 4.6 mm i.d.; 5 μ m), using mobile phases (H₂O and acetonitrile (ACN)) and non-polar stationary phase (octadecyl, C18). The injection volume was 20 μ l for all samples. The gradient elution profile is 15 mins 40:60 (H₂O: ACN), 15 min 90:10 (H₂O: ACN), and 5 min of 100:0 (H₂O: ACN) and the flow rate is 1 ml/min. The wavelength of the mass spectrometry detector is set at 214 nm and 220 nm at room temperature (25°C).

The concentrations of the solutes were calculated against a calibration curve that was prepared using standard solutions as follows: a primary stock solution of pure Sal A or Sal B at a concentration of 1 mg/ml was prepared in HPLC grade ACN. Analytical standards of 2, 5, 10, 20, 50, 70, and 80 ppm were obtained by appropriate dilution of the stock solution in ACN.

Stock solution was 9 mg dissolved into 15 mL, making it 0.6 mg/mL or 600 ppm. Volumes from the stock solution were drawn to which water was added to make

up the diluted concentrations. The volumes were calculated as shown in the example below for 10 ppm dilution.

$$c_1v_1 = c_2v_2$$

$$\text{For 10 ppm: } 600 \text{ ppm} \times v_1 = 10 \text{ ppm} \times 2000 \text{ }\mu\text{L}$$

$$v_1 = 33.33 \text{ }\mu\text{L stock solution}$$

$$1,983.33 \text{ }\mu\text{L ACN added}$$

$$V_{\text{total}} = 2,000 \text{ }\mu\text{L}$$

All samples were filtered in 0.2 μm filters before processing.

To prepare nanoparticle formulations for analysis, 450 μL of THF was added to 50 μL sample, which was vortexed and left at room temperature for 20 minutes. The sample was filtered (0.2 μm filter) into an HPLC autosampler vial, and analyzed by HPLC.

D. Nanoparticle Formulation

We used FNP in order to formulate ST1926 (control hydrophobic drug), Sal A, Sal B, and their derivatives into nanoparticles. The FNP setup required for the production and characterization of nanoparticles is established in the laboratory of Dr. Walid Saad, Department of Chemical Engineering at the American University of Beirut. A confined impinging jet (CIJ) mixer was used in which streams of solution were mixed at high velocity in the small chamber to make an output of 1:9 tetrahydrofuran (THF):H₂O. Flow rates were controlled using Harvard apparatus PHD2000 syringe pumps.

Formulation stability was manipulated through the type and size of the block copolymers used. Since it has been shown that particle size affects uptake into

mammalian cells, particle size can be modified either by adjusting the initial drug concentrations or through the addition of molecules with low water solubility (e.g. tocopherols, or hydrophobic polymers such as polystyrene) that will be co-encapsulated with the drug. In case the latter is used for control of particle size, growth inhibitory activity of the hydrophobic moiety added is evaluated as a control.

E. Dynamic Light Scattering

The particle size was determined using dynamic light scattering (DLS) Brookhaven Instrument BI-200SM dynamic light scattering instrument (Brookhaven Instruments, BI-200SM, Stonybrook, NY) immediately following nanoparticle formation. The instrument was powered up at least 30 min in advance of measurements to allow the laser to stabilize. The apparatus consisted of a continuous laser (wavelength 532 nm), and photomultiplier with detection angle 90° with the pinhole window set at either 100, 200, or 400 μm setting to maintain the signal intensity at the detector between 10 and 150 kHz. The chamber temperature was maintained at 25 °C. Samples were left to equilibrate in the chamber for at least 5 min prior to taking a size measurement. Cuvette of diluted sample was placed in the sample holder and three measurements of three minutes each in duration were taken per sample. Number-weighted particle size distributions were calculated by the software and plotted.

F. Scanning Electron Microscopy

Scanning Electron Microscopy (SEM) was performed in order to further characterize nanoparticle formulations by visualizing surface morphology of the nanoparticle. 10 μL of sample was dried completely on carbon coated stub by freeze-

drying. Stub surface was coated with gold by ion sputter at 10 mA for 2 minutes.

Images were recorded at 15-25 kV with a working distance of 15 mm.

G. Nanoparticle concentration for HPLC analysis

In order to separate drug that has not been encapsulated from nanoparticles for HPLC drug quantification analysis, Amicon-2 Ultrafiltration-30K device was used as follows. Two mL solution was added to the assembled device. It was stabilized with paper towels in 50 mL tubes at the proper orientation. It was spun for 20 minutes at 3220 rcf (g) using a swinging bucket rotor centrifuge. Solvent collected in the lower tube was analyzed by DLS to ensure no nanoparticles went through. Nanoparticles collected on the filter were resuspended in diH₂O and analyzed.

H. Cell culture

The MDA-MB-231, HCT-116 p53^{-/-}, and A549 cell lines were cultured in DMEM containing 10 % heat-inactivated FBS, 1 % sodium pyruvate, 1 % penicillin-streptomycin, and 1 % kanamycin antibiotics. The MCF-7, HCT-116, DU145, PC3, LAMA, K562, HL60, NB4, Jurkat, and MOLT-4 cell lines were cultured in RPMI containing 10 % heat-inactivated FBS, 1 % sodium pyruvate, 1 % penicillin-streptomycin, and 1 % kanamycin antibiotics. NCM460 cell line was cultured in M3:10 media. MCF-10a was cultured in DMEM F12 with horse serum. Cells were grown at 37 °C, 95 % air, and 5 % CO₂. When about 80 % confluent, adherent cells were passaged 1:10 while leukemic cell lines were maintained at optimal densities.

Table 2. Description of tested human cancer cell lines

Cell Line	Characterization	p53 Status
Colorectal		
NCM 460	Normal-like colorectal cells	Wild-type
HCT-116	Colorectal carcinoma	Wild-type
HCT-116 p53 ^{-/-}	Colorectal carcinoma	Knockout
Breast		
MCF 10A	Normal-like mammary epithelial cells	Wild-type
MCF-7	Breast adenocarcinoma	Wild-type
MDA-MB-231	Triple negative breast adenocarcinoma	Mutated
Lung		
A549	Non-small cell lung carcinoma	Wild-type
Prostate		
PC-3	Prostate adenocarcinoma	Knockout
DU-145	Prostate adenocarcinoma	Mutated
Chronic Myeloid Leukemia		
LAMA	Chronic myeloid leukemia	Wild type
K562	Chronic myeloid leukemia	Mutated
T-cell Acute Lymphoblastic Leukemia		
MOLT4	T-cell acute lymphoblastic leukemia	Wild-type
JURKAT	T-cell acute lymphoblastic leukemia	Mutated
Acute Promyelocytic Leukemia		
NB4	Promyelocytic leukemia	Mutated
HL60	Promyelocytic leukemia	Mutated

I. Cytotoxicity and Cell Growth Assays

Drug cytotoxicity was assayed after 6 h of treatment using CytoTox 96[®] assay; whereas, cell viability was assayed from 24 h up to 72 h of treatment, using CellTiter 96[®] assay, according to manufacturer's instructions (Promega Corp., Madison, WI). Triton-X 100, with concentrations up to 1 % of cell culture media was used as positive control in CytoTox 96[®] assays. The CytoTox 96[®] assay quantitatively measures the

activity of lactate dehydrogenase (LDH), a stable cytosolic enzyme that is released upon cell lysis. Released LDH in culture supernatants is measured with a coupled enzymatic assay which results in the conversion of a tetrazolium salt into a red formazan product, the absorbance of which is recorded at 490 nm using an ELISA microplate reader. The cytotoxicities of the tested compounds are then normalized relative to the maximum toxicity of a Lysis Buffer and tabulated as the mean \pm standard deviation (SD) of at least three measurements per condition. Cytotoxicity results were reproduced in two independent experiments using concentrations up to 25 $\mu\text{g/ml}$. The CytoTox 96[®] assay, when performed for short time points, such as 6 h, allows testing for an acute drug effect which is typically manifested by cell bursting and LDH release. Lysed cells quantified at later time points, such as 24 h or later, of drug exposure do not necessarily result from an acute response as most types of cell death also eventually lead to cell lysis after prolonged exposure to a drug.

Viability was assayed using the CellTiter 96[®] non-radioactive cell proliferation assay kit. This assay is an MTT-based method which, instead of quantifying lysed cells, measures the ability of metabolically active cells to convert tetrazolium salt into a blue formazan product, the absorbance of which is recorded at 570 nm using an ELISA microplate reader. Viability results were expressed as percentage of control and plotted as the mean \pm standard error (SE). The percentage of ethanol or DMSO used in all the treatments or in the control did not exceed 0.1% and did not affect cell growth.

J. Cell Cycle Analysis

Cell cycle analysis was performed using the propidium iodide assay (PI). PI is a membrane impermeant dye that is generally excluded from viable cells. This agent binds to double stranded DNA by intercalating between base pairs. For cell cycle analysis cells are permeabilized so they can uptake the dye which binds to DNA, analyzed by flow cytometry. About 500,000 cells were treated with drug for 24 or 48 h, cells were trypsinized, washed with 1X PBS, fixed with ice-cold 80% ethanol, and stored at -20°C for up to ten days. Next, the cells were washed with 1X PBS, and then incubated with 50 units RNase A (Roche) dissolved in 1X PBS for one hour at room temperature. Subsequently, the cells were stained with PI (50 µg/ml) (Sigma). Cell cycle analysis was done using FACScan flow cytometer (Becton Dickinson). Results are expressed as percentages of elements detected in the different phases of the cell cycle, namely pre-G₀, G₀/G₁, S, and G₂/M.

K. TUNEL Assay

The TUNEL (TDT-Mediated dUTP Nick-End Labeling) assay kit by Roche was used to measure late apoptosis since it detects single- and double-DNA strand breaks. The free 3'-OH termini found at the DNA strand breaks can be conjugated to dUTP-fluorescein under the action of the enzyme deoxynucleotidyl transferase and fluorescence can be measured through a FACScan flow cytometer.

Cells were seeded at 500,000 cells per 100 mm cell culture dish and harvested at 24 or 48 hours post-treatment. At the indicated time point, the cells were collected, washed with 1% BSA in 1X PBS, and then fixed in 4% formaldehyde at room temperature for 30 minutes. Subsequently, the cells were washed with 1X PBS and

incubated with 100 μ L of permeabilization solution (Sodium citrate, Triton X, and 1X PBS) for 2 minutes on ice. Positive control cells were incubated with 8 μ L of DNase for 30 minutes at room temperature, and then washed with 1X PBS. Meanwhile, the cells of the other conditions were washed with 1X PBS. Subsequently, all samples were incubated with TUNEL reagents for 1 h at 37°C in the dark: 50 μ l labeling solution for the negative control, and 50 μ l of TUNEL reagents mixture for the remaining conditions. The TUNEL reagents mixture is composed of 45 μ l labeling solution and 5 μ l enzyme solution. Cells were then washed with 1X PBS, resuspended in 300 μ l of 1X PBS, transferred into polystyrene round bottom tubes (Falcon) and fluorescence was measured through FACScan flow cytometer.

L. Immunoblot Analysis

Total cellular protein extracts were prepared from cells, washed twice with PBS, and scraped into SDS-lysis buffer (0.25 M Tris-HCl, pH 6.8, 20% glycerol, 4% SDS, 0.002% bromophenol blue, 10% β -mercaptoethanol). Protein concentrations were determined using a DC protein Assay Kit (Bio-Rad Laboratories, Hercules, California, USA) according to manufacturer's protocol. Equal amounts of total cellular proteins (up to 50 μ g) were resolved by 10 % SDS-polyacrylamide gel electrophoresis (PAGE), transferred onto nitrocellulose membranes (Amersham, Arlington, IL), and then probed with primary antibodies against GAPDH, PARP-1, p53, and p21 followed by secondary antibodies conjugated with horseradish peroxidase. Equal protein loading and quality were verified through GAPDH reprobing and Ponceau staining of membranes. The immunocomplexes were visualized using enhanced chemiluminescent kits obtained from Santa Cruz (ECL system).

M. Statistical Analysis

Data presented are the means \pm SE of n assays as noted in the figure legends. SPSS version 18.0 and Microsoft Office Excel 2010 were used to calculate the statistical significance. Statistical significance is claimed when the p -value is less than 0.05.

CHAPTER III

RESULTS

A. Drug Extraction and Characterization

1. Extraction optimization and purification of Sal A from Centaurea ainetensis

Since separation and purification procedures, using solid phase extraction (SPE), offered many limitations in respect to time consumption, excessive use of solvents, and molecule losses due to the presence of several steps in the purification process, Dr. Najat A. Saliba's group (Chemistry Department, American University of Beirut) was able to optimize and scale up the extraction and purification of Sal A from *Centaurea ainetensis* using both, analytical and preparative HPLC. Analytical HPLC is used to optimize the separation and identification procedure of Sal A, while the preparative HPLC is best suited for sample collection with an adopted version of the analytical HPLC method.

The analytical method consists of an automatic thermostated column compartment housing a C18 reversed-phase column (250 x 4.6 mm i.d.; 5 µm). The injection volume was 20 µl. The mobile phase consisted of acetonitrile (A) and water (B). The gradient elution profile was 15 min 50:50 (A: B), 15 min 90:10 (A: B), and 5 min of 100:0 (A: B), the flow rate is of 1 ml/min. The wavelength of the mass spectrometry detector was set at 210 and 214 nm at room temperature. HPLC chromatogram showed two peaks believed to belong to the sesquiterpene lactone family; the first one was confirmed as Sal A by comparison to a pure compound and the

retention time was at 3.5 min, the second peak was identified as Sal B at a retention time of 4.5 min.

The preparative HPLC separation was performed by injecting 3000 μl of filtered organic extract onto a Gilson GX-271 Prep (150 x 50 mm i.d.; 10 μm) Reprisil 100 C18 column. The pre-column is a Reprisil 100 C18 column (150 x 50 mm i.d.; 10 μm). Elution was performed using Gilson model 333 pumps to deliver a constant flow rate of 20 mL/min. The solvent system consists of an isocratic elution of acetonitrile and water (50:50) for 100 min. A total of 14 fractions were collected and the purification yield results of the collected fractions numbered from 1 to 14 were calculated. Fractions 1 to 7 contained the purified Sal A peak, while fractions 8 to 14 contained the new sesquiterpene lactone compound defined as Sal B (see Figure 8). Sal A and Sal B compounds were detected by UV absorbance at 214 and 210 nm, respectively using ultraviolet detection (UV/VIS-156). Sal A was collected between 5 and 10 min. Applying this method resulted in 1.2 % yield of pure Sal A (an increase of 1.1 % over the conventional method).

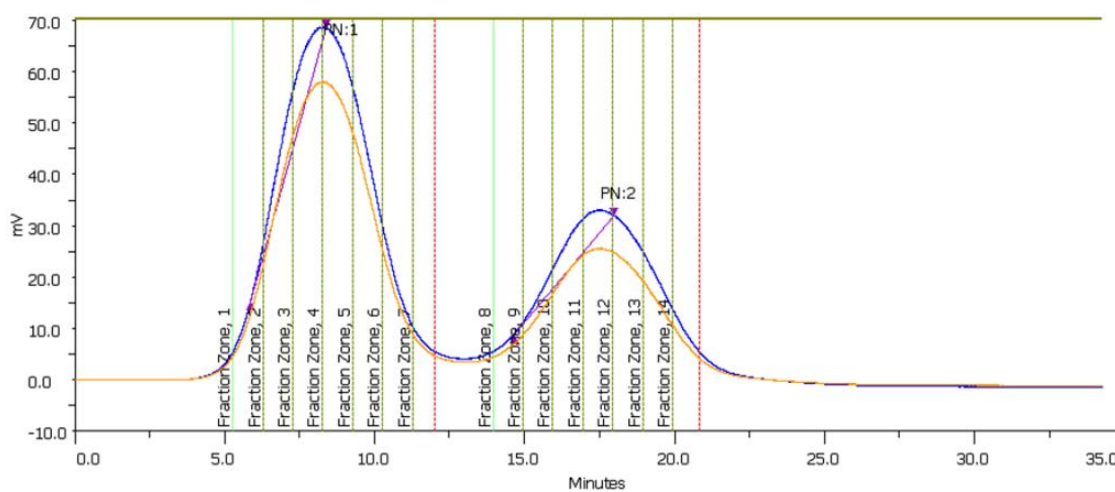


Figure 8. Preparative chromatogram of the *Centaurea ainetensis* extract for purification of Sal A and the new sesquiterpene lactone Sal B.

2. Spectroscopic measurements reveal the structures of Sal A and Sal B

The structure of Sal B was elucidated using FTIR, NMR, and GC-MS. Sal B has a molecular weight of 304 g/mol. ^1H and ^{13}C NMR spectroscopic analysis (Tables 1 and 2) showed the pronounced germinal coupling of the two olefinic proton signals at δ_{H} 6.28 (1H, d, $J = 3.4$ Hz) and 6.16 (1H, d, $J = 3$ Hz), and an unusually up field position of the proton in the trans position to the carbonyl group at C-11. These results indicated the presence of an α -OH at C-8. Furthermore, the ^{13}C NMR spectrum specified that the new sesquiterpene lactone compound contains four quaternary carbons, seven methyne, six methylene, and one methyl group. The molecular weight of the new compound suggests the presence of five oxygen atoms and one extra hydrogen atom. The ^{13}C NMR spectrum confirmed the presence of two carbonyl groups by exhibiting two carbon signals at δ 170.8 s and 169.6 s. The ester carbonyl belonged to an acetoxy group, as signals of acetyl methyl were present in both the ^{13}C (δ 21.3 q) and ^1H (δ 2.09 s) NMR spectra. The presence of the four remaining oxygen atoms was verified with three signals of secondary carbons bearing oxygens (δ 78.2 d, 51.7 d, and 74.6 d). Two of them belonged to the ester and the lactone and the remaining one was attached to hydroxyl group. The IR spectrum of this compound displayed the subsequent bands: hydrogen bonded OH at ν_{max} , 3503 cm^{-1} , lactonic carbonyl at ν_{max} , 1760 cm^{-1} , ester carbonyl at ν_{max} , 1731 cm^{-1} and C=C at ν_{max} , 1659 cm^{-1} . The suggested structure is represented in Figure 2.

All spectroscopic data were compared to the literature using Scifinder and was found to be identical to the guaianolide Sal B (3b-acetoxy-8a-hydroxy-1aH,5aH,6bH,7aH-guaia-4(15),10(14),11(13)trien-6,12-olide) or Kandavananolidide, already described for both *Centaurea* and *Cousinia* species [94-97].

A comparison between the spectroscopic ^1H and ^{13}C NMR data of Sal A and Sal B are shown in Tables 3 and 4. It is important to note that in Sal B, the normal shielding of the exomethylene protons 13a and 13b was attributed to the absence of a hydroxyl group at C-9. This was further validated by the additional CH_2 signal instead of a methyne group in the ^{13}C NMR spectrum of this molecule.

Table 3. ^1H -NMR spectral data for Sal A and Sal B (300 MHz, CDCl_3 , and J, in Hz)

H	Sal A	Sal B
1	2.92 m	3.03 ddd (11, 8, 8 Hz)
2 α	2.58 m	1.78 ddd (13.5, 11, 7.5 Hz)
2 β	1.85 ddd	2.36 ddd (13.5, 7.5, 7.5 Hz)
3	5.55 m	5.55 m (7.5, 7.5, 2.2 Hz)
5	2.92 m (9.48, 1.78, 3.78 Hz)	2.82 br dd (9.8 Hz)
6	3.93 dd (9.48, 9.37 Hz)	4.10 dd (10.5, 9 Hz)
7	2.97 ddd (9.37, 3.15, 10.38 Hz)	2.79 m (10.5, 9, 3.4, 3 Hz)
8	3.46 ddd (10.38, 8.06 Hz)	3.99 ddd (9.5, 4 Hz)
9 α	3.97 dd (8.06 Hz)	2.29 dd (14, 4 Hz)
9 β	-	2.67 dd (14, 5 Hz)
13a, 13b	6.40 dd (1.17, 3.15 Hz), 6.35 dd (1.17 Hz))	6.28 d (3.4 Hz), 6.16 d (3 Hz)
14a, 14b	5.50 d (0.88 Hz), 5.20 d (0.88 Hz)	5.12 br s, 5.00 br s
15a, 15b	5.47 t (1.78 Hz) 5.31 t (3.78 Hz)	5.52 br s (2 Hz), 5.33 br s (2 Hz)
2 x OH	3.59 m, 3.08 m	~ 4.00 br m
OAC	2.13 s	2.09 s

Table 4. ^{13}C -NMR spectral data for Sal A and Sal B (300 MHz, CDCl_3)

C	Sal A	Sal B
1	47.2 d	45.6 d
2	36.3 t	36.3 t
3	74.5 d	74.6 d
4	147.4 s	147.3 s
5	48.9 d	51.7 d
6	79.3 d	78.1 d
7	41.1 d	51.0 d
8	77.7 d	71.9 d
9	79.9 d	41.4 t
10	135.9 s	142.2 s
11	147.8 s	137.9 s
12	169.8 s	169.6 s
13	125.6 t	123.3 t
14	113.3 t	117.5 t
15	112.8 t	115.8 t
1'	170.7 q	170.8 s
2'	21.3 s	21.2 q

3. Sal A and Sal B derivatives were successfully synthesized and structurally elucidated

Our main purpose was to convert the biologically active compound Sal A into a more hydrophobic derivatives. In drug development, enhancing the drug's solubility and pharmacokinetic profile, as well as its efficacy, is crucial. A practical approach is through derivatization. From a chemical point of view, this can be achieved by altering the hydroxyl groups found on the structure of this compound by either their conversion to keto- or ester-groups. As for the oxidation, there are many methods for oxidizing a mono-hydroxyl group, however, in the case of Sal A the hydroxyl groups are found as a vicinal diol. Moreover, one of these hydroxyl groups is at an allylic position, and

therefore, we were limited by the available methods for such conversion. Three mild oxidation methods were attempted and unfortunately none gave the keto-form as expected, rather an opening of the carbocycle was seen. The three methods were: Swern oxidation (oxalyl chloride, dimethyl sulfoxide, at -78 °C), oxidation using the mild oxidant MnO₂ and finally using TEMPO.

Dr. Tarek Ghaddar's group (Chemistry Department, American University of Beirut) was able to successfully make derivatives of Sal A and Sal B by acylation to afford the three derivatives Sal A-1, Sal A-2 and Sal B-1 (Figure 9). ¹H NMR data is also shown below for the derivatives.

Sal A-1: ¹H NMR (500 MHz, CDCl₃): δ 6.22-6.25 (d, 1H, J= 3.6 Hz), 5.5-5.58 (m, 2H), 5.41-5.43 (t, 1H, J= 2.1Hz), 5.32 (s, 1H), 5.26-5.28 (t, 1H, J=2.1 Hz), 5.16 (s, 1H), 5.08-5.12 (m, 2H), 3.99-4.05 (t, 1H, J= 9.6Hz), 3.1-3.2 (m, 1H), 2.85-3.02(m, 2H), 2.48-2.57 (m, 1H), 2.08 (s, 3H), 2.05 (s, 3H), 2.01 (s, 3H), 1.75-1.81 (m, 1H).

Sal B-1: ¹H NMR (500 MHz, CDCl₃): δ 6.18-6.19 (d, 1H, J= 3.6 Hz), 5.57-5.58 (d, 1H, J= 3.6 Hz), 5.45-5.53 (m, 2H), 5.28-5.29 (t, 1H, J= 2.1Hz), 5.08 (s, 1H), 4.89-4.96 (m, 2H), 4.04-4.11 (t, 1H, J= 9.6Hz), 3.01-3.11 (m, 1H), 2.90-2.99(m, 1H), 2.73-2.8 (m, 1H), 2.57-2.64 (dd, 1H, J₁=14.7, J₂=5.4), 2.09 (s, 3H), 2.03 (s, 3H), 1.68-1.74 (m, 1H).

Sal A-2: ¹H NMR (300 MHz, CDCl₃): δ 6.22-6.25 (d, 1H, J= 3.6 Hz), 5.52-5.58 (m, 2H), 5.41-5.43 (t, 1H, J= 2.1Hz), 5.29 (s, 1H), 5.26-5.28 (t, 1H, J=2.1 Hz), 5.08-5.2 (m, 3H), 4.01-4.07 (t, 1H, J= 9.6Hz), 3.1-3.2 (m, 1H), 2.99-3.05 (m, 1H), 2.86-2.93 (m, 1H), 2.48-2.57 (m, 3H), 2.05 (s, 3H), 1.75-1.82 (m, 1H), 1.06-1.15 (m, 12H).

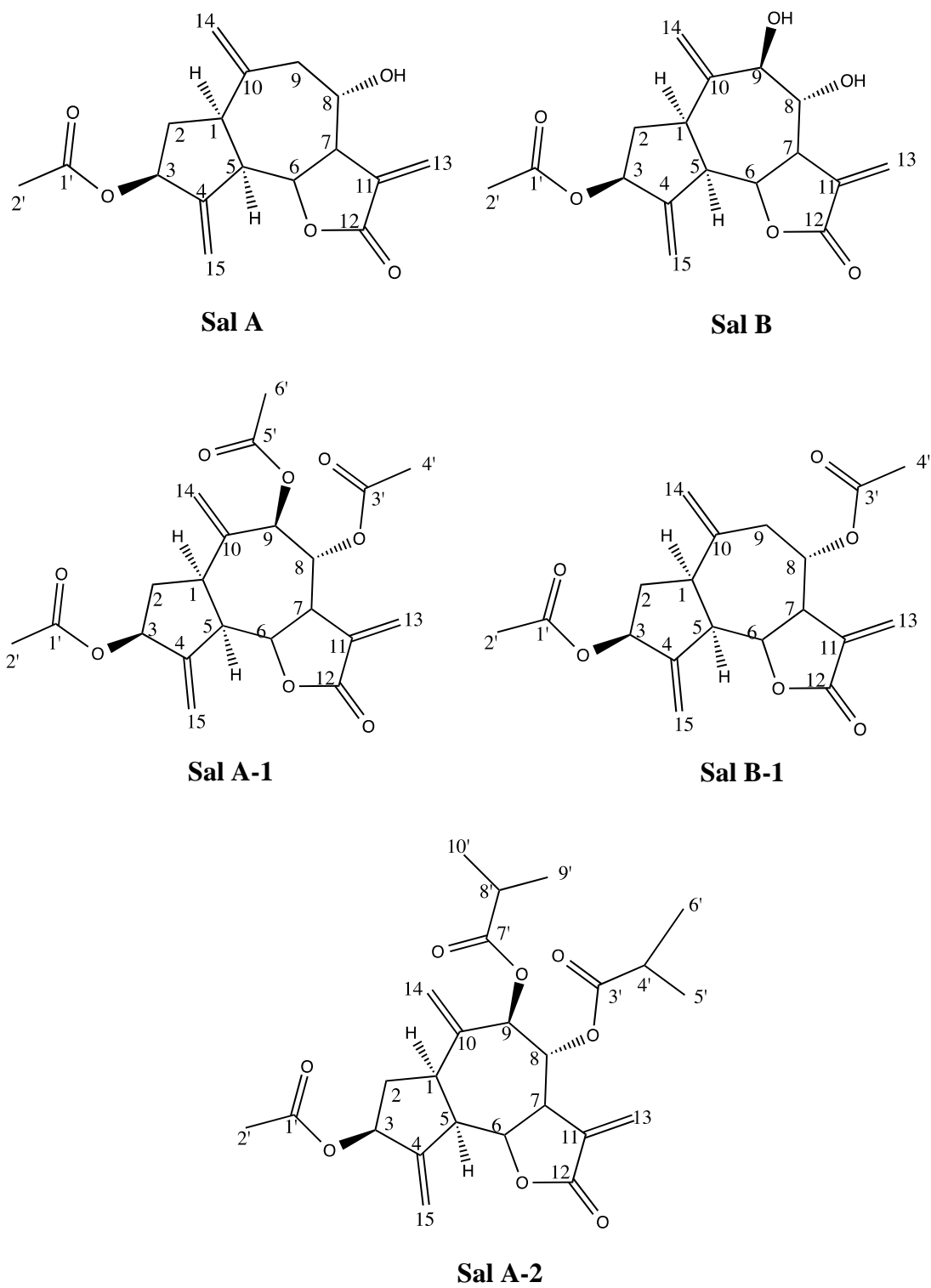


Figure 9. Structures of Sal A, Sal B, and their synthesized derivatives.

4. Sal B and derivatives were found to be more hydrophobic than Sal A

The aqueous solubility of Sal A and Sal B are reported here for the first time. Quantifying the solubility of Sal A and Sal B helps in guiding nanoparticle formulation development with FNP, a technology that relies on high supersaturation levels to induce controlled precipitation and stabilization of nanoparticles.

We developed an experimental method to determine solubility. Sal A and Sal B were dissolved in excess in a) water and b) 10% THF. Mixtures were subjected to vortexing, sonication, and shaking *via* mechanical shaker for 24 hours at room temperature. Finally, samples were centrifuged and filtered prior to analyzing the supernatant by HPLC as described above. Sal A and Sal B concentrations were computed using a calibration curve developed for method specific for each compound (See Figures 10 and 11). Sample chromatograms are shown in Figures 12 and 13. A comparison of solubility measurements of Sal A from three trials is shown in Figure 14. Measurements show precision, and also illustrate that our compounds are more soluble in organic solvents than in aqueous solvents (Figure 14).

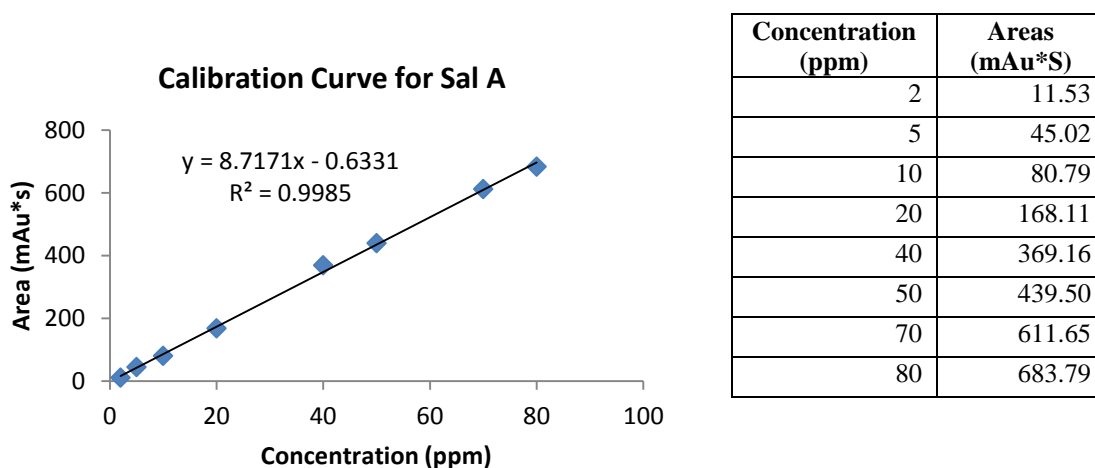


Figure 10. Calibration curve of Sal A obtained by HPLC.

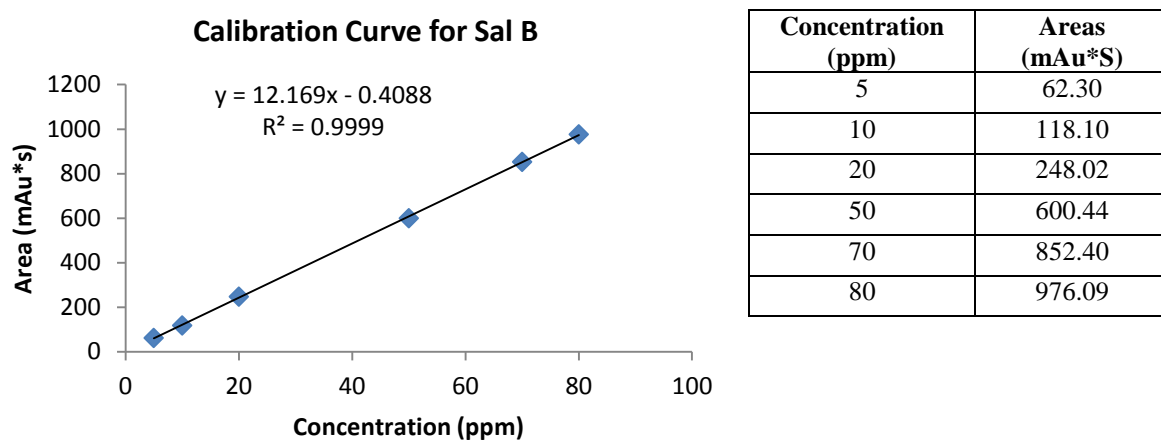


Figure 11. Calibration curve of Sal B obtained by HPLC.

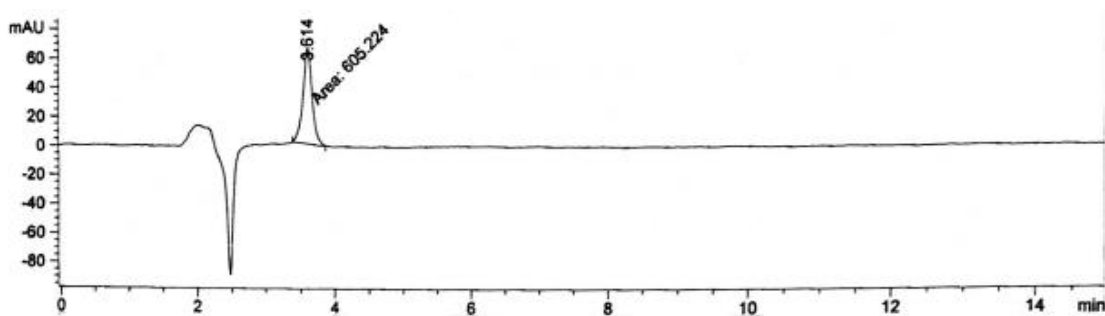


Figure 12. Sample chromatogram of Sal A obtained by HPLC.

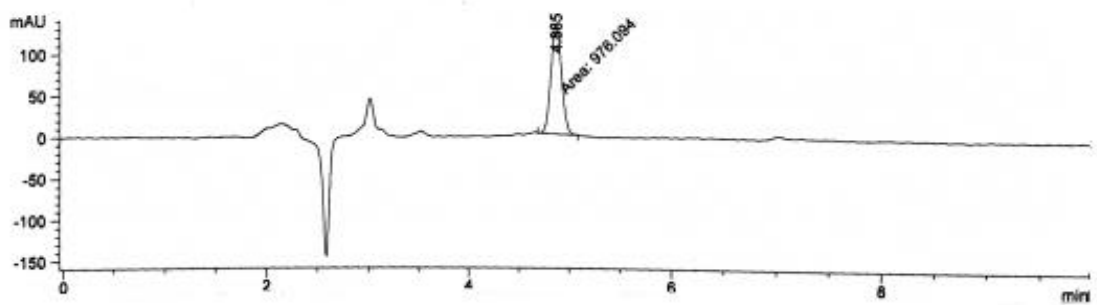


Figure 13. Sample chromatogram of Sal B obtained by HPLC.

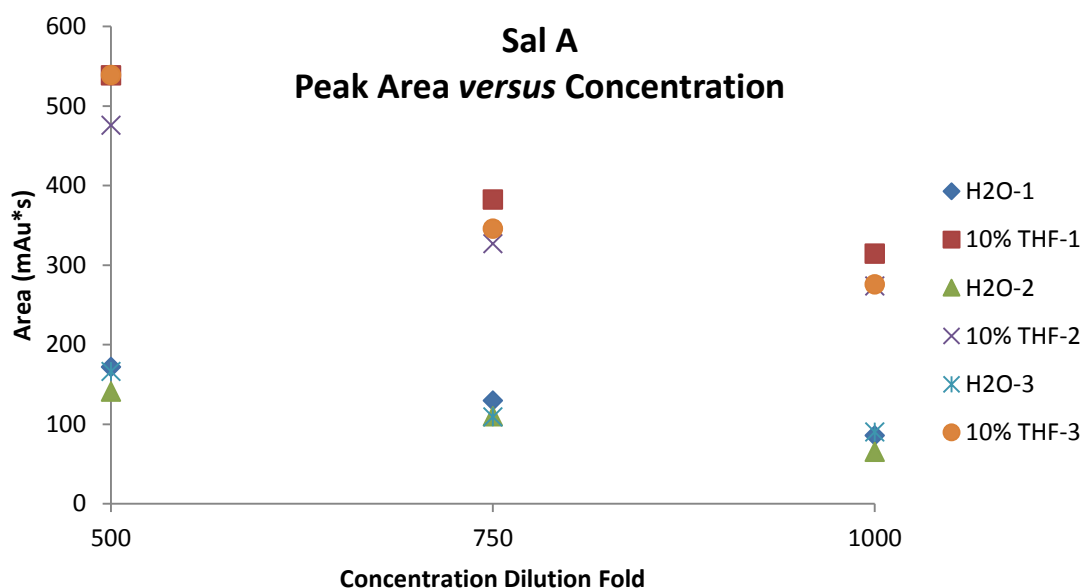


Figure 14. Comparisons of Sal A solubility measurements obtained in each trial for H₂O and 10% Tetrahydrofuran.

As an indicator of the extent of solubility levels of newly synthesized derivatives, Log P values were determined. Log P is an indicator of lipophilicity, where P is the octanol/water partition coefficient. Log P is a measure of how hydrophobic a compound is (the higher the number, the more hydrophobic). Additionally, this can be a useful tool for estimating the drug's distribution in the body as well as its biological activity. Hydrophobic drugs with high octanol/water partition coefficients are more readily distributed to hydrophobic compartments such as the lipid bilayers of cells, enhancing entry into the cells. Log P values, which are displayed for Sal A, Sal B, and the derivatives in Table 5, were obtained using ChemAxon, a data mining software.

Table 5. Table shows experimentally determined Sal A and Sal B aqueous solubility and calculated Log P values for Sal A, Sal B, and corresponding derivatives

Compound	Measured Solubility in Water	Predicted LogP value
Sal A	10.35 mg/mL	0.79
Sal B	1.06 mg/mL	1.71
Sal A-1	*	1.68
Sal A-2	*	4.16
Sal B-1	*	2.15

* indicates “not determined”

B. Drug Nanoparticle Formulation, Optimization, and Characterization

1. Nanoparticles were successfully formulated on a hydrophobic drug, ST1926

Prior to testing the FNP method on our SLs, due to limited amounts, we used a highly hydrophobic adamantyl retinoid, ST1926 ((2E)-3-[30-(1-adamantyl)-40-hydroxy[1,10-biphenyl]-4-yl]-2-propenoic acid), as a control for successful formulation. ST1926 was formulated into nanoparticles with a drug to polymer mass ratio of 1:5. 5 mg of ST1926 and 25 mg of polystyrene-b-poly(ethylene oxide) block copolymer (PS1.5-PEO2.4) with a polystyrene hydrophobic block size of 1,500 g/mole, and a poly(ethylene oxide) block size of 2,400 g/mole (Polymer Source) were dissolved in 3 mL of tetrahydrofuran (THF). The resulting solution was mixed at 12 ml/min with water at 108 ml/min using the CTF mixer. This nanoparticle suspension was collected at the mixer outlet and the particle size determined using dynamic light scattering (DLS) immediately following nanoparticle formation and following 24 hours of storage at room temperature (Figure 15). The initial particle size was 230 nm, and remained unchanged for over 48 hours of storage at room temperature.

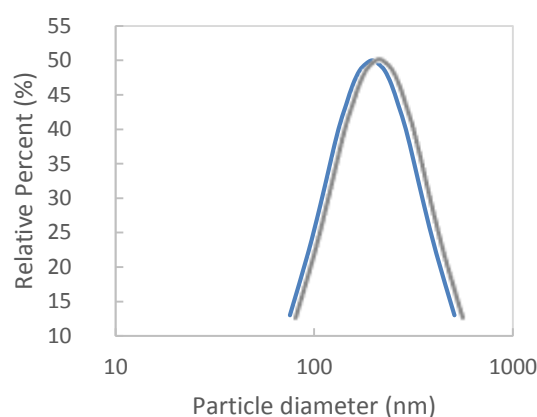


Figure 15. Number-based Particle Size Distribution as attained by Dynamic Light Scattering at time 0 and 24 h. The mean ST1926 nanoparticle was 230 nm, and remained stable in room temperature beyond 24 hours.

2. Nanoparticle formulation challenges for Sal A, Sal A-1, and Sal A-2

FNP relies on imposing high supersaturation conditions of the drug and a stabilizing amphiphilic block copolymer to produce controlled size nanoparticles. Supersaturation is achieved using solvent/non-solvent mixing under controlled conditions. In the case of Sal A, the supersaturation achieved through solvent/non-solvent mixing were not sufficient for stable particle formation. Further development of Sal A nanoparticle formulations was placed on hold to accommodate Sal B nanoparticles (Sal B-NP) formulation development. Focus shifted to Sal B-NP development due to favorable in vitro results demonstrated through the cytotoxicity and MTT assays discussed in the Cancer section of the results.

Sal A-1 and A-2 derivatives were also investigated for their nanoparticle formation via FNP with limited success. Although both derivatives exhibit lower water solubility than Sal A, which allows for higher supersaturation levels, both suspensions showed fast aggregation/crystallization within ten minutes of mixing using FNP. This behavior is attributed to the higher solubility of smaller particles in the resulting

solvent/non-solvent mixture. While this issue can be resolved via drug conjugation, our efforts will focus next on our lead compound, Sal B, which is investigated further below.

3. Nanoparticles were successfully formulated and characterized for Sal B

Sal B-NP were optimally prepared in 1:3 ratio of Sal B to polystyrene-b-poly(ethylene oxide) block copolymer (PS1.5-PEO2.4) with a polystyrene hydrophobic block size of 1,500 g/mole, and a poly(ethylene oxide) block size of 2,400 g/mole (Polymer Source) were dissolved in 3 mL of tetrahydrofuran (THF). Table 6 shows the nanoparticle formulation trials in which 1:3 drug to polymer ratio gave better physiochemical characteristics to 1:5 ratio.

Table 6. Trials for nanoparticle formulation of Sal B

Trial	Pre-mixing Concentrations	DLS Data
1	19.58 mg PSPEO + 6.16 mg Sal B	160 nm PDI: 0.4
2	19.2 mg PSPEO + 5.2 mg Sal B	194.7 nm PDI: 0.676
3	27 mg PSPEO + 10.66 mg Sal B	92.1 nm PDI: 0.356
4	28.7 mg PSPEO + 13.16 mg Sal B	90.6 nm PDI: 0.374
5	29.9 mg PSPEO + 11.28 mg Sal B	85.4 nm PDI: 0.387

The resulting solution was mixed at 12 ml/min with water at 108 ml/min using a custom-made, multiple inlet vortex mixer. The resulting nanoparticle suspension was collected at the mixer outlet and the particle size determined using dynamic light scattering (DLS) immediately following nanoparticle formation. The number-based nanoparticle size distribution is shown in Figure 16. Particle size increased over 24 hours of storage at room temperature. This increase is attributed to the presence of THF (10% by volume), which facilitates solvent mediated aggregation processes, including Ostwald-ripening. Formulation stability will be enhanced through solvent removal via dialysis subsequent to nanoparticle formation, which will limit Ostwald ripening.

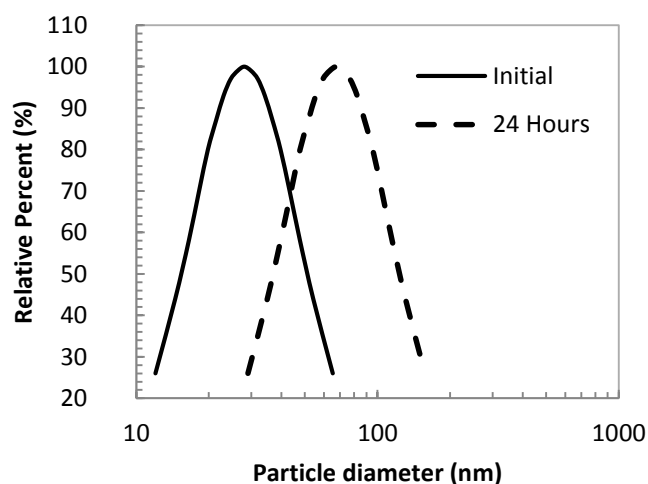


Figure 16. Number-based particle size distribution for Sal B-NP stabilized with PS1.5-PEO2.4 as determined by DLS. Particle size increased over 24 hours, most likely due to aggregation and Ostwald ripening in the presence of THF (10% by volume).

Morphology of the NPs were also confirmed by Scanning Electron Microscopy (SEM) (Figure 17).

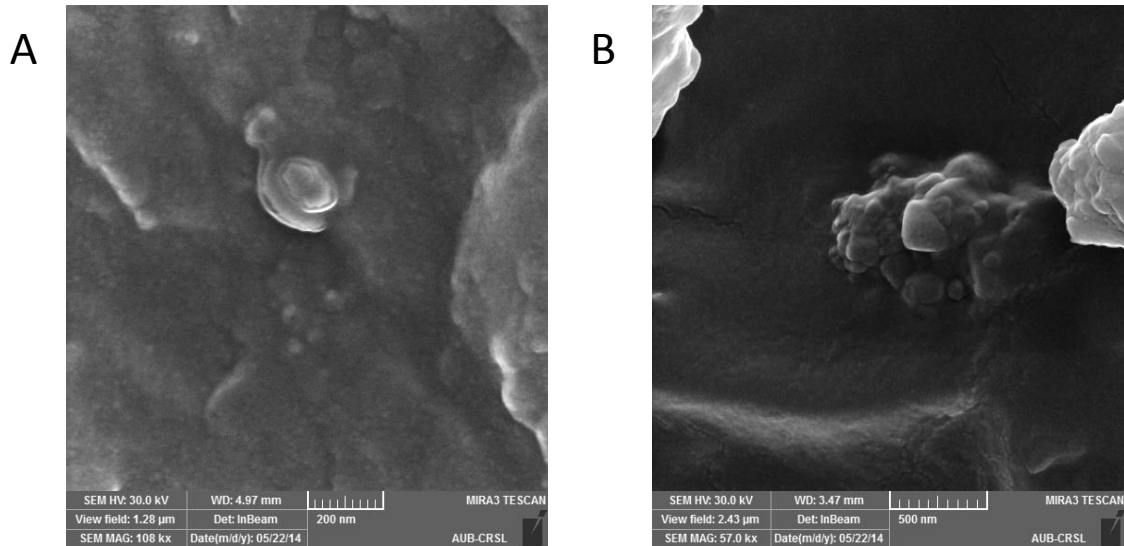


Figure 17. SEM images taken of Sal B Nanoparticles. The nanoparticles have a spherical diameter that is less than 200 nm and are round in morphology (A). Nanoparticles tend to aggregate during the freeze-drying process, as shown in (B).

C. Anti-cancer Activities of Native Drugs and Nanoparticle Formulations

1. Sal B and derivatives reveal increased potency in human colorectal and breast cancer cells with different p53 status compared to Sal A

We have assessed the effects of Sal A and Sal B, and their derivatives on the growth and viability of human tumor cells *versus* their normal counterparts. Towards this end, we used MTT cell proliferation assay and well-characterized human *in vitro* models of colorectal and breast tumor models as described in the Introduction and Methods. Viability results were expressed as percentage of control and plotted as the mean \pm Standard Error (SE) of at least three independent experiments. IC₅₀ concentrations with 50% growth inhibitory effects were obtained (see Figures 18-22 and corresponding Table 7). Our results clearly indicate that colorectal and breast tumor cells are more sensitive to Sal A derivatives as well as Sal B and derivatives (Table 7).

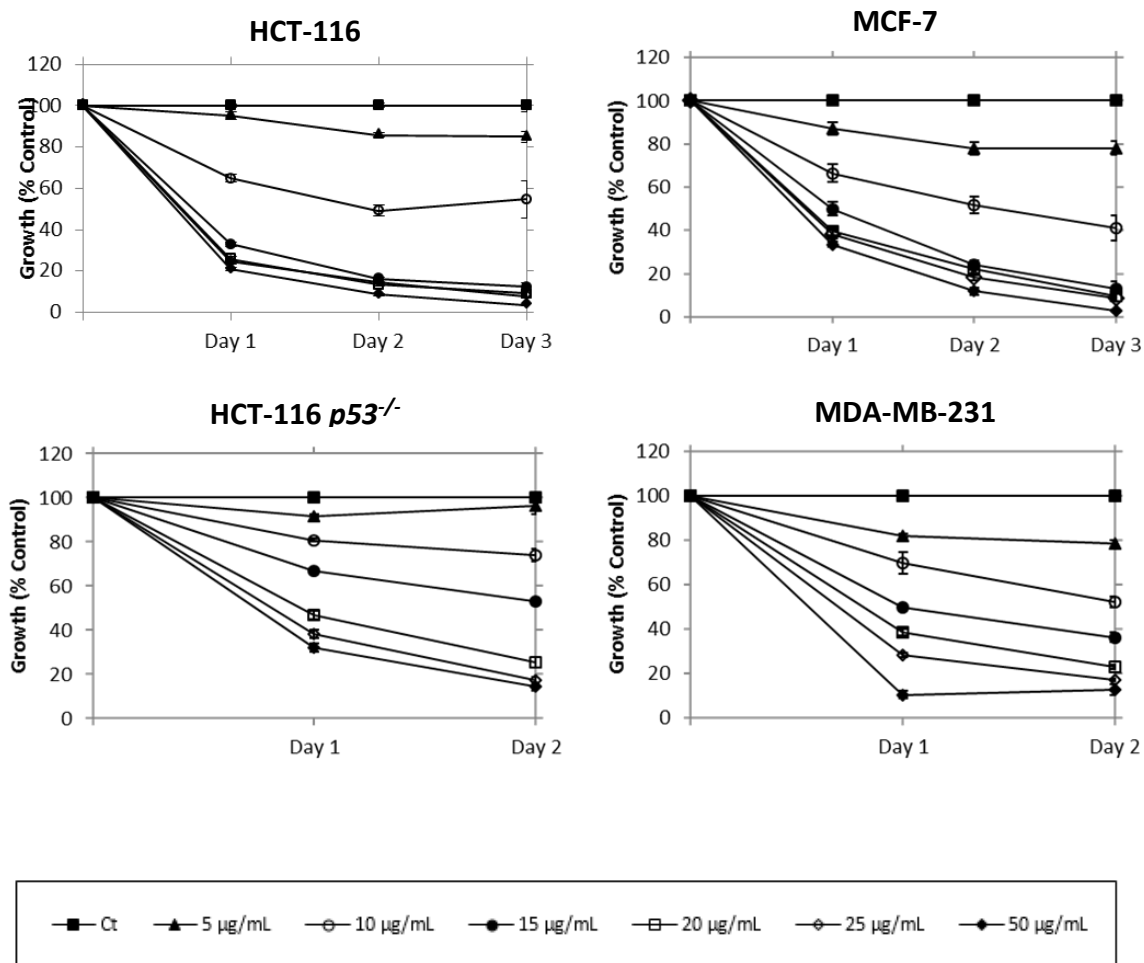


Figure 18. The effect of Sal A on the growth of colorectal and breast cancer cells. Cells were seeded in 96-well plates and treated with 0.1% ethanol or the indicated drug concentrations up to 3 days. Cell growth was assayed in triplicate wells using the cell proliferation MTT CellTiter 96[®] Assay. Results are expressed as percentage of control (0.1% ethanol) and represent the average of three independent experiments \pm SE.

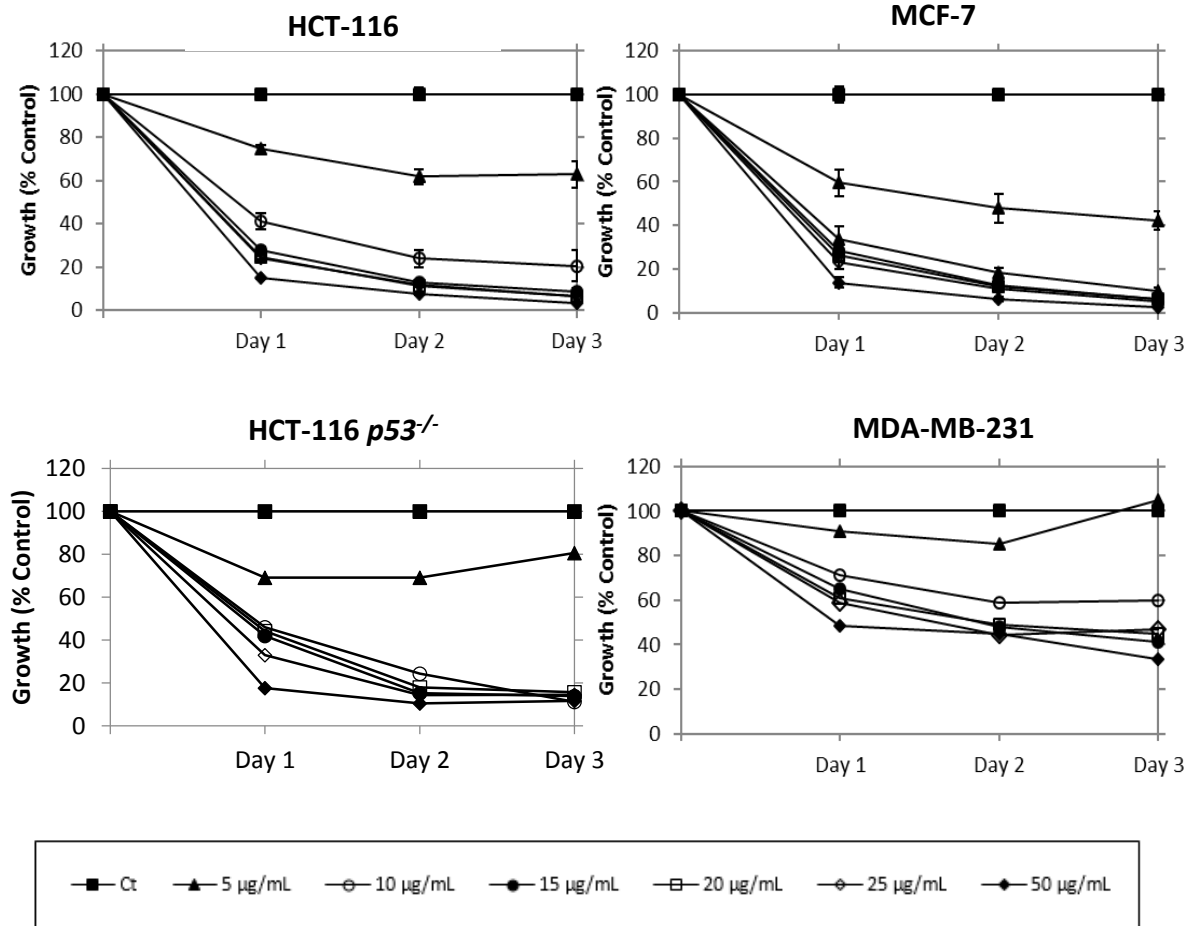


Figure 19. The effect of Sal B on the growth of colorectal and breast cancer cells. Cells were seeded in 96-well plates and treated with 0.1% ethanol or the indicated drug concentrations up to 3 days. Cell growth was assayed in triplicate wells using the cell proliferation MTT CellTiter 96[®] Assay. Results are expressed as percentage of control (0.1% ethanol) and represent the average of three independent experiments \pm SE.

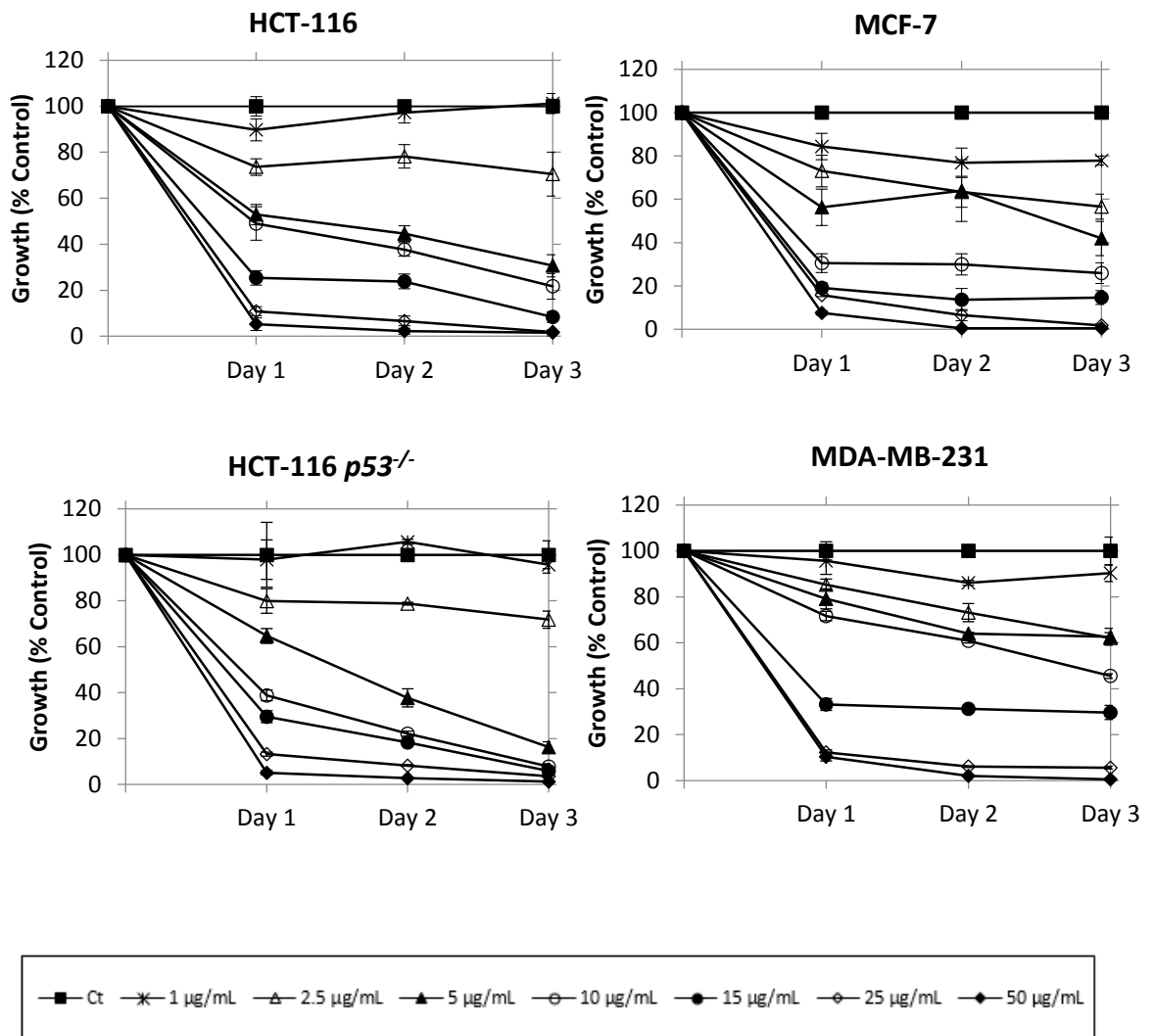


Figure 20. The effect of Sal A-1 on the growth of colorectal and breast cancer cells. Cells were seeded in 96-well plates and treated with 0.1% DMSO or the indicated drug concentrations up to 3 days. Cell growth was assayed in triplicate wells using the cell proliferation MTT CellTiter 96[®] Assay. Results are expressed as percentage of control (0.1% DMSO) and represent the average of three independent experiments \pm SE.

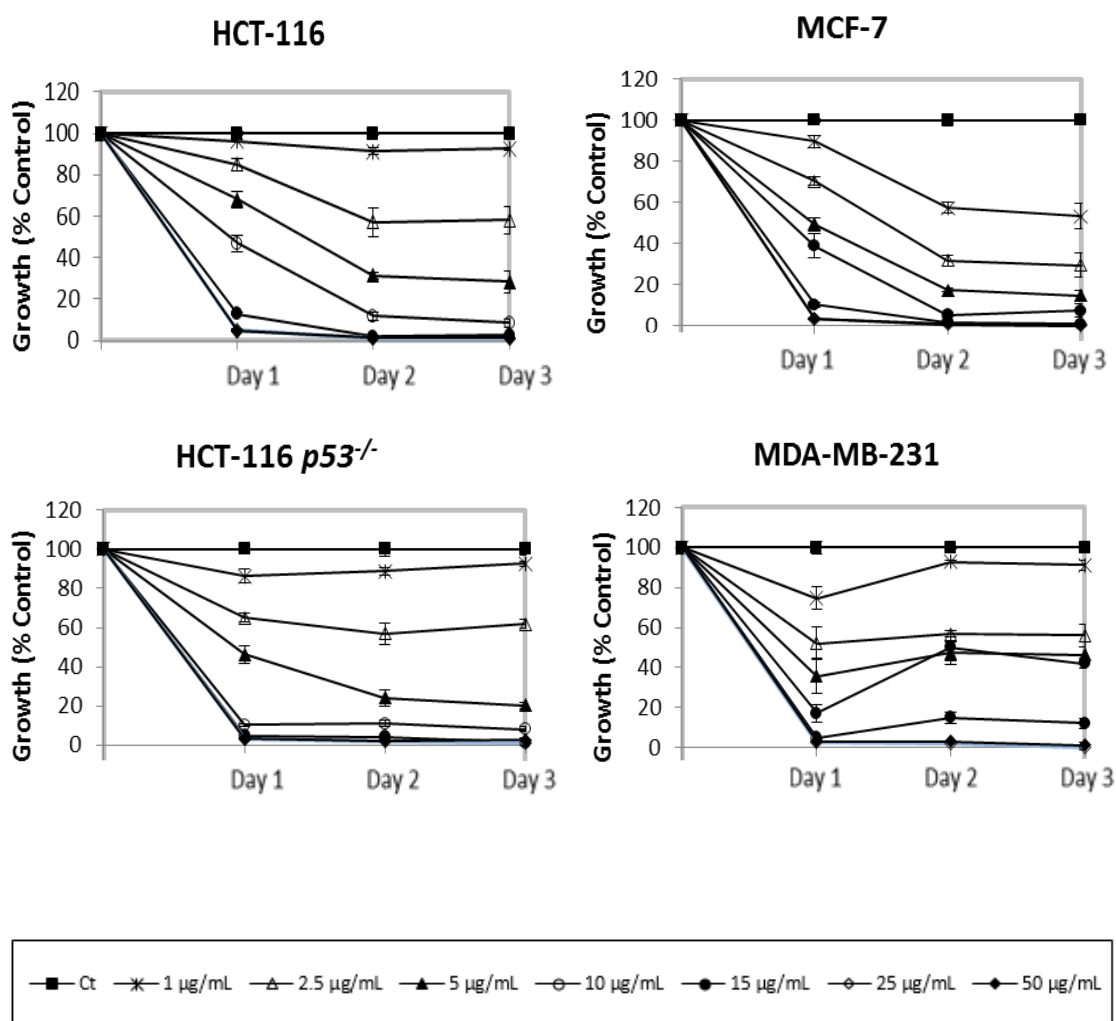


Figure 21. The effect of Sal A-2 on the growth of colorectal and breast cancer cells. Cells were seeded in 96-well plates and treated with 0.1% DMSO or the indicated drug concentrations up to 3 days. Cell growth was assayed in triplicate wells using the cell proliferation MTT CellTiter 96[®] Assay. Results are expressed as percentage of control (0.1% DMSO) and represent the average of three independent experiments \pm SE.

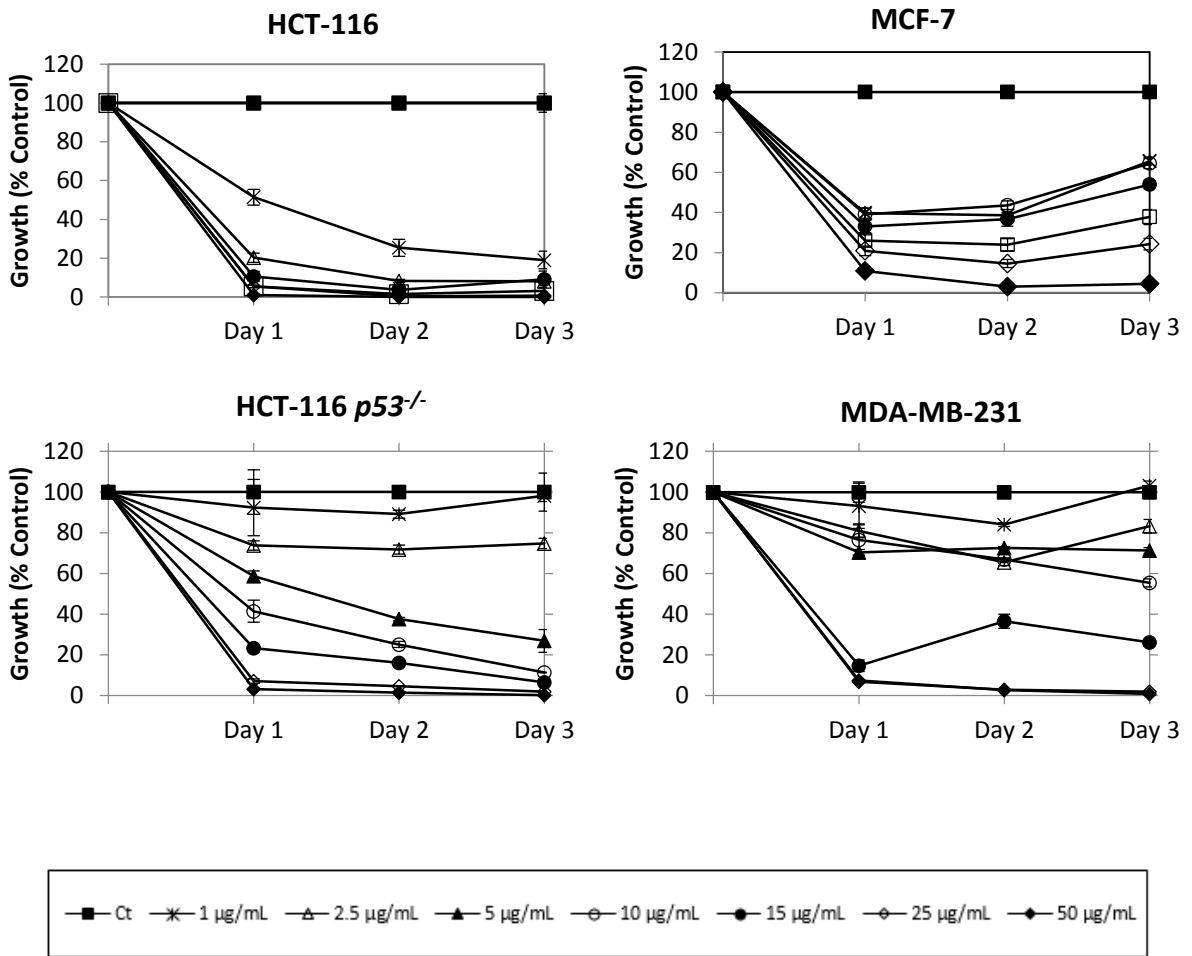


Figure 22. The effect of Sal B-1 on the growth of colorectal and breast cancer cells. Cells were seeded in 96-well plates and treated with 0.1% ethanol or the indicated drug concentrations up to 3 days. Cell growth was assayed in triplicate wells using the cell proliferation MTT CellTiter 96[®] Assay. Results are expressed as percentage of control (0.1% ethanol) and represent the average of three independent experiments \pm SE.

Table 7. IC₅₀ values of Sal A, Sal B, and derivatives for inhibition of tumor cell growth at 24 hours post-treatment

Drug	IC ₅₀ * (µg/ml)			
	HCT-116	HCT-116 p53 ^{-/-}	MCF-7	MDA-MB-231
Sal A	10	20	15	15
Sal B	8	8	6	15
Sal A-1	5	7	5	12
Sal A-2	6	8	10	11
Sal B-1	5	7	5	11

*IC₅₀ are approximate values.

2. Sal A and Sal B are relatively non-cytotoxic to normal versus tumor cells

Cytotoxicity assays measured by LDH release from cells at six hours of treatment demonstrate that Sal A and Sal B are not cytotoxic up to 15 and 25 µg/ml, respectively, in the different tested normal-line colorectal and breast cancer cells, whereas the corresponding derivatives show cytotoxic effects from 5-10 µg/mL concentrations (See Figures 23-25). Finally, our cytotoxicity experiments showed that Sal B was the least cytotoxic to the different normal-like cells among the different tested compounds.

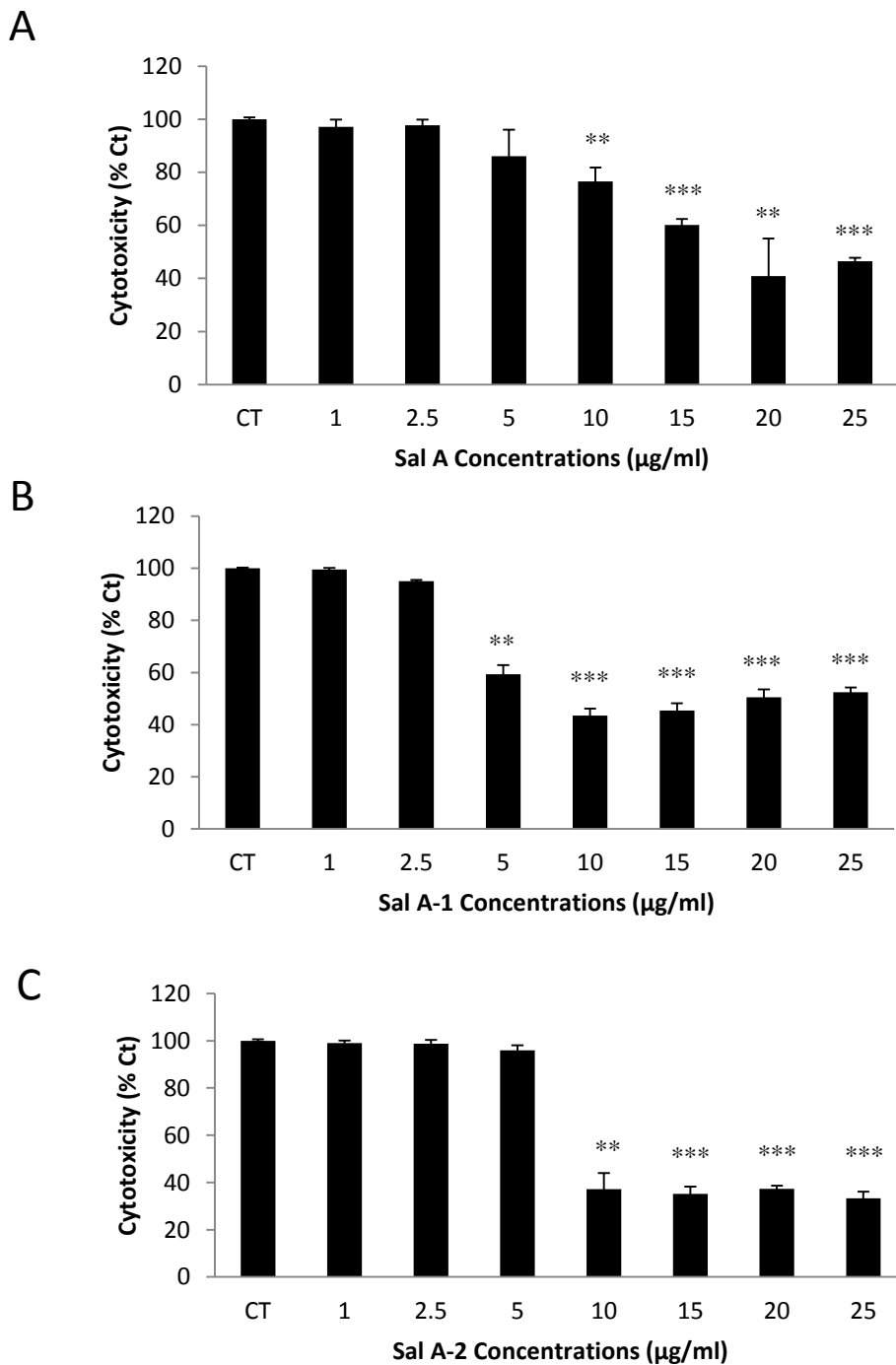


Figure 23. The normal-like colorectal cell line NCM460 was treated with (A) Sal A and derivatives (B) Sal A-1 and (C) Sal A-2 for 6 hours and the cytotoxic activity was determined by the lactate dehydrogenase assay as described in Materials and Methods. Data are representative of two independent experiments done in triplicate wells expressed as percentage of control cells and plotted as the mean \pm SD. *, $p < 0.05$; **, $p < 0.01$; ***, $p < 0.001$

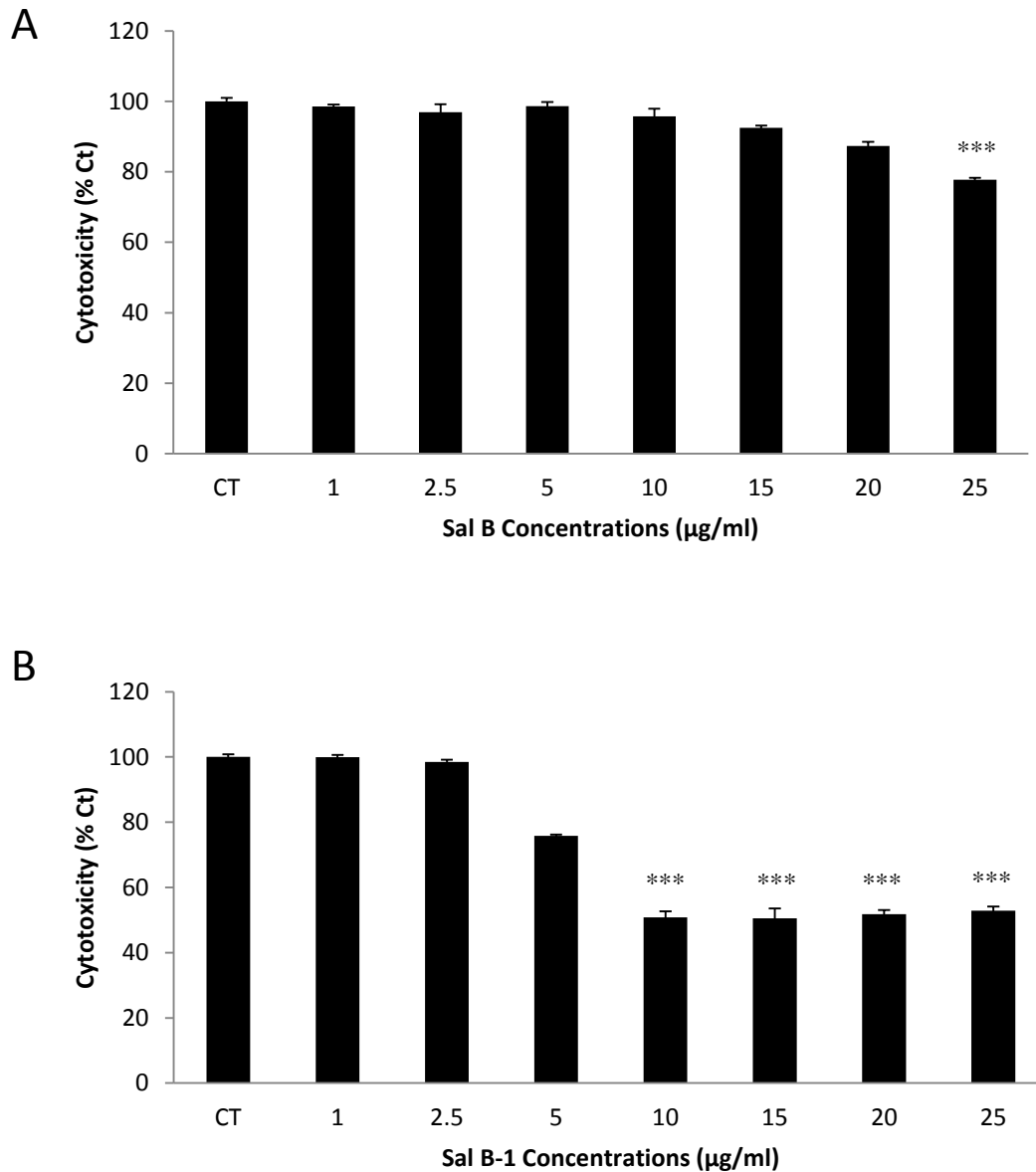


Figure 24. The normal-like colorectal cell line NCM460 was treated with A) Sal B and B) Sal B-1 for 6 hours and the cytotoxic activity was determined by the lactate dehydrogenase assay as described in Materials and Methods. Data are representative of two independent experiments done in triplicate wells expressed as percentage of control cells and plotted as the mean \pm SD. *, $p < 0.05$; **, $p < 0.01$; ***, $p < 0.001$

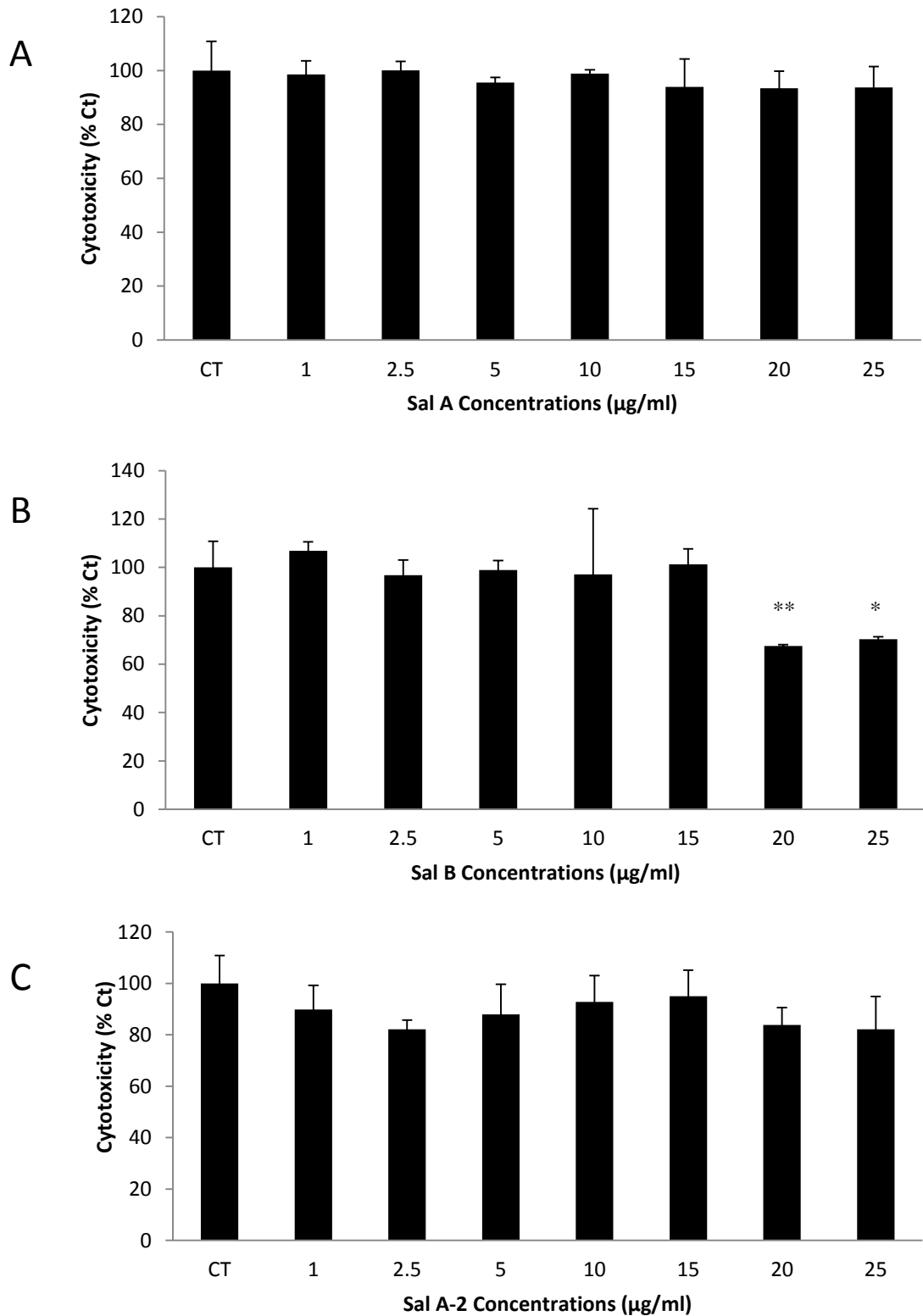


Figure 25. The normal-like breast cell line MCF10A was treated with (A) Sal A, (B) Sal B and (C) Sal A-2 for 6 hours and the cytotoxic activity was determined by the lactate dehydrogenase assay as described in Materials and Methods. Data are representative of two independent experiments done in triplicate wells and expressed as percentage of control cells and plotted as the mean \pm SD. *, $p < 0.05$; **, $p < 0.01$

3. Nanoparticles show a similar cytotoxicity profile as native drug on tumor cells

Sal B and Sal B-NP were found to be non-cytotoxic up to 25 $\mu\text{g/ml}$ in the HCT-116 colorectal cancer cells (Figure 26) and MCF-7 breast cancer cells after 6 hours of treatment (Figure 27).

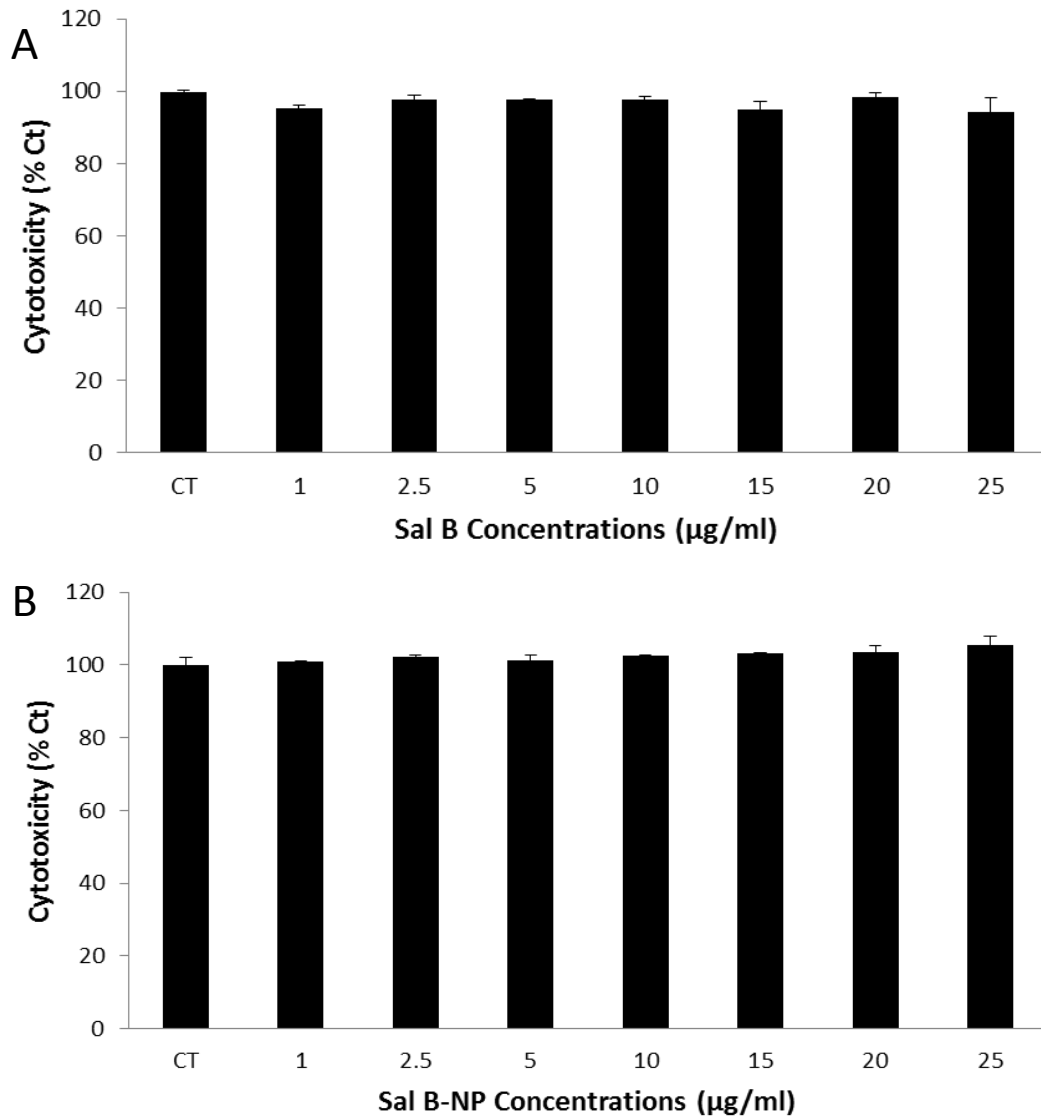


Figure 26. Sal B and Sal B nanoparticles are relatively non-cytotoxic to HCT-116 cells. The HCT-116 colorectal cancer cells were treated with Sal B (A) or Sal B nanoparticles (B) for 6 hours and the cytotoxic activity was determined by the lactate dehydrogenase (LDH) release assay as described in Materials and Methods. Results represent the average of one independent experiment done in quadruplicate wells and expressed as percentage of control-treated cells and plotted as the mean \pm SD. *, $p < 0.05$; **, $p < 0.01$

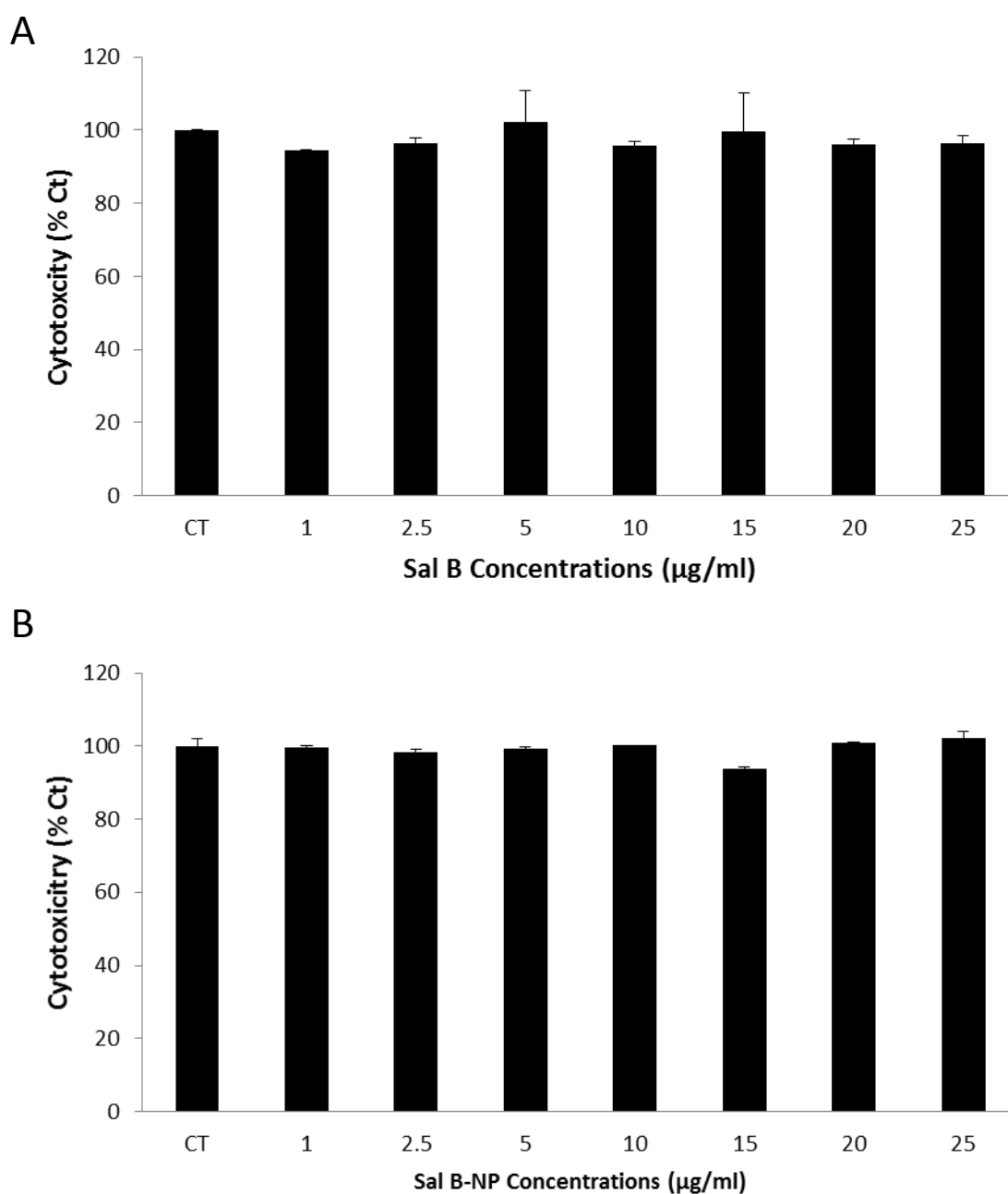


Figure 27. Sal B and Sal B nanoparticles are relatively non-cytotoxic to MCF-7 cells. The MCF-7 breast cancer cells were treated with Sal B (A) or Sal B-NP (B) for 6 hours and the cytotoxic activity was determined by the lactate dehydrogenase release assay as described in Materials and Methods. Results represent the average of one independent experiment done in quadruplicate wells and expressed as percentage of control-treated cells and plotted as the mean \pm SD. *, $p < 0.05$; **, $p < 0.01$

4. Screening Sal A, B, A-2 on prevalent human solid and hematological tumor cells

Our previous testing of the different drugs on the growth and cytotoxicity of tumor *versus* normal cells led us to select Sal B and Sal A-2 as lead drugs and to compare their anti-tumor activities *versus* Sal A. A panel of human cancer cells and their normal counterparts were treated with Sal A, Sal B, and Sal A-2 up to 72 h using the MTT cell proliferation assay (Figures 28-33). Viability results are expressed as percentage of control done in triplicate wells and plotted as the mean \pm Standard Error (SE) of at least three independent experiments. IC₅₀ concentrations with 50% growth inhibitory effects are calculated for the anti-tumor activities and are presented in Tables 8 and 9.

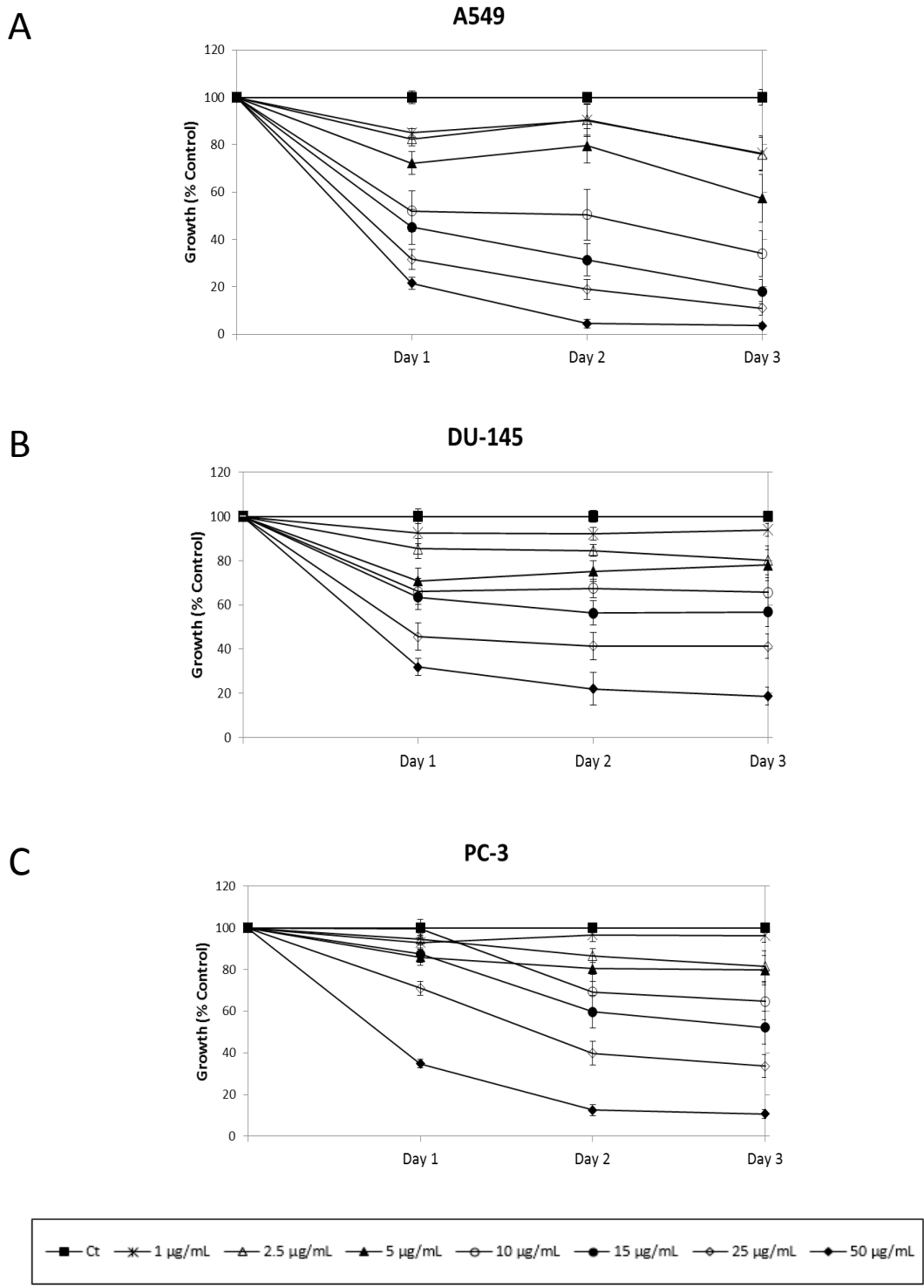


Figure 28. The effect of Sal A on the growth of A) lung A549, B) prostate DU-145, and C) prostate PC-3 cells. Cells were seeded in 96-well plates and treated with the drug solvent or the indicated drug concentrations up to 3 days. Cell growth was assayed in triplicate wells using the cell proliferation MTT CellTiter 96[®] Assay. Results are expressed as percentage of control and represent the average of three independent experiments ± SE.

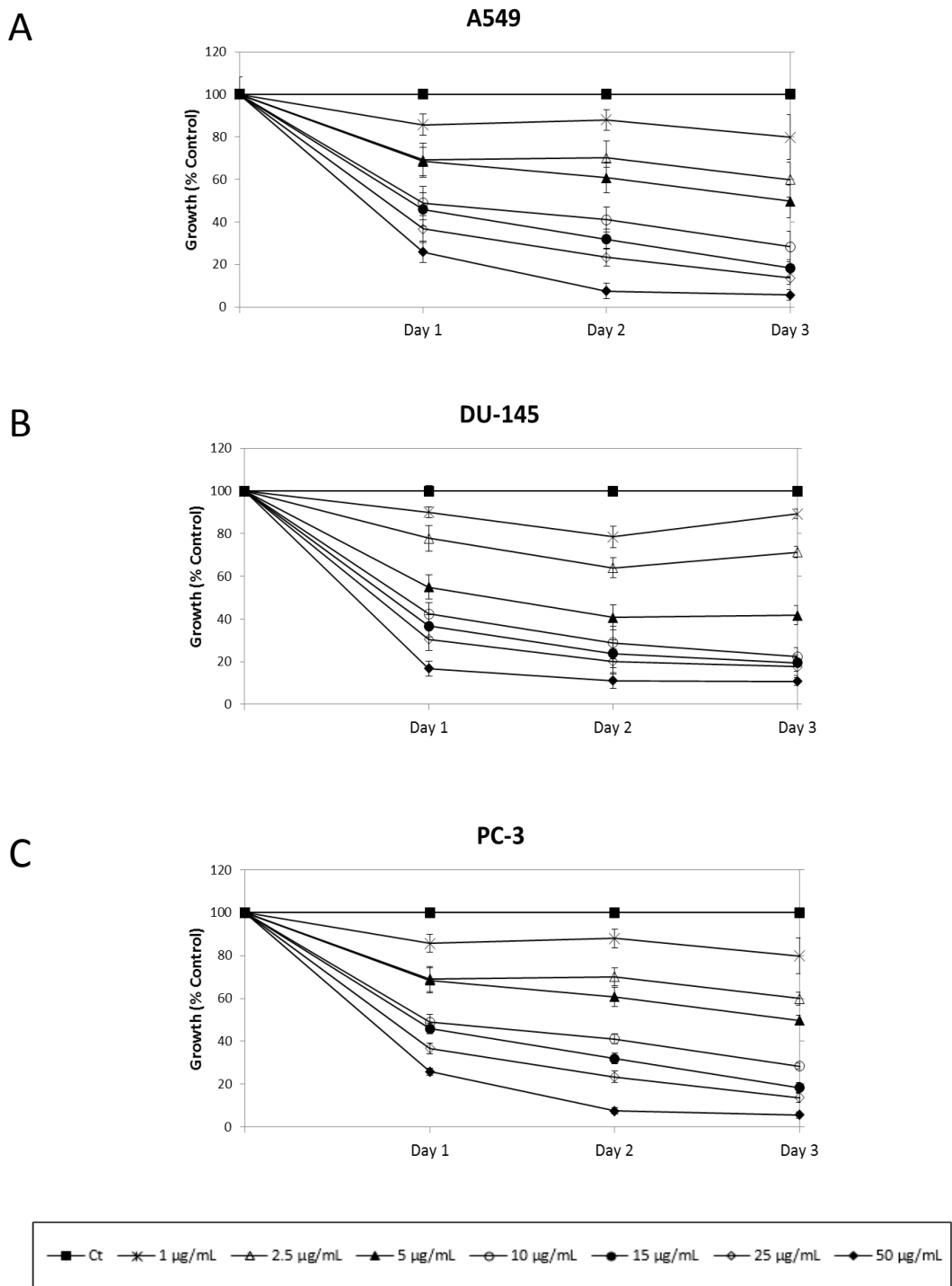


Figure 29. The effect of Sal B on the growth of A) lung A549, B) prostate DU-145, and C) prostate PC-3 cells. Cells were seeded in 96-well plates and treated with the drug solvent or the indicated drug concentrations up to 3 days. Cell growth was assayed in triplicate wells using the cell proliferation MTT CellTiter 96[®] Assay. Results are expressed as percentage of control and represent the average of three independent experiments \pm SE.

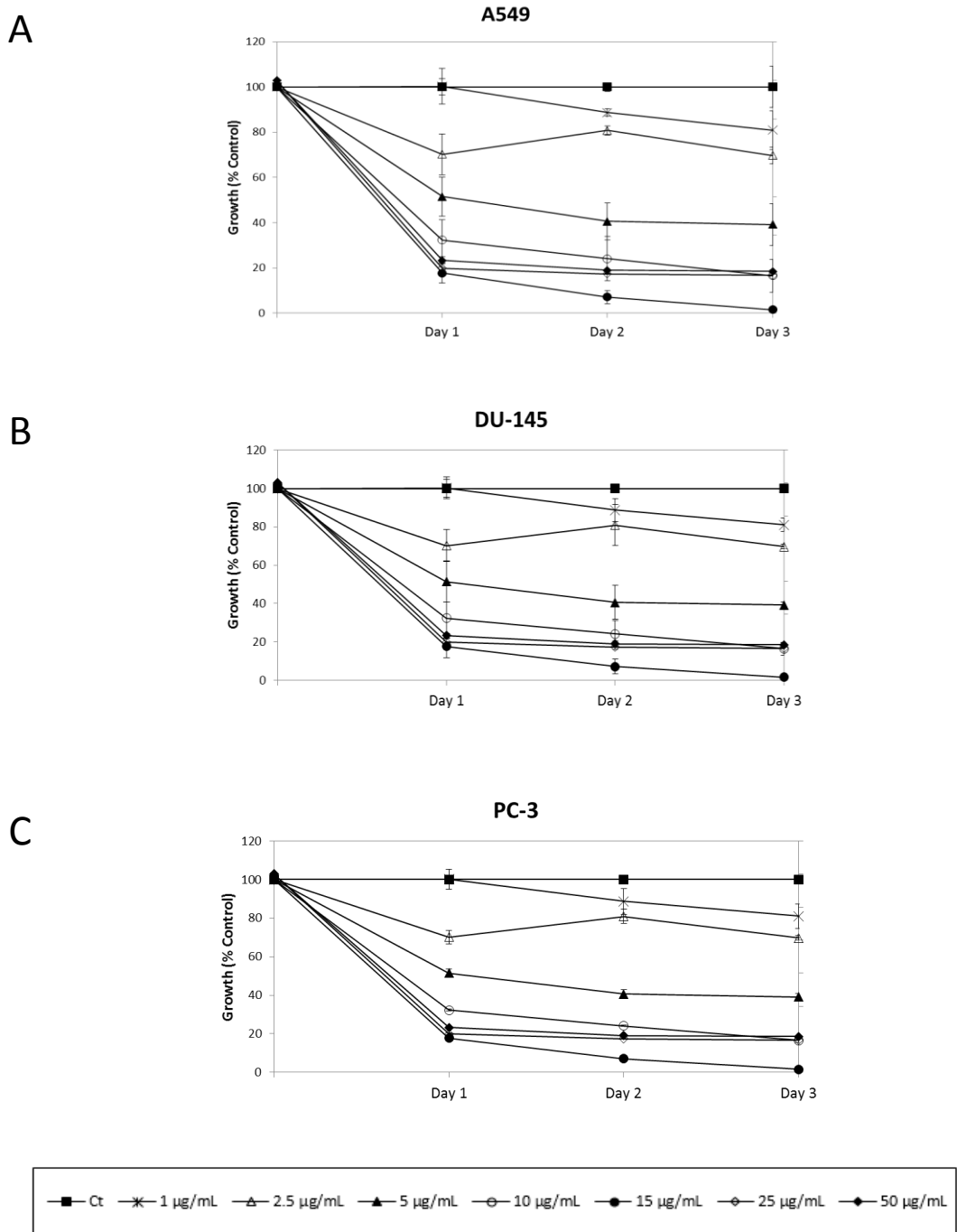


Figure 30. The effect of Sal A-2 on the growth of A) lung A549, B) prostate DU-145, and C) prostate PC-3 cells. Cells were seeded in 96-well plates and treated with the drug solvent or the indicated drug concentrations up to 3 days. Cell growth was assayed in triplicate wells using the cell proliferation MTT CellTiter 96[®] Assay. Results are expressed as percentage of control and represent the average of three independent experiments \pm SE.

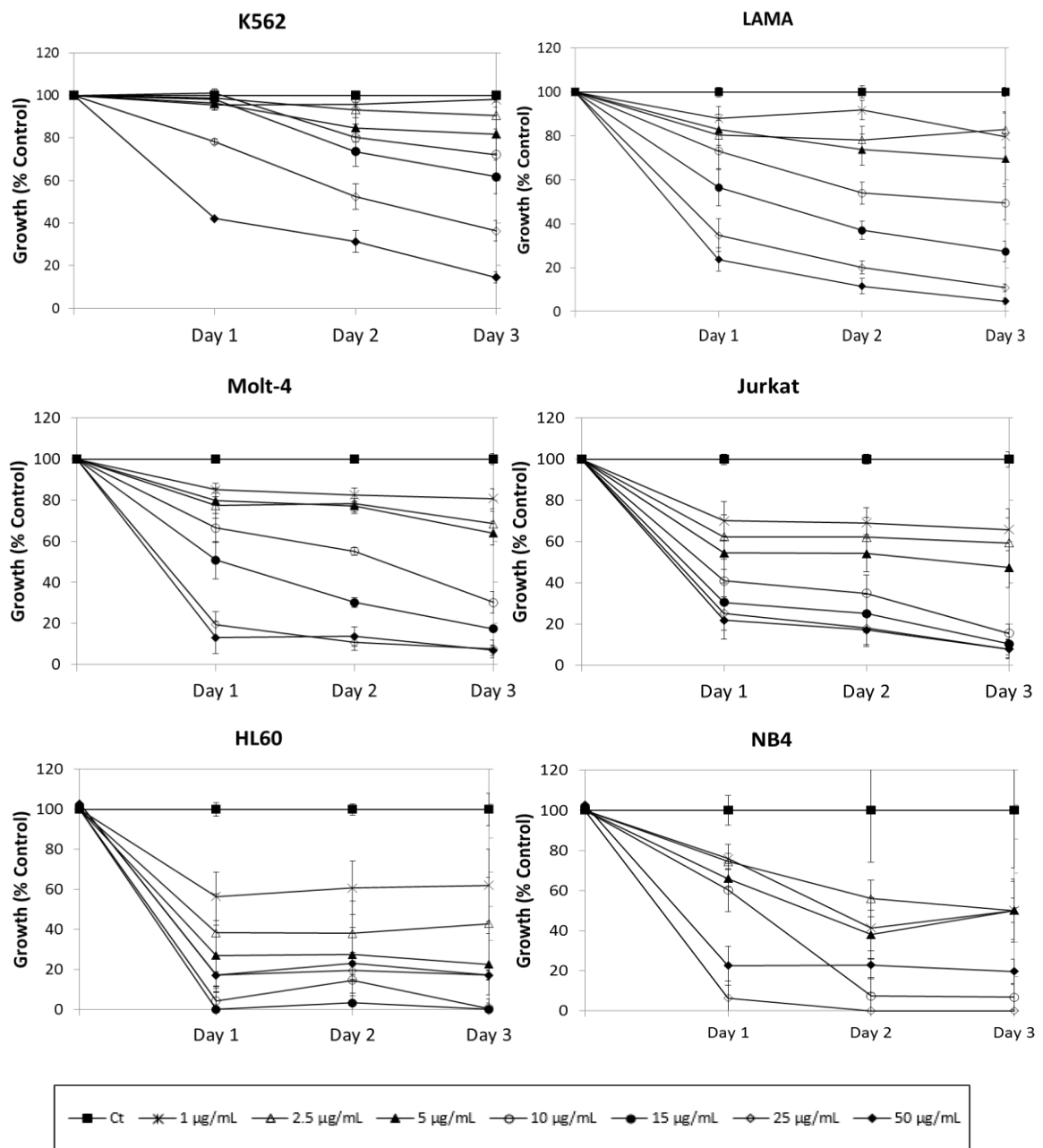


Figure 31. The effect of Sal A on the growth of representative human hematological tumor cells. Chronic myeloid leukemia cells (K562, LAMA), T-cell acute lymphoblastic leukemia cells (Molt-4, Jurkat), and acute promyelocytic leukemia cells (HL60, NB4) were seeded in 96-well plates and treated with the drug solvent or the indicated drug concentrations up to 3 days. Cell growth was assayed in triplicate wells using the cell proliferation MTT CellTiter 96[®] Assay. Results are expressed as percentage of control and represent the average of three independent experiments \pm SE.

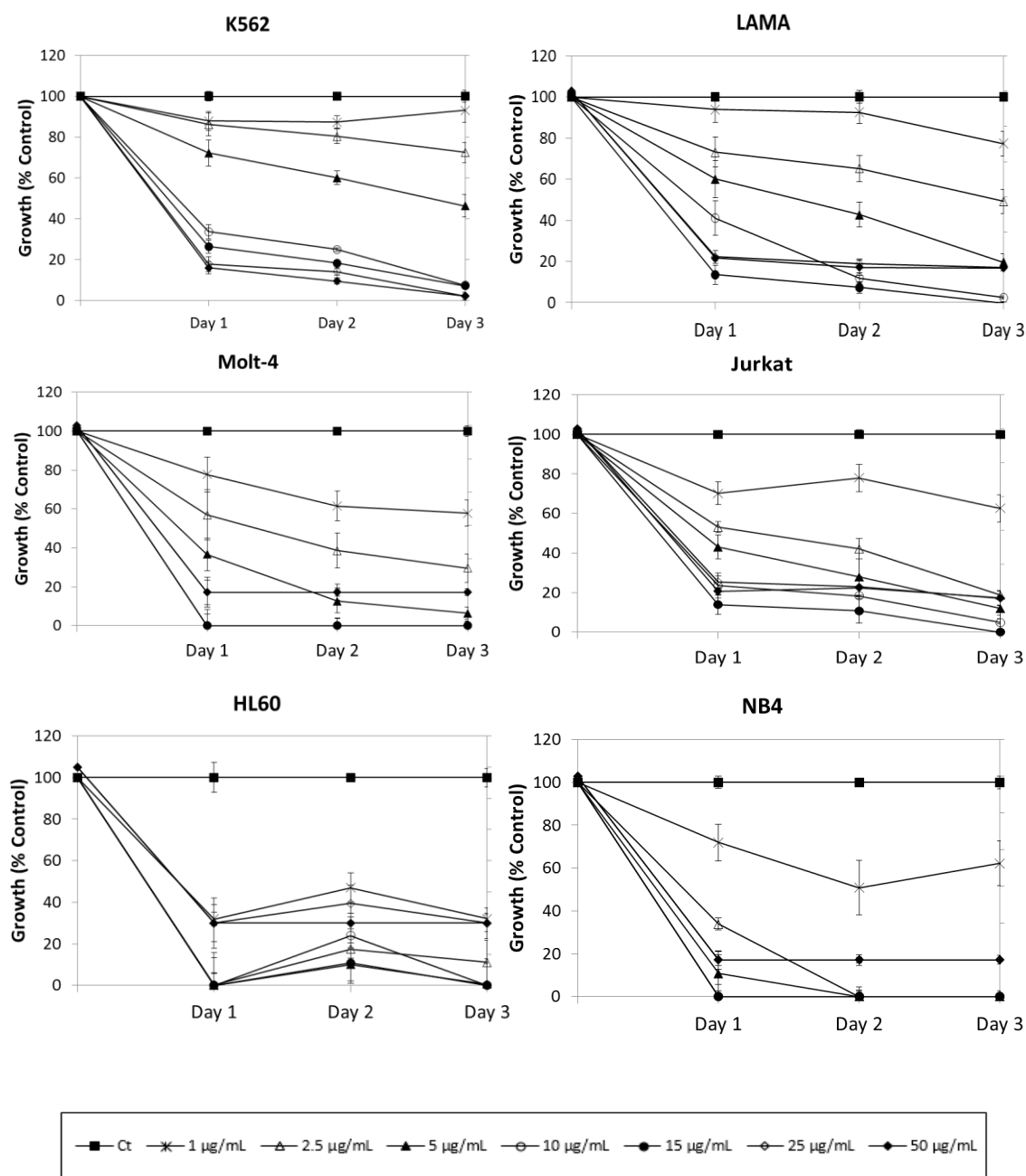


Figure 32. The effect of Sal B on the growth of representative human hematological tumor cells. Chronic myeloid leukemia cells (K562, LAMA), T-cell acute lymphoblastic leukemia cells (Molt-4, Jurkat), and acute promyelocytic leukemia cells (HL60, NB4) were seeded in 96-well plates and treated with the drug solvent or the indicated drug concentrations up to 3 days. Cell growth was assayed in triplicate wells using the cell proliferation MTT CellTiter 96[®] Assay. Results are expressed as percentage of control and represent the average of three independent experiments \pm SE.

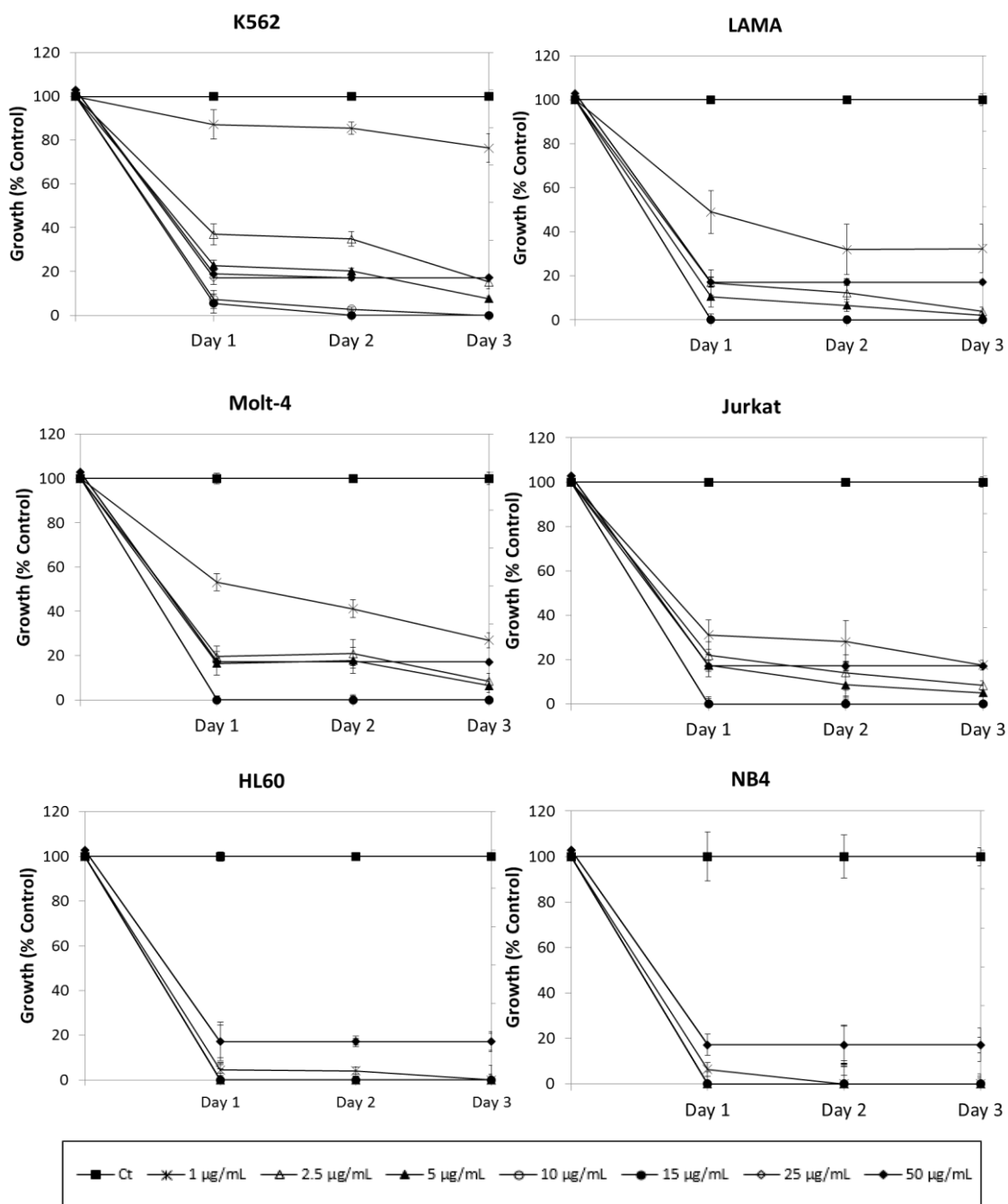


Figure 33. The effect of Sal A-2 on the growth of representative human hematological tumor cells. Chronic myeloid leukemia cells (K562, LAMA), T-cell acute lymphoblastic leukemia cells (Molt-4, Jurkat), and acute promyelocytic leukemia cells (HL60, NB4) were seeded in 96-well plates and treated with the drug solvent or the indicated drug concentrations up to 3 days. Cell growth was assayed in triplicate wells using the cell proliferation MTT CellTiter 96[®] Assay. Results are expressed as percentage of control and represent the average of three independent experiments \pm SE.

Table 8. IC₅₀ values of Sal A, Sal B, and Sal A2 for inhibition of solid tumor cell growth at 24 hours post-treatment

Drug	IC ₅₀ * (µg/ml)						
	HCT-116	HCT-116 p53 ^{-/-}	MCF-7	MDA-MB-231	A-549	DU145	PC3
Sal A	10	20	15	15	15	25	25
Sal B	8	8	6	15	10	5	5
Sal A-2	6	5-10	10	10-15	5	5	1-2.5

* IC₅₀ are approximate values

Table 9. IC₅₀ values of Sal A, Sal B, and Sal A-2 for inhibition of hematological tumor cell growth at 24 hours post-treatment

Drug	IC ₅₀ * (µg/ml)					
	K562	LAMA	Molt-4	Jurkat	NB4	HL60
Sal A	25-50	15-25	15	5	10	5
Sal B	5-10	5-10	2.5	2.5	1-2.5	1
Sal A-2	1-2.5	1-2.5	1	1	0-1	1

* IC₅₀ are approximate values

5. ST1926 nanoparticles have comparable anti-tumor activities to native drug in in vitro human colorectal and cancer models

The synthetic retinoid ST1926 is a highly hydrophobic drug and was therefore used as a control drug for successful nanoparticle formulations during the process. We assessed the efficacy of ST1926 nanoparticles (ST-NP) in *in vitro* human colorectal cancer models: HCT-116 (wild-type *p53*) and HCT-116 *p53*^{-/-} cell lines. ST1926 was successfully formulated into nanoparticles which exhibited comparable potent anti-cancer activities to native ST1926 in tested colorectal cancer cells, at pharmacologically achievable µM concentrations, which was validated by MTT cell viability assay (Figure 34). Additionally apoptotic assay results also suggest that OST-NP, comparable to the

native ST1926, induced apoptosis in colorectal and breast cancer cells, as demonstrated by TUNEL assay (data not shown).

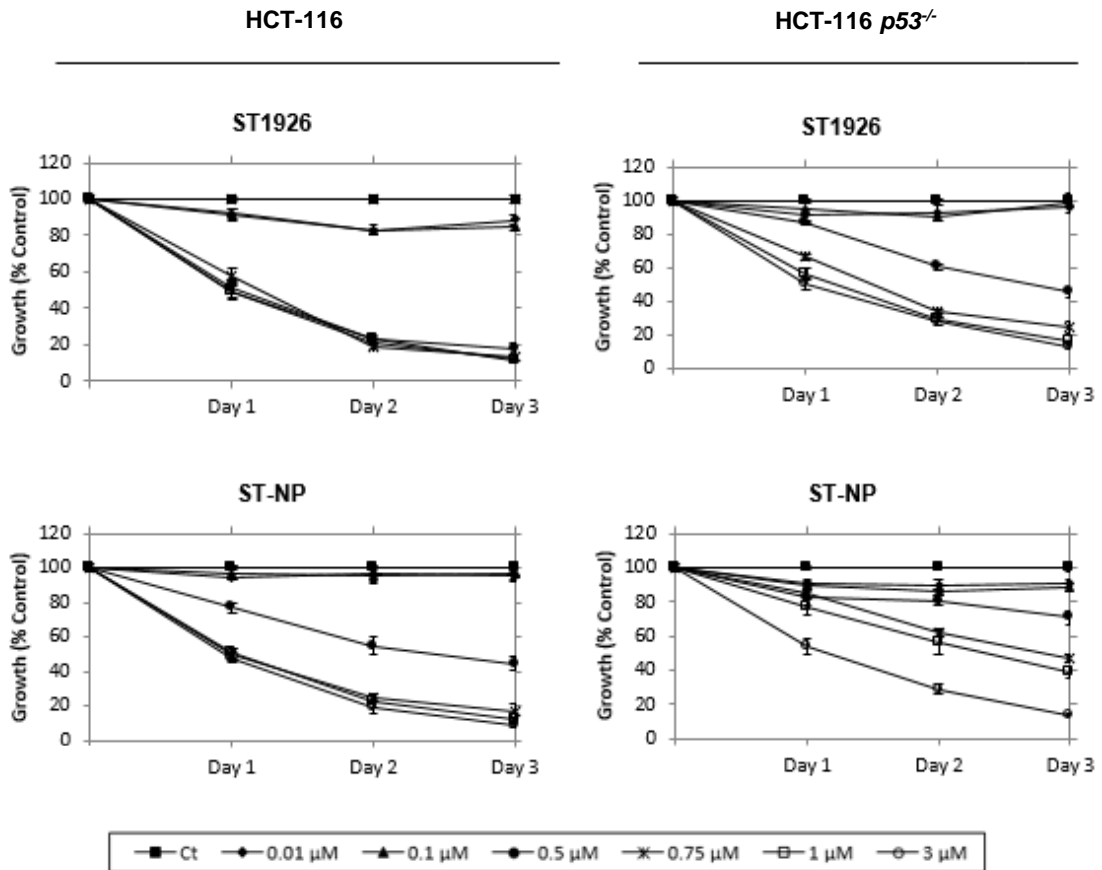


Figure 34. ST1926 and its nanoparticle formulation inhibit colorectal cancer cell growth independently of *p53*. Cells were seeded in 96-well plates and treated with the indicated ST1926 and ST-NP (ST1926 nanoparticles) concentrations up to 3 days. Cell growth was assayed in triplicate wells using the cell proliferation MTT CellTiter 96 Assay. The results are expressed as percentage of control (0.1% DMSO) and are the average \pm SE of three independent experiments.

6. Sal B nanoparticles have comparable anti-cancer activities to native drug *in vitro*

We assessed the efficacy of Sal B nanoparticles in *in vitro* human colorectal and breast cancer models, HCT-116 and MCF-7 (Figures 35 and 36) and they were found to have comparable anti-tumor activities. Furthermore, Sal B and its nanoparticle formulation affected the confluency and morphology of treated HCT-116 and MCF-7 cells as shown by microscopic images represented in Figures 37 and 38.

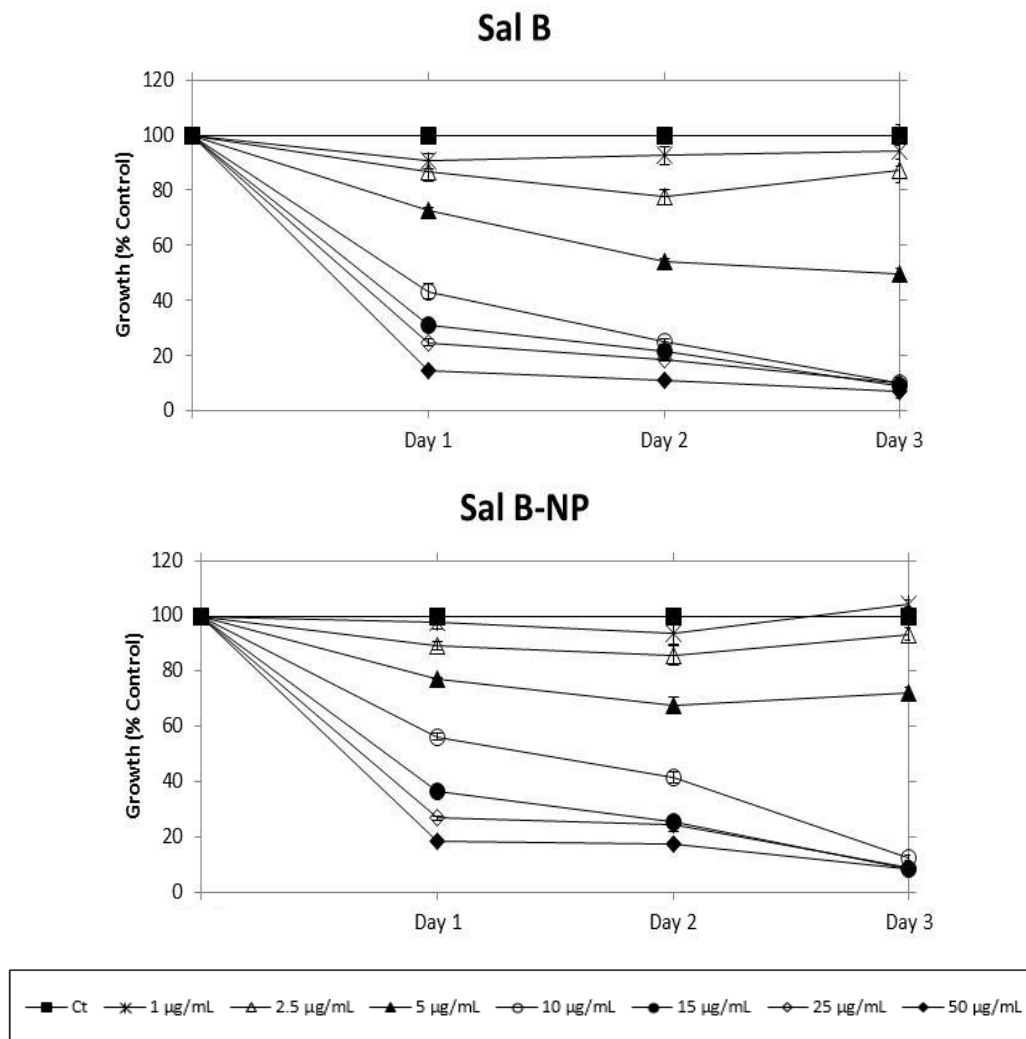


Figure 35. Sal B and its nanoparticle formulation inhibit growth of HCT-116 colorectal cancer cells. Cells were seeded in 96-well plates and treated with the indicated Sal B and Sal B-NP (Sal B nanoparticles) concentrations up to 3 days. Cell growth was assayed in triplicate wells using the cell proliferation MTT CellTiter 96 Assay. The results are expressed as percentage of control (0.1% ethanol or NP vehicle) and are the average \pm SE of two independent experiments.

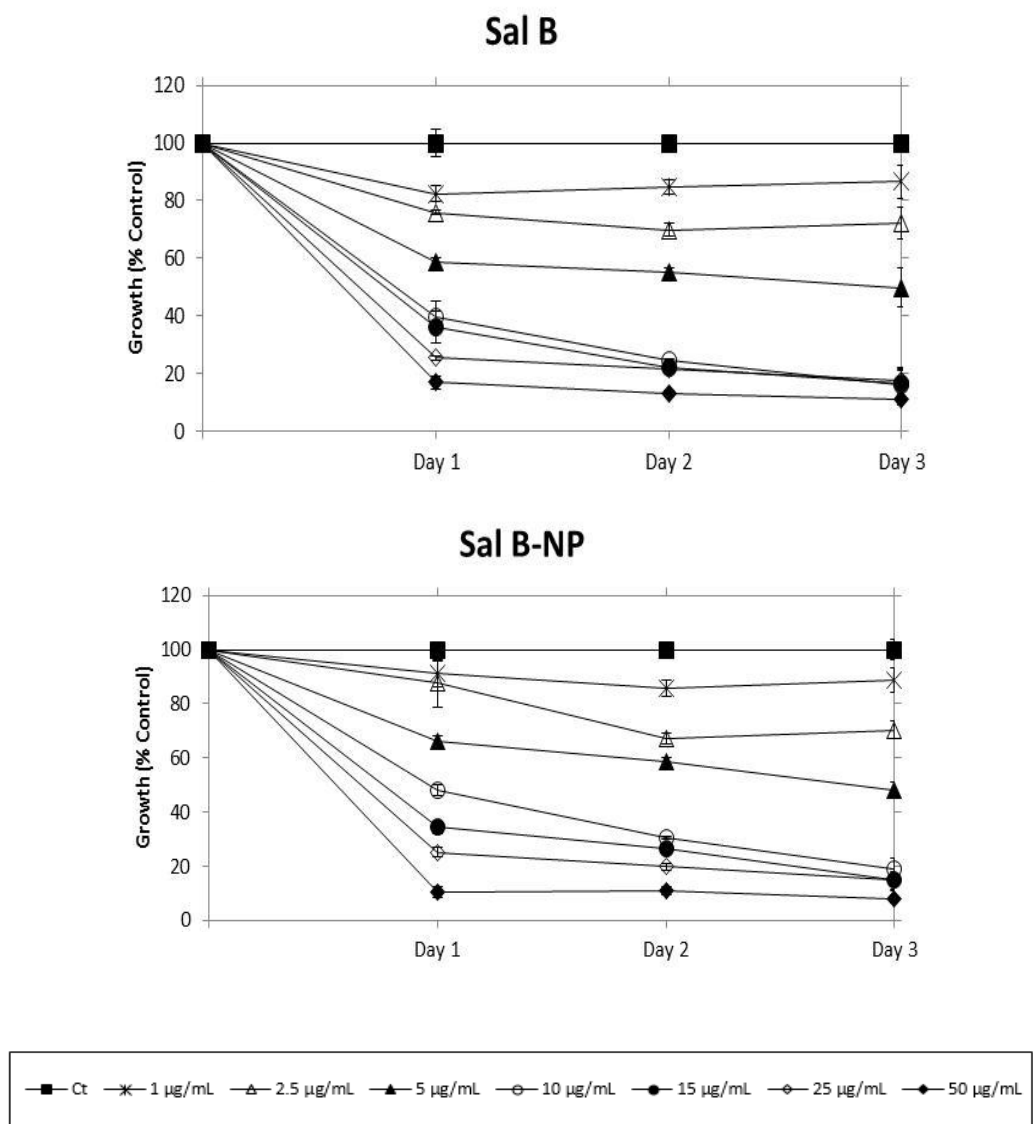


Figure 36. Sal B and its nanoparticle formulation inhibit the growth of MCF-7 breast cancer cells. Cells were seeded in 96-well plates and treated with the indicated Sal B and Sal B-NP (Sal B nanoparticles) concentrations up to 3 days. Cell growth was assayed in triplicate wells using the cell proliferation MTT CellTiter 96 Assay. The results are expressed as percentage of control (0.1% ethanol or NP vehicle) and are the average \pm SE of two independent experiments.

HCT-116

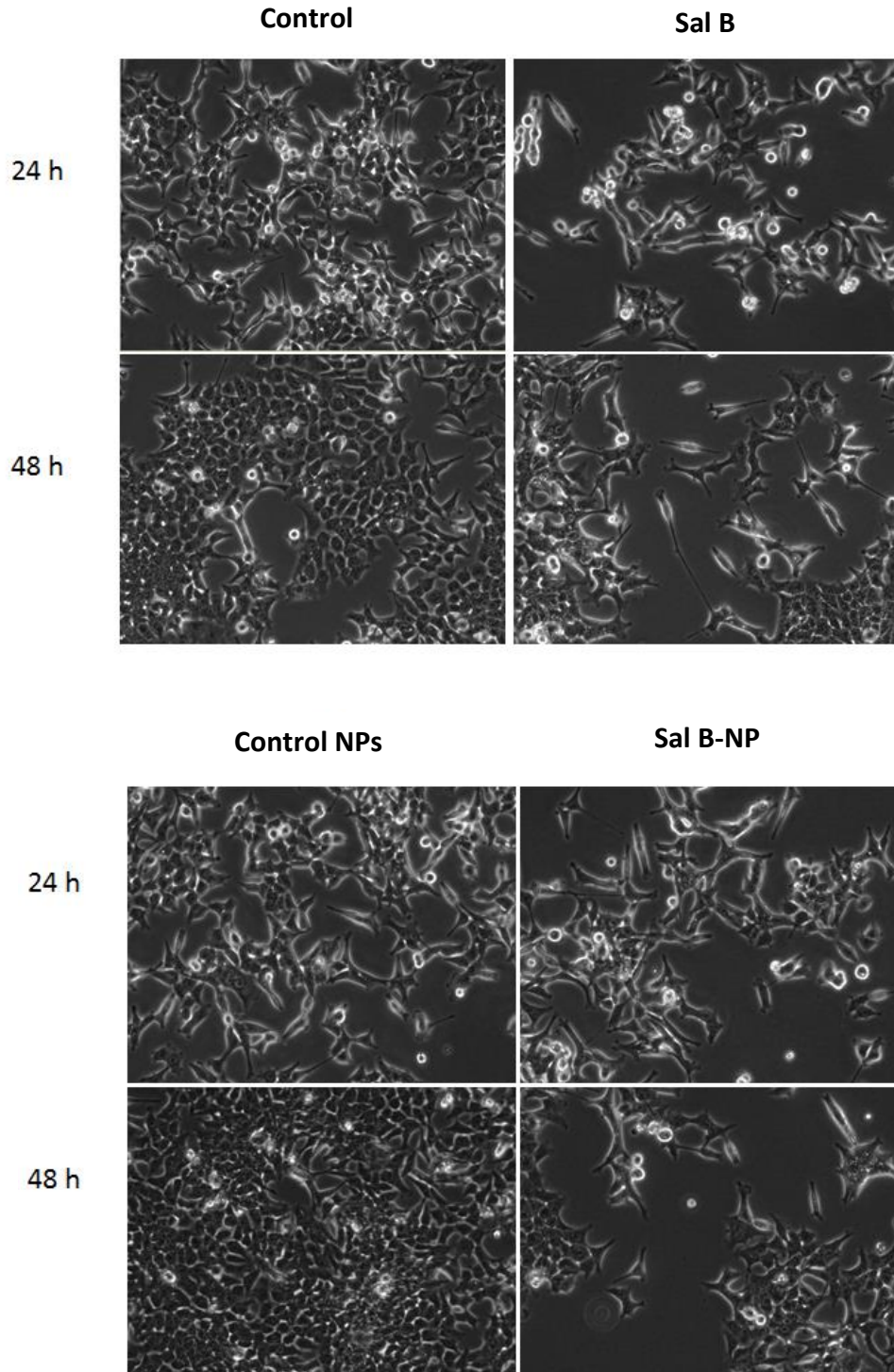


Figure 37. Sal B and its nanoparticle formulation affect the confluency and morphology of treated HCT-116 cells. 500,000 cells were seeded in 100 mm plates and treated with 10 $\mu\text{g/ml}$ Sal B and Sal B-NP (Sal B nanoparticles) concentrations up to 2 days. Representative micrographs of post-treated HCT-116 cells were taken at 10x magnification.

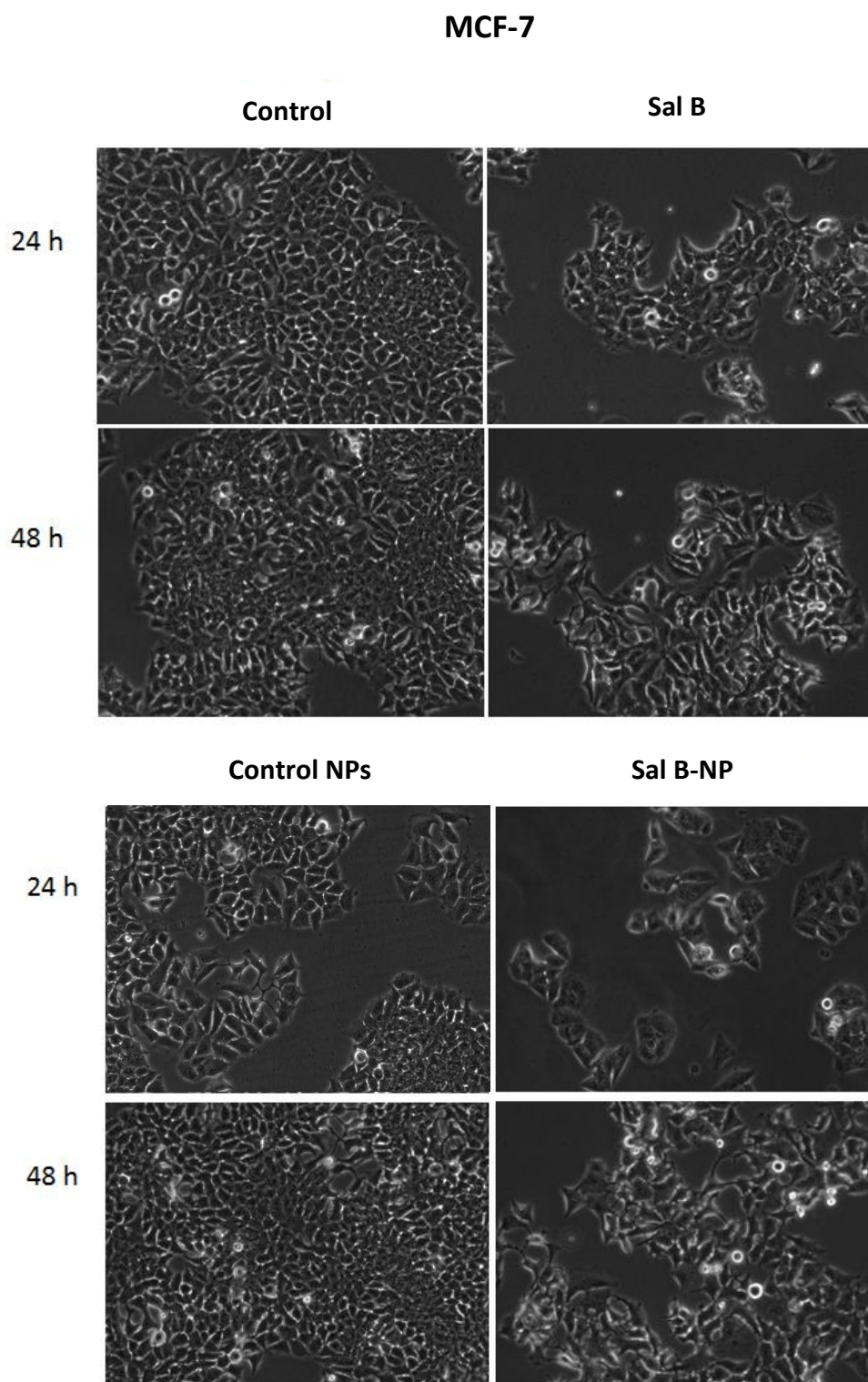


Figure 38. Sal B and its nanoparticle formulation affect the confluency and morphology of treated MCF-7 cells. 500,000 cells were seeded in 100 mm plates and treated with 10 $\mu\text{g/ml}$ Sal B and Sal B-NP (Sal B nanoparticles) concentrations up to 2 days. Representative micrographs of post-treated HCT-116 cells were taken at 10x magnification.

7. Native Sal B and Sal B nanoparticles treated cells accumulate in the S phase of the cell cycle

In order to investigate the mechanism of growth inhibition and cell death induced by native Sal B and its nanoparticle formulation in colorectal cancer cells. Cell cycle analysis was conducted using cell cycle analysis by flow cytometry (as described in Methods). HCT-116 cells were treated with 5 $\mu\text{g}/\text{mL}$ Sal B or Sal B-NP. Sal B and Sal B-NP caused an accumulation of treated cells in the S-phase of the cell cycle (Figure 39 and Table 10). We are in the process of completing experiments at 10 $\mu\text{g}/\text{mL}$ concentrations as to induce a more potent effect on cell death and accumulation of cells in the presumably apoptotic pre-G₁ region of the cell cycle.

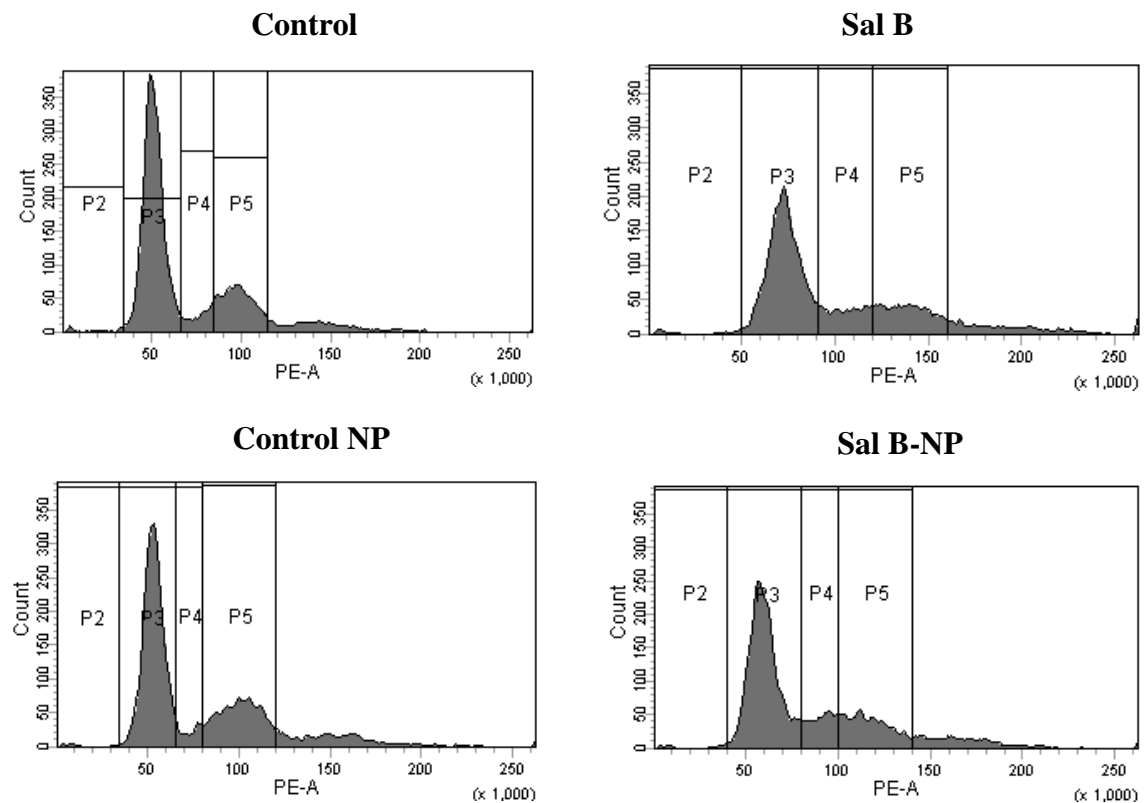


Figure 39. Sal B and its nanoparticle formulation treatment of HCT-116 cells induces S phase accumulation in the cell cycle. HCT-116 cells were treated with 5 $\mu\text{g}/\text{mL}$ Sal B or Sal B-NP for up to 48 hours while control cells were treated with 0.1% ethanol or THF with the NP vehicle. The results are representative of two independent experiments.

Table 10. Effect of Sal B and Sal B nanoparticle treatment at 5 µg/ml for 48 hours on the cell cycle distribution of colorectal cancer cells

Phases (% of total)	Control	Sal B	Control-NP	Sal B-NP
Pre-G ₁	2	3	2	2
G ₀ /G ₁	69	60	62	62
S	7	15	5	14
G ₂ /M	22	22	31	22

8. Native Sal B and Sal B nanoparticles-treated cells show differential regulation of p53 and p21 proteins

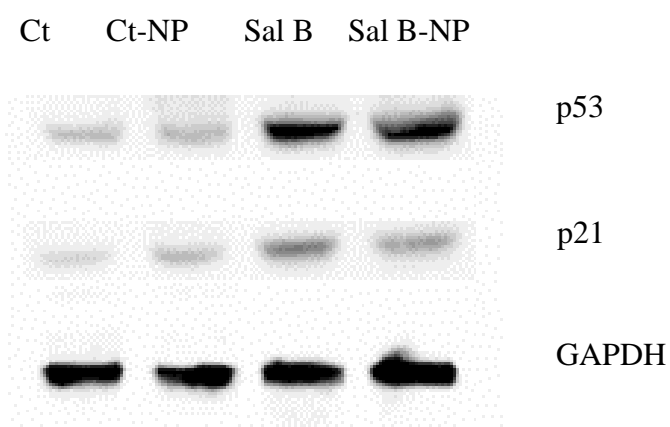


Figure 40. Sal B and Sal B-NP treatment of HCT-116 cells results in differential upregulation of *p53* and *p21* proteins. Cells were seeded at a density of 1×10^6 cells/ml and treated with 5 µg/ml Sal B or Sal B-NP up to 48 hours. Whole SDS lysates (50 µg/ml) were prepared and immunoblotted against *p53* and *p21* antibodies. Blots were re-probed with GAPDH antibody to ensure equal protein loading. Similar trend was observed in two independent experiments.

9. Native Sal B and Sal B nanoparticles induce apoptosis in treated tumor cells

Native Sal B and Sal B-NP treatment cause apoptosis of colorectal cells as evidenced by PARP cleavage (figure 41) and TUNEL assay (Figures 42 and 43).

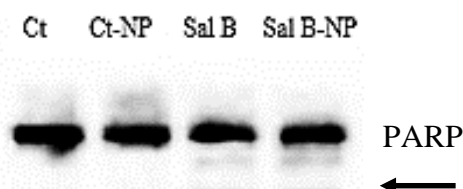


Figure 41. Sal B and Sal B-NP treatment of HCT-116 cells induces apoptosis as shown by PARP cleavage. Cells were seeded at a density of 1×10^6 cells/ml and treated with $5 \mu\text{g/ml}$ Sal B or Sal B-NP up to 48 hours. Whole SDS lysates ($50 \mu\text{g/ml}$) were prepared and immunoblotted against PARP antibody. Arrow indicates cleaved PARP. Similar trend was observed in two independent experiments.

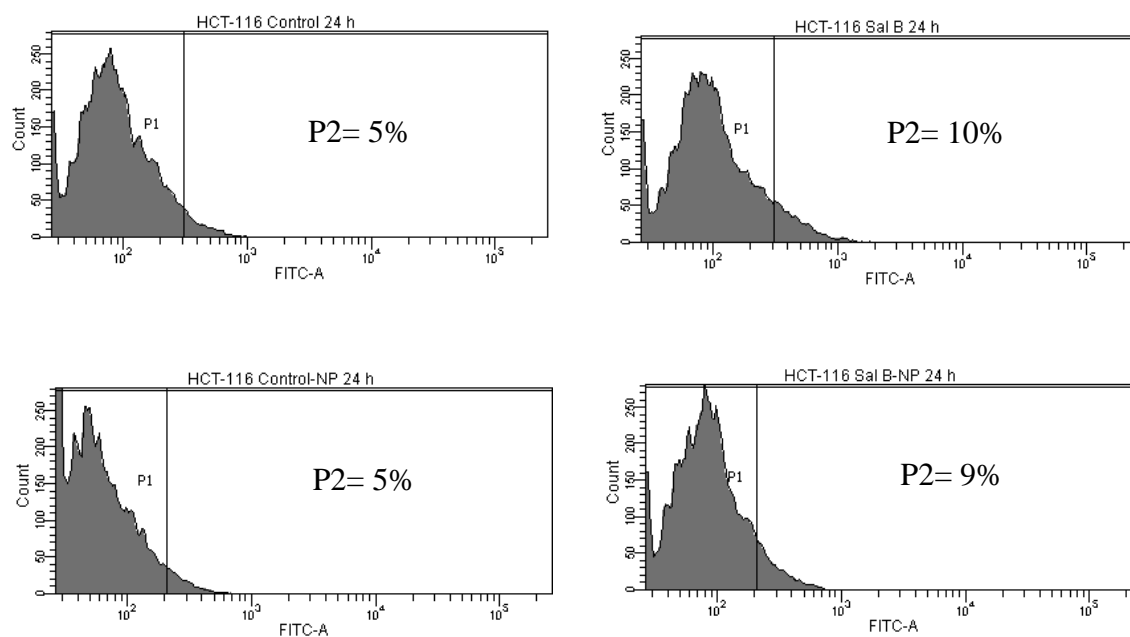


Figure 42. Sal B and its nanoparticle formulation treatment for 24 hours induce apoptosis in HCT-116 cells. HCT-116 cells were treated with $5 \mu\text{g/mL}$ Sal B or Sal B-NP. Control cells were treated with 0.1% ethanol or THF with NP vehicle. TUNEL analysis was performed on treated cells as described.

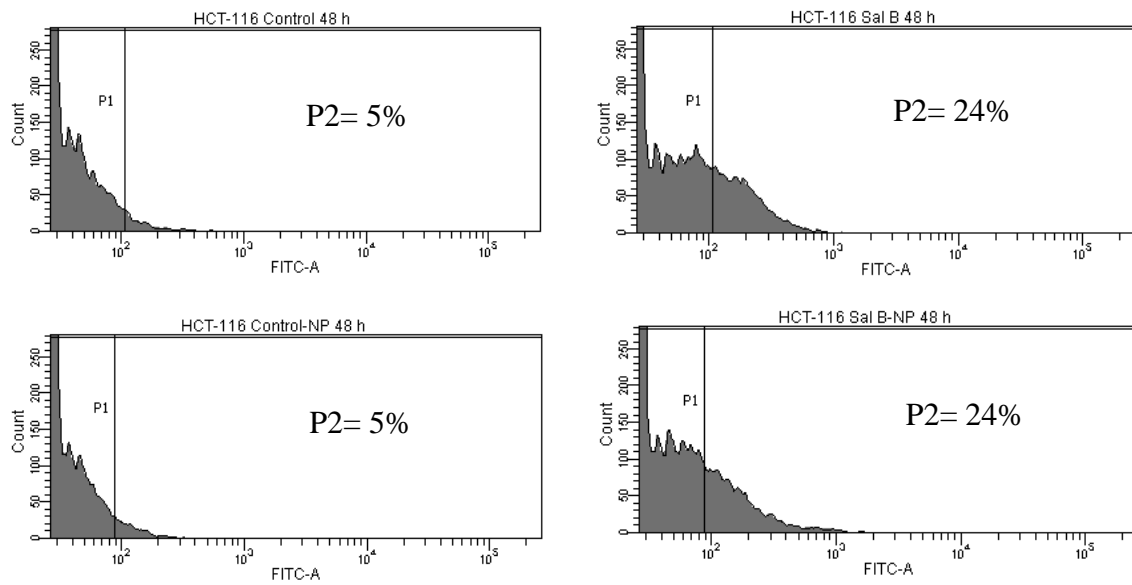


Figure 43. Sal B and its nanoparticle formulation treatment for 48 hours induce apoptosis in HCT-116 cells. HCT-116 cells were treated with 5 $\mu\text{g}/\text{mL}$ Sal B or Sal B-NP. Control cells were treated with 0.1% ethanol or THF with NP vehicle. TUNEL analysis was performed on treated cells as described.

CHAPTER IV

DISCUSSION

Natural compounds are at the forefront of anti-cancer drug development and PSMs from medicinal plants are responsible for these therapeutic properties. In particular, SLs have shown promise as they possess a broad range of anti-tumor properties and several have been tested in cancer clinical trials. We have previously extracted and purified Sal A from *Centaurea ainetensis* and shown that this SL possesses anti-tumor properties in *in vitro* and *in vivo* tumor models. Here, we aimed to develop more bioavailable and clinically desirable derivatives of Sal A and to optimize its extraction and drug formulation into nanoparticles. Nanoparticle formulations can help provide drug delivery strategies for increased stability, selectivity, efficacy, and bioavailability. This leads to reduced drug cytotoxicity, a common undesirable effect of chemotherapy, by allowing administered drug concentration to be lower than with native drug. Furthermore, nanoparticle formulations of Sal A may address drug quantity limitations which is a common feature of drug development from natural sources.

Thus, we undertook this study in order to develop Sal A as an anti-cancer drug candidate, while enhancing the drug through biotechnological approaches such as derivatization and nano-formulation. Our aim was to use these strategies to develop more effective and less toxic lead drugs from natural sources. This required an interdisciplinary team, where we must first scale up drug extractions, characterize our drugs, and synthesize derivatives with the help of our collaborators in the Chemistry Department, namely Dr. Najat Saliba and Dr. Tarek Ghaddar. Next, we applied the

expertise of Dr. Walid Saad from the Chemical Engineering Department for nanotechnology-based strategies to address any solubility limitations associated with Sal A and its derivatives, and to optimize drug bioavailability and drug efficacy in order to achieve a more clinically desirable product. Finally, we evaluated drugs and nanoparticle formulations in several *in vitro* models of cancer. This drug development dynamic was established through continuous interaction among multidisciplinary collaborators where extraction and derivatization fed into the biological evaluation of the drug, providing feedback for further derivatization and optimization. This drove drug formulation optimization, in which nanoformulations were developed and assessed in *in vitro* models. Every step of this system became crucial towards the success of the overall drug development process.

Drug development of Sal A was aimed towards the cancer clinic. Given that cancer persists as a worldwide problem, and the need for novel anti-cancer agents is in high demand, we studied the effect of Sal A, derivatives, and nanoparticle formulations on a panel of representative cell lines of the most pervasive cancers, namely colorectal, breast, lung, prostate, and hematological cancers [52]. Cell lines were selected to represent both early and late stages of human cancers with different *p53* status. Of note, *p53* is widely studied since it is one of the most deregulated genes in human cancers [98]. To decipher the mechanism of action of the different anti-cancer drugs, we selected the human colorectal cancer *in vitro* model as this neoplasm is one of the most common worldwide as well as regionally. Furthermore, this *in vitro* model consists of widely used and characterized isogenic cell lines with various *p53* status.

We began our study by scaling up drug extraction. Interestingly, during the extraction and purification of Sal A, another SL with similar physiochemical properties

eluted at a later time point. This compound was identified in the literature as Sal B [94-97] where its structure has been elucidated and anti-fungal activity studied. However, no anti-tumor properties of Sal B have been reported so far. Interestingly, only plant batches collected in summer 2012 and 2013 contained Sal B but none was detected in previous years. The plants collected during these two years were subjected to stress conditions due to drought and it is plausible that *Centaurea ainetensis* produced Sal B, a more hydrophobic compound better suited to stress conditions. In fact, many plant species respond to water stress by slowing growth while continuing to produce PSMs at a rate that results in higher concentrations of these compounds [99]. For example, the SL and diterpene content of the leaves of the desert sunflower *Helianthus ciliaris* doubled from 0.40% to 0.79% under moderate water stress [100]. According to this study, the accumulation of these PSMs might have been an adaptive response to stress that allows for survival of the plant. When overall water supply is limiting, one might expect an increased investment in defenses that are more effective at lower concentrations such as with Sal B.

The chemical structure of Sal B was elucidated by FTIR, NMR, and GC-MS, and showed to have a decreased polarity relative to Sal A due to the missing hydroxyl group on the ninth carbon. Interestingly, Sal B was shown to be relatively non-cytotoxic to normal cells at the tested concentrations and more potent than Sal A. However, simply depending on Sal A and Sal B's natural structures was not sufficient. With properties such as high hydrophobicity and low polarity, Sal A and Sal B necessitate modifications to the bioactive molecules in order to improve their solubility and pharmacokinetic profile. Nanoparticle formulation afforded the ability to

enhance these physiochemical properties of the drugs but the method required special considerations for solubility.

In search of more bioavailable and suitable drugs for nanoparticle formulation, more hydrophobic derivatives of Sal A and Sal B were synthesized, namely Sal A-1, Sal A-2, and Sal B-1. In drug development, enhancing the drug's solubility and pharmacokinetic profile, as well as its efficacy, is crucial towards clinical success. We pursued a practical approach through derivatization whereby the hydroxyl groups found on the structure of the compounds were converted to keto- or ester-groups, consequently decreasing the drugs' polarity. To our knowledge, the derivatization of Sal A and Sal B, solubility, and supersaturation levels were reported for the first time and may lead to good knowledge of the most potent derivative bioavailability.

Solubility experiments further confirmed increased hydrophobicity due to the modified structures. These chemical properties may lend insight into the altered function of the drug when it comes to efficacy and potency. These five compounds exhibited anti-cancer activities in a variety of human cancer cell lines where the different derivatives have shown at least a two-fold increased potency relative to Sal A. When all compounds were tested, Sal A, Sal B, and Sal A-2 had the most potent activity at relatively non-cytotoxic concentrations to normal counterparts. In fact, among the compounds tested, Sal B proved to be least cytotoxic to normal cells. Solid and hematological tumor cells treated with Sal B and Sal A-2 were more sensitive in comparison to Sal A. This increased potency may be attributed to their increased hydrophobicity, facilitating ease of intake into the cell, however, this needs further investigation. Alternatively, the increased activities may be explained by a kinetically driven process whereby the hydrolyzation of the hydroxyl bond leads to increased

cellular intake. Over time, the more hydrophobic derivative accumulates faster in the cell than parental compound but eventually converts back to the parental compound once in the cell.

The potency of the tested Sal A, Sal B, and their derivatives is primarily attributed to the characteristic alkylating center of SLs, the α -methylene- γ -lactone functional group, which targets and inhibits the activity of several functional proteins [101]. However, since the α -methylene- γ -lactone moiety is common to all tested compounds, the observed differential growth inhibitory effects may be ascribed to the difference in the attached functional groups such as the hydroxyl or isopropyl groups. Further investigation of the structure-activity relationship of these different SLs will shed light on whether increased anti-tumor activities is due to enhanced lipophilicity and/or type of functional groups. Docking experiments, computerized modeling and bioinformatics software is in process in order to understand and compare the structure-function relationship of the drugs and possible targeted pathways in tumor cells.

In addition to characterizing the chemical structure of the compounds, determination of aqueous and organic solubilities allowed us to ascertain their suitability for producing nanoparticles. By combining nanotechnology with medicine, we aimed for more efficient drug delivery; increasing stability, bioavailability, and reducing drug toxicity, which are common challenges in drug development. Towards this end, we proceeded to formulate and characterize nanoparticles of the different SLs and to assess their anti-cancer effects in established *in vitro* models of human colorectal and breast cancer.

Sal A, Sal B, and derivatives were attempted to be formulated into nanoparticles using FNP. However, Sal A could not be developed into nanoparticles using our

method due to its high solubility in 10% THF. Therefore, more hydrophobic derivatives of Sal A, namely Sal A-1 and Sal A-2, were synthesized but they proved to be highly unstable drug formulations, exhibiting drug crystallization that prevented chemical interaction with the polymer. We are currently investigating other types of polymers that may work best with Sal A-1 and Sal A-2 based on solubility profiles. So far, only Sal B proved most successful as a nanoparticle formulation and became our lead drug based on anti-tumor feedback biological assays.

Our results showed that native Sal B and its nanoparticle formulation had comparable anti-tumor activities in colorectal and breast cancer cells of different *p53* status, while being non-cytotoxic to normal cells at effective tested concentrations. Naked Sal B and nanoparticle formulation induced apoptosis as well as accumulation of cells in the S phase of the cell cycle. We will monitor and optimize Sal B nanoparticle formulation stability over time through DLS and HPLC. Dialysis or other techniques for solvent removal will be used. Additionally, Sal B nanoparticles will be further characterized in order to quantify drug loading content and encapsulation efficiency. These formulation properties will then be optimized based on feedback biological assays. In particular, we are interested in monitoring cellular intake behavior through use of isotopes or fluorescent tagging. This will allow us to further compare structure-function relationships to explain enhanced drug effect.

A major challenge in drug development from natural sources is a continuous and sufficient supply of drugs. For example, the most used anti-cancer drug Taxol® was initially isolated from the bark of the Pacific yew tree (*Taxus brevifolia*). However, due to difficulties harvesting enough bark for Taxol® and complexities involved in synthesis of this compound, development toward the clinic was slow. Clinical trials

became possible when a method was derived to extract a precursor of Taxol®, 10-deacetyl-baccatin III, from the leaves of the common yew *Taxus baccata*. The precursor was then converted by chemical synthesis to Taxol® [6]. In order to get enough quantities of Sal B for pre-clinical drug development *in vivo*, we aim to synthesize Sal B from its precursor, Sal A. Ideally we would like to fully synthesize Sal B but this possibility remains challenging due to the complexity of the cyclic structures. Additionally, we will attempt to synthesize other derivatives that might show success as nanoparticle formulations with enhanced stability.

Several limitations need to be addressed before proceeding with the preclinical *in vivo* testing, including limited drug quantities and problems with nanoparticle stability. Additionally, though *in vitro* nanoparticles demonstrate comparable potency against cancer cells to native drug, there is a possibility that they may not show success *in vivo* as they may be rapidly hydrolyzed and cleared from the system. However, we remain optimistic since nanoparticles exhibit a characteristically enhanced effect *in vivo* especially through the aforementioned EPR effect. We, therefore, expect increased efficacy of nanoparticles *versus* native drug but this needs further validation.

Native Sal B and its nanoparticle formulation will be further evaluated in tumor xenograft animal models with the ultimate aim of providing novel colorectal and breast cancer therapies. The plasma retention time of Sal B and nanoparticle formulations will be assessed *in vivo* as it is one of the crucial factors affecting the *in vivo* availability and efficacy of a drug. Lipophilic nanoparticle carriers enhance the plasma retention time of drugs, in particular those with low aqueous solubility, due to the high probability of the drug partitioning back into the carrier [88]. We will then generate tumor xenograft models in mice. Human colorectal and breast cancer cells will be injected into severe

combined immunodeficient (SCID) mice. Histological characteristics of the tumors, including volume, morphology, cell proliferation, apoptotic markers, and vascularization, will be monitored over time before and during the treatment. Success *in vivo* will allow the advancement of the drug development in translational research.

In summary, these studies highlight the use of Sal B and its nanoparticle formulation as promising lead anti-cancer drug candidates for further preclinical investigation. For the first time, these drugs have been tested on several human *in vitro* solid and hematological models and further characterized on colorectal cancer models. They have shown increased potency and reduced cytotoxicity to normal cells relative to Sal A, producing supporting evidence for further drug development.

REFERENCES

1. Azaizeh, H., et al. *Traditional Arabic and Islamic medicine, a re-emerging health aid*. Evidence-Based Complementary and Alternative Medicine, 2010. **7**(4): p. 419-424.
2. Pierpoint, W.S. *Salicylic-acid and its derivatives in plants -medicines, metabolites and messenger molecules*. Advances in Botanical Research, Vol 20, 1994. **20**: p. 163-235.
3. Balunas, M.J. and A.D. Kinghorn. *Drug discovery from medicinal plants*. Life Sciences, 2005. **78**(5): p. 431-441.
4. Harvey, A.L. *Natural products in drug discovery*. Drug Discovery Today, 2008. **13**(19–20): p. 894-901.
5. Zubrod, C.G. *Origins and development of chemotherapy research at the National Cancer Institute*. Cancer Treat Rep, 1984. **68**(1): p. 9-19.
6. Cragg, G.M. *Paclitaxel (Taxol): a success story with valuable lessons for natural product drug discovery and development*. Med Res Rev, 1998. **18**(5): p. 315-31.
7. Nehmé, M. *Wild Flowers of Lebanon*. 1978: National Council for Scientific Research.
8. Rouwayha, A. *Alatadawi Bil Aa'shab*. Dar El Qualam, Beirut, Lebanon, 1981.
9. Hart, N. *Inviting all the world's crops to the table: supporting traditional crops to supply future needs*, in *Global Facilitation Unit for Underutilized Species*. 2007: Rome, Italy.
10. Kingston, D.G. and D.J. Newman. *Taxoids: cancer-fighting compounds from nature*. Curr Opin Drug Discov Devel, 2007. **10**(2): p. 130-44.
11. Newman, D.J. and G.M. Cragg. *Natural products as sources of new drugs over the last 25 years*. Journal of Natural Products, 2007. **70**(3): p. 461-477.
12. Ganapathy, H.S., R.S. Nagarajan, and H. Ihara. *Recent advances in cancer therapy using phytochemicals*, in *Nanomedicine and Cancer Therapies*. 2012, Apple Academic Press. p. 69-74.
13. Saeidnia, S. and M. Abdollahi. *Perspective studies on novel anticancer drugs from natural origin: a comprehensive review*. International Journal of Pharmacology, 2014. **10**(2): p. 90-108.
14. Kossel, A. *Ueber die chemische Zusammensetzung der Zelle*. Archiv für physiologie, 1891: p. 181-186.
15. Czapek, F. *Biochemie der Pflanzen*. 1922.
16. Harborne, J.B. *Arsenal for survival: secondary plant products*. Taxon, 2000. **49**(3): p. 435-449.
17. Pichersky, E. and D.R. Gang. *Genetics and biochemistry of secondary metabolites in plants: an evolutionary perspective*. Trends Plant Sci, 2000. **5**(10): p. 439-45.
18. Wink, M. *Phytochemical diversity of secondary metabolites*. Encycl Plant Crop Sci, 2004: p. 915-9.
19. Acamovic, T. and J. Brooker. *Biochemistry of plant secondary metabolites and their effects in animals*. Proceedings of the Nutrition Society, 2005. **64**(03): p. 403-412.

20. Wink, M. *Importance of plant secondary metabolites for protection against insects and microbial infections*. *Advances in Phytomedicine*, 2006. **3**: p. 251-268.
21. Li, J., et al. *Arabidopsis flavonoid mutants are hypersensitive to UV-B irradiation*. *The Plant Cell Online*, 1993. **5**(2): p. 171-179.
22. Harborne, J.B. *Classes and functions of secondary products from plants*. *Chemicals from Plants*, 1999: p. 1-25.
23. Gurib-Fakim, A. *Medicinal plants: traditions of yesterday and drugs of tomorrow*. *Molecular Aspects of Medicine*, 2006. **27**(1): p. 1-93.
24. Savel, H. *The metaphase-arresting plant alkaloids and cancer chemotherapy*. *Progress in Experimental Tumor Research*, 1965. **8**: p. 189-224.
25. Athar, M., et al. *Resveratrol: a review of preclinical studies for human cancer prevention*. *Toxicology and Applied Pharmacology*, 2007. **224**(3): p. 274-283.
26. Kunnumakkara, A.B., et al. *Curcumin potentiates antitumor activity of gemcitabine in an orthotopic model of pancreatic cancer through suppression of proliferation, angiogenesis, and inhibition of nuclear factor- κ B-regulated gene products*. *Cancer Research*, 2007. **67**(8): p. 3853-3861.
27. Ding, M., et al. *Cyanidin-3-glucoside, a natural product derived from blackberry, exhibits chemopreventive and chemotherapeutic activity*. *Journal of Biological Chemistry*, 2006. **281**(25): p. 17359-17368.
28. Afaq, F., et al. *Inhibition of ultraviolet B-mediated activation of nuclear factor κ B in normal human epidermal keratinocytes by green tea Constituent (-)-epigallocatechin-3-gallate*. *Oncogene*, 2003. **22**(7): p. 1035-1044.
29. Lu, Y.-P., et al. *Topical applications of caffeine or (-)-epigallocatechin gallate (EGCG) inhibit carcinogenesis and selectively increase apoptosis in UVB-induced skin tumors in mice*. *Proceedings of the National Academy of Sciences*, 2002. **99**(19): p. 12455-12460.
30. Schiff, P.B., J. Fant, and S.B. Horwitz. *Promotion of microtubule assembly in vitro by taxol*. 1979.
31. Zhang, S., et al. *Anti-cancer potential of sesquiterpene lactones: bioactivity and molecular mechanisms*. *Current Medicinal Chemistry-Anti-Cancer Agents*, 2005. **5**(3): p. 239-249.
32. Heinrich, M., et al. *Ethnopharmacology of Mexican asteraceae (compositae)*. *Annual Review of Pharmacology and Toxicology*, 1998. **38**(1): p. 539-565.
33. Kaij-a-Kamb, M., M. Amoros, and L. Girre. *Search for new antiviral agents of plant origin*. *Pharmaceutica Acta Helvetiae*, 1991. **67**(5-6): p. 130-147.
34. Zhang, S., C.-N. Ong, and H.-M. Shen. *Critical roles of intracellular thiols and calcium in parthenolide-induced apoptosis in human colorectal cancer cells*. *Cancer Letters*, 2004. **208**(2): p. 143-153.
35. Wen, J., et al. *Oxidative stress-mediated apoptosis the anticancer effect of the sesquiterpene lactone parthenolide*. *Journal of Biological Chemistry*, 2002. **277**(41): p. 38954-38964.
36. Lee, K.-H., et al. *Sesquiterpene antitumor agents: inhibitors of cellular metabolism*. *Science*, 1977. **196**(4289): p. 533-536.
37. Ghantous, A., et al. *What made sesquiterpene lactones reach cancer clinical trials?* *Drug Discovery Today*, 2010. **15**(15): p. 668-678.

38. Pajak, B., B. Gajkowska, and A. Orzechowski. *Molecular basis of parthenolide-dependent proapoptotic activity in cancer cells*. *Folia Histochemica et Cytobiologica*, 2008. **46**(2): p. 129-135.
39. Neelakantan, S., et al. *Aminoparthenolides as novel anti-leukemic agents: Discovery of the NF- κ B inhibitor, DMAPT (LC-1)*. *Bioorganic & Medicinal Chemistry Letters*, 2009. **19**(15): p. 4346-4349.
40. Sweeney, C.J., et al. *The sesquiterpene lactone parthenolide in combination with docetaxel reduces metastasis and improves survival in a xenograft model of breast cancer*. *Molecular Cancer Therapeutics*, 2005. **4**(6): p. 1004-1012.
41. Nasim, S. and P.A. Crooks. *Antileukemic activity of aminoparthenolide analogs*. *Bioorganic & Medicinal Chemistry Letters*, 2008. **18**(14): p. 3870-3873.
42. El-Najjar, N., et al. *Anti-colon cancer effects of Salograviolide A isolated from *Centaurea ainetensis**. *Oncology Reports*, 2008. **19**(4): p. 897-904.
43. Saikali, M., et al. *Sesquiterpene lactones isolated from indigenous Middle Eastern plants inhibit tumor promoter-induced transformation of JB6 cells*. *BMC Complementary and Alternative Medicine*, 2012. **12**(1): p. 89.
44. Ghantous, A., et al. *Purified Salograviolide A isolated from *Centaurea ainetensis* causes growth inhibition and apoptosis in neoplastic epidermal cells*. *International Journal of Oncology*, 2008. **32**(4): p. 841-849.
45. Talhouk, R.S., et al. *Anti-inflammatory bio-activities in water extract of *Centaurea ainetensis**. *Journal of Medicinal Plants Research*, 2008. **2**(2): p. 24-33.
46. Saliba, N.A., et al. *Bio-guided identification of an anti-inflammatory guaianolide from *Centaurea ainetensis**. *Pharmaceutical Biology*, 2009. **47**(8): p. 701-707.
47. Mabberley, D. *The Plant Book*. 1997, Cambridge, Cambridge University Press.
48. Karamenderes, C., et al. *Total phenolic contents, free radical scavenging activities and inhibitory effects on the activation of NF- κ B of eight *Centaurea L. species**. *Phytotherapy Research*, 2007. **21**(5): p. 488-491.
49. Skliar, M., M. Toribio, and D. Oriani. *Antimicrobial activity of *Centaurea diffusa**. *Fitoterapia*, 2005. **76**(7): p. 737-739.
50. Koukoulitsa, E., et al. *Bioactive sesquiterpene lactones from *Centaurea species* and their cytotoxic/cytostatic activity against human cell lines in vitro*. *Planta Medica*, 2002. **68**(7): p. 649-652.
51. Barrero, A.F., et al. *Biomimetic cyclization of cnicin to malacitanolide, a cytotoxic eudesmanolide from *Centaurea malacitana**. *Journal of Natural Products*, 1997. **60**(10): p. 1034-1035.
52. Siegel, R.L., K.D. Miller, and A. Jemal. *Cancer statistics, 2015*. *CA Cancer J Clin*, 2015. **65**(1): p. 5-29.
53. Russo, J. and I. Russo. *Pathogenesis of breast cancer*, in *Molecular Basis of Breast Cancer*. 2004, Springer Berlin Heidelberg. p. 137-180.
54. Shamseddine, A., et al. *Cancer incidence in postwar Lebanon: findings from the first national population-based registry, 1998*. *Annals of Epidemiology*, 2004. **14**(9): p. 663-668.
55. Soule, H.D., et al. *Isolation and characterization of a spontaneously immortalized human breast epithelial cell line, MCF-10*. *Cancer Res*, 1990. **50**(18): p. 6075-86.

56. Merlo, A., et al. *5' CpG island methylation is associated with transcriptional silencing of the tumour suppressor p16/CDKN2/MTS1 in human cancers.* Nat Med, 1995. **1**(7): p. 686-92.
57. Debnath, J., S.K. Muthuswamy, and J.S. Brugge. *Morphogenesis and oncogenesis of MCF-10A mammary epithelial acini grown in three-dimensional basement membrane cultures.* Methods, 2003. **30**(3): p. 256-268.
58. Soule, H.D., et al. *A human cell line from a pleural effusion derived from a breast carcinoma.* J Natl Cancer Inst, 1973. **51**(5): p. 1409-16.
59. Levenson, A.S. and V.C. Jordan. *MCF-7: the first hormone-responsive breast cancer cell line.* Cancer Res, 1997. **57**(15): p. 3071-8.
60. Lacroix, M. and G. Leclercq. *Relevance of breast cancer cell lines as models for breast tumours: an update.* Breast Cancer Res Treat, 2004. **83**(3): p. 249-89.
61. Chavez, K.J., S.V. Garimella, and S. Lipkowitz. *Triple negative breast cancer cell lines: one tool in the search for better treatment of triple negative breast cancer.* Breast Disease, 2010. **32**(1-2): p. 35-48.
62. Moyer, M., et al. *NCM460, a normal human colon mucosal epithelial cell line.* In Vitro Cellular & Developmental Biology - Animal, 1996. **32**(6): p. 315-317.
63. Bunz, F., et al. *Requirement for p53 and p21 to sustain G2 arrest after DNA damage.* Science, 1998. **282**(5393): p. 1497-1501.
64. Cragg, G.M. and D.J. Newman. *Plants as a source of anti-cancer agents.* Journal of Ethnopharmacology, 2005. **100**(1-2): p. 72-79.
65. Cragg, G.M., D.G.I. Kingston, and D.J. Newman. *Anticancer agents from natural products.* 2005: CRC Press.
66. Newman, D.J., G.M. Cragg, and K.M. Snader. *Natural products as sources of new drugs over the period 1981-2002.* Journal of Natural Products, 2003. **66**(7): p. 1022-1037.
67. Savas, P., B. Hughes, and B. Solomon. *Targeted therapy in lung cancer: IPASS and beyond, keeping abreast of the explosion of targeted therapies for lung cancer.* J Thorac Dis, 2013. **5 Suppl 5**: p. S579-92.
68. Hortobagyi, G.N. *Opportunities and challenges in the development of targeted therapies.* Semin Oncol, 2004. **31**(1 Suppl 3): p. 21-7.
69. Phelps, M.A. and A. Sparreboom. *A snapshot of challenges and solutions in cancer drug development and therapy.* Clin Pharmacol Ther, 2014. **95**(4): p. 341-6.
70. Kwok, B.H.B., et al. *The anti-inflammatory natural product parthenolide from the medicinal herb Feverfew directly binds to and inhibits I κ B Kinase.* Chemistry & Biology, 2001. **8**: p. 759-766.
71. Yip-Schneider, M.T., et al. *Efficacy of dimethylaminoparthenolide and sulindac in combination with gemcitabine in a genetically engineered mouse model of pancreatic cancer.* Pancreas, 2013. **42**(1): p. 160-167.
72. Piccionello, A.P., et al. *Fluorinated and pegylated polyaspartamide derivatives to increase solubility and efficacy of Flutamide.* Journal of Drug Targeting, 2012. **20**(5): p. 433-444.
73. McNeil, S. *Unique Benefits of Nanotechnology to Drug Delivery and Diagnostics,* in *Characterization of nanoparticles intended for drug delivery,* S.E. McNeil, Editor. 2011, Humana Press. p. 3-8.
74. Wilczewska, A.Z., et al. *Nanoparticles as drug delivery systems.* Pharmacological Reports, 2012. **64**(5): p. 1020-1037.

75. Sivasankar, M. and B.P. Kumar. *Role of nanoparticles in drug delivery system*. International Journal of Research in Pharmaceutical and Biomedical Sciences, 2010. **1**(2): p. 41-66.
76. Mitragotri, S., P.A. Burke, and R. Langer. *Overcoming the challenges in administering biopharmaceuticals: formulation and delivery strategies*. Nat Rev Drug Discov, 2014. **13**(9): p. 655-672.
77. Hubbell, J.A. and A. Chilkoti. *Nanomaterials for drug delivery*. Science, 2012. **337**(6092): p. 303-305.
78. Maeda, H., et al. *Tumor vascular permeability and the EPR effect in macromolecular therapeutics: a review*. Journal of Controlled Release, 2000. **65**(1): p. 271-284.
79. Jhaveri, A.M. and V.P. Torchilin. *Multifunctional polymeric micelles for delivery of drugs and siRNA*. Frontiers in Pharmacology, 2014. **5**.
80. Fang, J., H. Nakamura, and H. Maeda. *The EPR effect: Unique features of tumor blood vessels for drug delivery, factors involved, and limitations and augmentation of the effect*. Adv Drug Deliv Rev, 2011. **63**(3): p. 136-51.
81. Duncan, R. and R. Gaspar. *Nanomedicine(s) under the microscope*. Mol Pharm, 2011. **8**(6): p. 2101-41.
82. Jong, W.H.D. and P.J. Borm. *Drug delivery and nanoparticles: applications and hazards*. International Journal of Nanomedicine, 2008. **3**(2): p. 133.
83. Alexis, F., et al. *Targeted Nanoparticle-Polypeptide Bioconjugates for Breast Cancer Therapy*. Nanotech, 2007. **2**.
84. Merisko-Liversidge, E.M. and G.G. Liversidge. *Drug nanoparticles: formulating poorly water-soluble compounds*. Toxicologic Pathology, 2008. **36**(1): p. 43-48.
85. Savjani, K.T., A.K. Gajjar, and J.K. Savjani. *Drug solubility: importance and enhancement techniques*. ISRN Pharmaceutics, 2012. **2012**: p. 195727.
86. Kumar, A., et al. *Review on solubility enhancement techniques for hydrophobic drugs*. Pharmacie Globale, 2011. **3**(3): p. 001-007.
87. Johnson, B.K., W. Saad, and R.K. Prud'homme. *Nanoprecipitation of pharmaceuticals using mixing and block copolymer stabilization*. in ACS symposium series. 2006. Oxford University Press.
88. Ansell, S.M., et al. *Modulating the therapeutic activity of nanoparticle delivered paclitaxel by manipulating the hydrophobicity of prodrug conjugates*. Journal of Medicinal Chemistry, 2008. **51**(11): p. 3288-3296.
89. Svenson, S. *What nanomedicine in the clinic right now really forms nanoparticles?* Wiley Interdisciplinary Reviews: Nanomedicine and Nanobiotechnology, 2014. **6**(2): p. 125-135.
90. Svenson, S. *Clinical translation of nanomedicines*. Current Opinion in Solid State and Materials Science, 2012. **16**(6): p. 287-294.
91. Torchilin, V.P. *Multifunctional, stimuli-sensitive nanoparticulate systems for drug delivery*. Nature Reviews Drug Discovery, 2014. **13**(11): p. 813-827.
92. Mathur, M. and G. Vyas. *Role of nanoparticles for production of smart herbal drug— An overview*. Indian Journal of Natural Products and Resources, 2013. **4**(4): p. 329-338.
93. Karmakar, A., et al. *Nanodelivery of parthenolide using functionalized nanographene enhances its anticancer activity*. RSC Adv, 2015. **5**(4): p. 2411-2420.

94. Daniewski, W.M., et al. *Sesquiterpene lactones of Centaurea salonitana*. *Phytochemistry*, 1993. **34**(2): p. 445-447.
95. Marco, J.A., et al. *Bisabolene derivatives and sesquiterpene lactones from Cousinia species*. *Phytochemistry*, 1993. **32**(2): p. 395-400.
96. Vajs, V., et al. *Guaianolides from Centaurea nicolai: antifungal activity*. *Phytochemistry*, 1999. **52**(3): p. 383-386.
97. Rustaiyan, A. and S. Ardebili. *New guaianolides from Centaurea kandavanensis*. *Planta medica*, 1984. **50**(4): p. 362-362.
98. Vogelstein, B., S. Sur, and C. Prives. *p53: the most frequently altered gene in human cancers*. *Nature Education*, 2010. **3**(9): p. 6.
99. Gershenzon, J. *Changes in the levels of plant secondary metabolites under water and nutrient stress*, in *Phytochemical Adaptations to Stress*, B. Timmermann, C. Steelink, and F. Loewus, Editors. 1984, Springer US. p. 273-320.
100. Rogers, C.E., et al. *Terpenes of wild sunflowers (Helianthus): an effective mechanism against seed predation by larvae of the sunflower moth, Homoeosoma electellum (Lepidoptera: Pyralidae)*. Vol. 16. 1987. 586-592.
101. Kupchan, S.M., M.A. Eakin, and A.M. Thomas. *Tumor inhibitors. 69. Structure-cytotoxicity relations among the sesquiterpene lactones*. *Journal of Medicinal Chemistry*, 1971. **14**(12): p. 1147-1152.